RD-90/32, I

ACM-651

DOT/FAA/RD–90/32,I

Research and
Development Service
Washington, D.C. 20591

Runway Exit Designs for Capacity Improvement Demonstrations

Phase I — Algorithm Development

A.A. Trani
A.G. Hobeika
H.D. Sherali
B.J. Kim
C.K. Sadam

Virginia Polytechnic Institute and State University
University Center for Transportation Research
Blacksburg, Virginia 25061

June 1990

This document is available to the public through the
National Technical Information Service,
Springfield, Virginia 22161

U.S. Department of Transportation
Federal Aviation Administration

NOTICE

This document is disseminated under the sponsorship of the U.S. Department of Transportation in the interest of information exchange. The U.S. Government assumes no liability for its contents or use thereof.

Technical Report Documentation Page

1. Report No. DOT/FAA/RD-90/32, I	2. Government Accession No.	3. Recipient's Catalog No.
4. Title and Subtitle Runway Exit Designs for Capacity Improvement Demonstrations (Phase 1)		5. Report Date June 1990
		6. Performing Organization Code
7. Author(s) Trani, A.A., Hobeika, A.G., Sherali, H., Kim, B.J. and Sadam, C.K.		8. Performing Organization Report No. CTR-R-1-90
9. Performing Organization Name and Address Center for Transportation Research 106 Faculty Street Virginia Tech University, Blacksburg, VA 24061		10. Work Unit No. (TRAIS)
		11. Contract or Grant No. NAS1-18471-15
12. Sponsoring Agency Name and Address Federal Aviation Administration, ARD-200 800 Independence Avenue Washington, D.C., 20591		13. Type of Report and Period Covered Technical Report
		14. Sponsoring Agency Code FAA ARD-200

15. Supplementary Notes

A.A. Trani, A.G. Hobeika and H. Sherali: Virginia Tech University, Blacksburg VA. 24061. H. Tomita (FAA) and D. Middleton (NASA LARC) Project Monitors.

16. Abstract

A description and results are presented of a study to locate and design rapid runway exits under realistic airport conditions. The study developed a PC-based computer simulation-optimization program called REDIM (runway exit design interactive model) to help future airport designers and planners to locate optimal exits under various airport conditions. The model addresses three sets of problems typically arising during runway exit design evaluations. These are the evaluation of existing runway configurations, addition of new rapid runway turnoffs and the design of new runway facilities. The model is highly interactive and allows a quick estimation of the expected value of runway occupancy time. Aircraft populations and airport environmental conditions are among the multiple inputs to the model to execute a viable runway location and geometric design solution. The results presented in the report suggest that possible reductions on runway occupancy time (ROT) can be achieved with the use of optimally tailored rapid runway designs for a given aircraft population. Reductions of up to 9-6 seconds are possible with the implementation of 30 m/sec. variable geometry exits.

17. Key Words Runway Exits, Runway Occupancy Times High-Speed Exits	18. Distribution Statement This document is available to the public through the National Technical Information Service, Springfield, Virginia 22161.

19. Security Classif. (of this report) Unclassified	20. Security Classif. (of this page) Unclassified	21. No. of Pages 160	22. Price

Form DOT F 1700.7 (8-72) Reproduction of completed page authorized

Table of Contents

1.0 Introduction **1**

1.1 Previous Turnoff Geometry Research 5

1.2 Mathematical Models for Optimal Turnoff Locations 9

1.3 Approach and Scope of the UCTR/VPI Research 13

1.4 Model Overview 18

2.0 Input Module **22**

2.1 Data Classification 22

2.2 Input/Output Relationship 25

2.3 Data Input Method 27

2.4 Procedures in Input Module 28

2.4.1 Starting a New Problem 28

2.4.2 Editing Aircraft Data 32

2.4.3 Editing the Master File 32

3.0 Dynamic Module **37**

3.1 Air Distance 37

3.2 Free Roll Distances 40

3.3 Braking Distance 42

3.4 Turnoff Algorithm 44

3.5 Comfort Factor Considerations 53

3.6 Exit Assignment Algorithm 58

3.7 Airport Environmental Variables 59

3.8 Aircraft Characteristics 60

4.0 Optimization Module **64**

4.1 Generation of a Complete Set of Candidates 65

4.2 Estimation of Runway Occupancy Times 67

4.3 Finding Optimal Locations 69

4.3.1 Mathematical Model 70

4.3.2 Dynamic Programming Formulation 72

4.4 Aircraft Exit Assignment 75

4.5 A Simple Example 75

4.6 Modified Algorithm for 'Improvement' Analysis 76

5.0 Output Module 78

5.1 View the Output 78

5.1.1 Evaluate an Existing Runway 80

5.1.2 Improve an Existing Runway 84

5.1.3 Design of a New Runway 92

5.2 Print the Report 98

5.3 Help 99

6.0 Use of the Model 100

6.1 Example 1 (Evaluating a Runway Facility) 101

6.2 Example 2 (Improving a Runway Facility) 112

7.0 Conclusions 124

7.1 Suggested High-speed Standard Geometry 124

7.2 Comparison of REDIM Geometries 130

8.0 Model Recommendations 136

8.1 Postoptimization Algorithm 136

8.2 Human Behavioral Factors 137

8.3 Turnoff Angle Parameters 138

Bibliography 139

Appendix A. Glossary of Aircraft Characteristics 143

Appendix B. Optimality Through a Discrete Search 146

Appendix C. Approximation of Turnoff Times 148

Foreword

This report details the work performed by the Center for Transportation Research at Virginia Polytechnic Institute and State University in the area of optimal location of runway turnoffs. The report addresses the first phase of contract NAS1-18471 Task No. 15 with the Federal Aviation Administration (FAA) and the National Aeronautics and Space Administration.

The work presented here would not have been possible without the contributions and support of many people. Mr. David Middleton (NASA) acted as project monitor for this task and his guidance is highly appreciated. Mr. Hisao Tomita, Project Manager at the Federal Aviation Administration (ARD-200), provided this research team with the necessary resources to complete this task. His interest and suggestions during the project execution were of paramount importance to achieve our goal. Finally we would like to thank NASA and FAA for their trust and confidence in the Virginia Tech research team.

A.G. Hobeika

A.A. Trani

H.D. Sherali

B.J. Kim

C.K. Sadam

List of Figures

Figure 1.1. Turnoff Geometry Specification Graph [Horonjeff, 1958]. 7

Figure 1.2. 30 Degree High-Speed Turnoff Geometry. 8

Figure 1.3. 45 Degree High-Speed Turnoff Geometry. 8

Figure 1.4. A Modified High-Speed Turnoff Geometry. 10

Figure 1.5. Comparison of a Standard and Modified High Speed Turnoff Geometry. 10

Figure 1.6. Hypothetical Aircraft Landing Distance Frequency Distribution. 15

Figure 1.7. Typical Projected Turnoff Locations for a Hypothetical Runway. 16

Figure 1.8. Sample Turnoff Geometries for Different Aircraft Categories. 17

Figure 1.9. REDIM Model Flowchart Organization. 19

Figure 1.10. Aircraft Landing Events Modeled in the Analysis. 21

Figure 2.1. Input Module Functional Flow Diagram. 23

Figure 2.2. I/O Relationship for 'Evaluation' Analysis. 26

Figure 2.3. I/O Relationship for 'Improvement' Analysis. 26

Figure 2.4. I/O Relationship for 'Design' Analysis. 27

Figure 2.5. Main Menu Screen. 29

Figure 2.6. Type of Analysis Menu. 29

Figure 2.7. Data Related to Type of Analysis Screen. 30

Figure 2.8. Aircraft Mix Data Menu. 31

Figure 2.9. Aircraft Characteristics Data Screen. 31

Figure 2.10. Airport Environmental Data Screen. 33

Figure 2.11. Airport Operational Data Screen. 33

Figure 2.12. Runway Gradients Screen. 34

Figure 2.13. Weather and Exit Speeds Menu. 34

Figure 2.14. Edit Menu Screen. 35

Figure 2.15. Edit Menu Screen for Master File. 35

Figure 2.16. Adding a New Aircraft Screen. 36

Figure 3.1 Dynamic Module Functional Flow Diagram. 38

Figure 3.2 Runway Clearance Point Nomenclature....47
Figure 3.3 Comparative Lift-to-Weight Ratios for High-Speed Taxiing Aircraft....48
Figure 3.4 Comparison of Aircraft Turnoff Tracks With and Without Lifting Forces....48
Figure 3.5 Skid Friction Variations with Tire Pressure and Speed....49
Figure 3.6 Aircraft Turnoff Paths using Two Integration Algorithms....52
Figure 3.7 Possible Passenger Comfort Factor Indifference Curves....55
Figure 3.8 Comparison of Turnoff Track for Various Aircraft....56
Figure 3.9 Aircraft Kinematic Behavior Nomenclature....61
Figure 3.10 Aircraft Geometric Characteristics....62
Figure 4.1. Best Turnoff Locations abd Their Weights....65
Figure 4.2. Optimization Procedure Flow Chart....66
Figure 4.3. The Components of T_{ijk} Time....68
Figure 5.1. Output Functional Flow Diagram....79
Figure 5.2. Output Menu....80
Figure 5.3. Functional Flow Diagram for the 'Evaluation' Mode (Runmode 1)....81
Figure 5.4. View Menu for 'Runmode 1'....82
Figure 5.5. ROT/Reliability Table Results....82
Figure 5.6. Turnoff Location Along the Runway Downrange....85
Figure 5.7. Standard FAA 30-Degree Turnoff....85
Figure 5.8. Standard FAA 45-Degree Turnoff....86
Figure 5.9. Standard FAA 90-Degree Turnoff....86
Figure 5.10. Functional Flow Diagram for Runmode '2'....87
Figure 5.11. View Menu for Runmodes '2' and '3'....89
Figure 5.12. ROT Table of Results....89
Figure 5.13. Comparision of Centerline Turnoff Geometries....90
Figure 5.14. Functional Flow Diagram for Runmode '3'....93
Figure 5.15. Table of Turnoff Geometry Coordinates....94
Figure 5.16. Variable Turnoff Geometry (REDIM)....96
Figure 5.17. Aircraft Statistics and Their ROT's....96
Figure 6.1. ROT Parameter vs. Exit Speed and Airfield Elevation (BAe-146-200)....99

Figure 6.2. ROT Parameter vs. Exit Speed and Airfield Temperature.....100
Figure 6.3. ROT and Exit Location Sensitivities to Aircraft Landing Mass.....101
Figure 6.4. Main Menu to Start Example 1.....102
Figure 6.5. Evaluation Mode for Example 1.....102
Figure 6.6. Selecting Existing Turnoffs and Their Type for Example 1.....103
Figure 6.7. Aircraft Mix Editor Screen for Example 1.....103
Figure 6.8. Airport Operational Values for Example 1.....105
Figure 6.9. Airport Environmental Values for Example 1.....105
Figure 6.10. Runway Gradients and for Example 1.....106
Figure 6.11. Weather Characteristics and Exit Speeds for Example 1.....106
Figure 6.12. Main 'Output Menu' for Example 1.....108
Figure 6.13. 'View Menu' for Example 1.....108
Figure 6.14. Partial ROT / Reliability Table for Example 1.....111
Figure 6.15. Turnoff Locations and Their Geometries for Example 1.....111
Figure 6.16. Existing 90-Degree Standard Turnoff Geometry for Example 1.....112
Figure 6.17. Definition of Weather Conditions and Exit Speeds for Example 2.....114
Figure 6.18. Partial Dynamic Simulation Results for Improved Single Runway.....114
Figure 6.19. Partial ROT/Table Results for Improved Single Runway with 5 exits.....116
Figure 6.20. Partial ROT/Table Results for Improved Single Runway with 6 exits.....119
Figure 6.21. Runway Exit Locations for Example 2 with 6 Turnoffs.....117
Figure 6.22 Centerline Geometry Comparison for Example 2 with 6 exits.....117
Figure 6.23. Complete Turnoff Geometry for Fifth Exit of Example 2 (6 Exits).....118
Figure 6.24. Input Data Summary Report for Example 2.....118
Figure 6.25. Analysis Results Format for Example 2.....119
Figure 6.26. Analysis Results Format for Example 2 (Continuation).....120

List of Tables

Table 1.1. Arrival Runway Occupancy Times. 3

Table 1.2. Arrival In-Trail Separation Criteria. 5

Table 3.1. Aircraft Approach Category Classification. 32

Table 3.2. Aircraft Characteristics. 48

Table 4.1. T_{ijk} Data for Three Aircraft 61

Table 4.2. Aircraft Assignments. 61

Table 6.1. REDIM Baseline Exit Speeds for Standard FAA Turnoffs. 139

Executive Summary

This report presents the results of a study performed by the Center for Transportation Research (CTR) at Virginia Polytechnic Institute and State University concerning the development of rapid runway turnoffs to be used in existing and future airport scenarios. This study was conducted for the Federal Aviation Administration (FAA) Office of Airport Research and Development (ARD-200) to assess the impact of optimal runway turnoff locations and their corresponding geometries in runway occupancy time and ultimately in runway capacity. The report emphasizes in the development of a combined simulation and optimization methodology to ascertain the impact of runway turnoff placement in the weighted average runway occupancy time (WAROT) for realistic aircraft populations operating from a single runway. The methodology developed was extended into a user-friendly computer program called REDIM - Runway Exit Design Interactive Model - to estimate the WAROT performance index for user defined aircraft populations under various airport atmospheric conditions. The accompanying computer software developed in this research requires a minimum of 512 Kbytes of memory and an ordinary IBM or compatible computer.

The results of this investigation can be summarized as follows:

1) Evidence suggests that existing runway turnoff geometries are not being used near their design speeds. The small existing database in high-speed runway exit use indicates that commercial aircraft are regularly using these exits 10-15 knots below their design speeds. The major consequence of this being higher runway occupancy times as aircraft have to spend more time decelerating on the runway.

2) Significant reductions in runway occupancy time (ROT) were observed (i.e., from 7 to 18 %) with the use of three, four and five optimally located runway turnoffs. The magnitude of these ROT reductions was, as expected, a strong function of the exit speeds used.

3) For all practical purposes a good approximation of a fully variable variable turnoff geometry can be obtained with two radii of curvature ending at a generally small exit angle. The differences observed between the approximation and the actual fully variable geometries are insignificant for small exit angles and should not compromise safety and comfort factors while maneuvering on the turnoff.

4) It seems feasible to design rapid runway turnoff designs for entry speeds of up to 35 m/s. (78 MPH) for aircraft TERP categories C and D. For these designs a smaller exit angle would be required to increase the deceleration distance available along the tangent turnoff geometry. This will add confidence to the pilot before arriving to the nearest taxiway junction. An alternative to this reduction in exit angle is to increase the current lateral separation minima between a runway and parallel taxiway centerline distance from 183 m. (600 ft.) to 228 m. (750 ft.).

5) It is suggested that further investigations be made on the aircraft stability and control implications at speeds above 35 m/s. to determine safety boundaries while executing turns at moderate ground turn rates.

6) Very low exit angles (i.e., < 15 degrees) should be avoided as they contribute to large turnoff and runway occupancy times due to long exposure of the aircraft wing or tailplane tip within the runway bounds. Optimal exit angle geometries seem to be in the 17-30 degree range depending on the specific aircraft and exit speed. The lower exit angles might have better acceptance among pilots as they would provide added distances to decelerate before a taxiway is reached. However, they would involve slightly higher costs and land use.

7) A computer simulation/optimization model to assess the runway optimal location and geometries of runway turnoffs was successfully implemented in a personal computer. The program requires a definition of the aircraft population and environmental conditions of the airport facility to optimize the weighted average runway occupancy time (WAROT). The

program executes a typical linear network optimal assignment problem including the simulation of the aircraft kinematic trajectories. The program is suitable for use at existing facilities in process of upgrading as well as for entirely new runways planned for the future.

8) Preliminary results at the runway capacity level indicate that rapid runway designs could increase runway hourly capacity by up to 10-12% if further reductions are accomplished in the in-trail separation distances allowed for successive arrivals planned for future airport environments (i.e., 2/4/5 nautical mile rule).

1.0 Introduction

The subject of airport congestion and delays has received a great deal of attention in recent years due to the rapid growth of air transportation services coupled with a relatively stagnant airport infrastructure. Current statistics indicate that approximately two billion dollars are paid by air travelers due to system imposed delays in the United States alone [FAA, 1987]. These delays are likely to increase as air travel demand builds up from 416 billion passenger revenue mile flown in 1988 to an estimated 750 billion passenger revenue mile by the end of the century or equivalent to an average annual growth of roughly 6 percent [Aviation Week & Space Technology, 1989]. The problem is further aggravated when one considers that the current air transportation system has been operating in a pseudo-stagnant mode with almost the same infrastructure in terms of airport facilities since the early seventies. The Federal Aviation Administration (FAA) has estimated that eleven major airports now experience severe chronic operational delays -more than 20,000 hours of system imposed delays per year - as a result of traffic congestion [FAA, 1989]. According to the FAA this number will increase to thirty two by the year 1996 and possibly fifty by the end of the century [FAA, 1988]. One fifth of these airport facilities will experience more than 50,000 hours of system imposed delays according to the same study. Delays at these key airports are not simply local problems; the effects ripple outward to other airports with flights connecting to these hubs and ultimately to the entire air transportation network [Transportation Research Board, 1988].

To illustrate the magnitude of the capacity restrictions at a typical major airport facility consider the Los Angeles International Airport (LAX). According to the City of Los Angeles Department of Airports, Facilities Planning Bureau, the design capacities of LAX are 147 and 128 aircraft operations per hour under Visual and Instrument Flight Rules (VFR and IFR), respectively [Los Angeles City Department of Airports, 1988]. Due to strict noise abatement procedures this capacity is reduced to 114 operations per hour for both VFR and IFR conditions. Furthermore, during the hours of midnight to 6:30 A.M. the terminal airport capacity

is restricted to 32 operations per hour. This last point has tremendous operational effects on this facility due to its strategic location for transpacific flights. Similar capacity restrictions have been applied to Chicago O'Hare International Airport prompted by a large increase in the number of operational errors at the terminal control center [Aviation Week and Space Technology, 1988].

The capacity of an airport facility is dictated by the critical capacity of the following four components: 1) the airspace, 2) the runway, 3) the taxiway, and 4) the apron-gate component (i.e., assuming a well designed ground access system). Although the interrelations between these four components could be significant for certain airport configurations it has been customary to study in detail each component independently and then select the most restrictive one as that defining the capacity of the facility. Obviously, capacity is also affected by many external factors such as meteorological conditions, airfield configuration, aircraft characteristics, and air traffic control system performance.

The challenge faced by today's system developers is how to increase system capacity without violating present operational norms and degrading system safety. Research and development programs at FAA and NASA are addressing several issues of the airfield problems, foremost of which are the improvement of operational use of runways, provision of efficient flow control, spacing and management of aircraft in the terminal airspace, upgrading of the computer/communication technology usage, and the resolution of the effects of wake vortex and aircraft noise.

Improving the operational use of runways, the reduction of runway occupancy times using high-speed exits is one of the research activities carried by the FAA and NASA. The efficiency of the runway component is dictated primarily by the runway occupancy time (ROT) and its variability from aircraft to aircraft. ROT is the time an aircraft spends on the runway or its vicinity until a new arrival or departure can be processed. Table 1.1 illustrates typical values of ROT and its variablity for several aircraft classes using current and future technologies according to a recent study conducted at the MITRE Corporation [Barrer and Dielh, 1988]. The study quantified the potential increases to runway capacity resulting from improvements to the

Table 1.1 Arrival Runway Occupancy Times (Adapted from Barrer & Dielh, 1988).		
TERP Category	ROT Mean Value (seconds) Present	Future (1996)
A	43	35
B	45	37
C	46	40
D	50	45

Air Traffic Control System (ATC) performance parameters (i.e., reducing in-trail landing separations, better planned runway exits, improved ground-based radar surveillance capability, etc.) and concluded that gains of up to 20% in the capacity of a single runway are possible if these control actions were to be implemented. Other studies support similar gains if advanced systems are used [Lebron, 1987; Simpson et al, 1988]. On the airspace component a critical parameter directly related to capacity is the arrival in-trial separation (AIT). AIT values are dictated by safety criteria to avoid the effects of the wake vortex generated by a leading aircraft during landing. Current and future arrival in-trail separation values taken from the same study are shown in Table 1.2. Values of equivalent arrival in-trail separation have been added to show that even with the projected fixed distance separation standards large in-trail separation times remain for some operational scenarios (i.e., a small aircraft operating behind a heavy heavy jet). Moreover, one must recognize that challenges remain to be solved in terms of the technology available to support some of these control actions. For example, the wake vortex separation criteria envisioned in the MITRE study would necessitate of a completely revised scheme in how aircraft control systems are designed or through sophisticated approach sequences which might not only include curved paths but also real-time advisories of the progress of preceeding landing aircraft. The first point is probably the most debatable since the vortex wake generated by a heavy aircraft requires a significant amount of time to decay to harmless levels and the reduction of the current separation criteria could result in substantial increases in vortex wake penetration [Rossow and Tinglin, 1988].

The second approach seems more promising with the introduction of the microwave landing system (MLS) coupled with area navigation procedures (RNAV) and its well publicized multipath approach capabilities although more flight testing is necessary to validate potential MLS-RNAV procedures for heavy aircraft operations in the "near" terminal control area [Branstetter et al, 1988]. The automation of the future Air Traffic Control (ATC) activities in the terminal control aerea seem to promise a small reduction in the interarrival time and runway occupancy time buffers currently applied under manual control ATC conditions [Swedish , 1979]. If these reductions were to take place in the near future, the runway subsystem could in fact become the '"bottleneck" of the airport system and thus airport capacity could then be dictated by the runway occupancy times achieved during realistic operations. Under the simple assumption of considering an average ROT value in the future, if the 2/4/5 n.m. distance in-trail separation rule were implemented in the future then the average runway occupancy time (ROT) necessary to accomodate this level of arrival rates would be 39 seconds with a 1.4% intervention rate [Swedish, 1979]. According to observations made by Koenig [Koenig, 1978] at six major airports this average is below the 42-51 second average ROT experienced by short/medium size transport-type aircraft and the 51-58 second average ROT observed in heavy jet VFR operations. It is interesting to observe that these averages have not significantly changed for more than a decade suggesting that the current runway subsystem needs to be modified if future gains in average ROT are to be achieved. It seems desirable to investigate high-speed turnoff alternatives that could reduce the present average ROT values by 4 to 10 seconds (i.e., depending upon the operating aircraft mix) to balance the expected future interarrival separation standards with the average runway occupancy times and thus improving runway capacity under mixed operations.

Parallel research studies are currently being conducted to address the air space and runway capacity issues in order to improve the level of service of existing and future facilities. It is important to emphasize that a reduction in the in-trail separation rules will have to be followed by a corresponding reduction in ROT times if significant improvements in the airport capacity are to be achieved. The use of highly advanced avionics coupled with the installation of modern navigation facilities (i.e., microwave landing system, four-dimensional navigation,

etc.) and the strategic location of turnoffs seem to promise some reductions in the in-trail separation, ROT and their corresponding variabilities to warrant changes in runway capacity.

Among the several alternatives to improve airport capacity one being addressed in this research is the use of high-speed turnoffs in airport runways to reduce the aircraft runway occopancy times. It should be clear that although some of the major airport facilities have adopted the 30-degree high-speed FAA turnoff standard and newly proposed spiral designs it seems possible to improve the level of service of a runway facility (i.e., decreasing the runway occupancy time or increasing the runway acceptance rate) by tailoring the turnoff geometry and location to an existing or forecasted population of aircraft. That is the population of aircraft operating in a particular airfield should dictate not only the location but also the characteristic turnoff geometries associated with that runway.

1.1 Previous Turnoff Geometry Research

Past studies by Horonjeff et al [Horonjeff et al, 1958, 1959, and 1960] recognized the critical relationship between turnoff location and turnoff geometry and developed a mathematical model to locate exit taxiways for a limited number of scenarios (i.e., two exit taxiway speeds and a reduced aircraft population). The results of this model concluded that the optimum location of runway turnoffs is quite sensitive to aircraft population, number of exits, and exit speeds. The same model used external atmospheric corrections to modify the baseline results due to meteorological and geographical conditions. However, only two exit speeds (i.e., 40 and 60 mph) and a limited number of aircraft populations were investigated thus making the model of limited use. Furthermore, since the aircraft populations used comprised "old" aircraft by current standards the results need revision. The pioneering effort of the Horonjeff team, however, generated a good amount of information regarding the cornering capabilities of aircraft and also obtained data on several lighting schemes to help pilots negotiate these turnoffs under adverse weather conditions. The Horonjeff team performed extensive experiments to find the acceptable turning radius at a given exit speed. The results suggested

Table 1.2 Arrival In-Trail Separation Criteria.

Lead Aircraft	Current Values (nautical miles) (seconds)			Future Goal (1996) (nautical miles) (seconds)		
	Small	Large	Heavy	Small	Large	Heavy
Small	2.5 82	2.5 64	2.5 60	2.0 65	2.0 51	2.0 48
Large	4.0 131	2.5 64	2.5 60	3.0 98	2.0 51	2.0 48
Heavy	6.0 196	5.0 129	4.0 96	5.0 163	4.0 103	3.0 72

Assumed speeds for three aircraft classes:
Small - 110 knots
Large - 140 knots
Heavy - 150 knots

two centered curves for the turnoff geometry with specifications shown in Table 1.3 and Figure 1.1 [Horonjeff et.al., 1958].

In 1970, FAA (1970, AC 150/5335-1A) made standards of high speed exits, angled exits with 30^0 and 45^0. The new FAA standard employed Horonjeff's suggested ending radius of 1800 feet which equates to an exit speed of 60 MPH. Another standard adopted for smaller aircraft was a 45 degree angle exit with a radius of curvature of 800 ft. which could well serve aircraft exiting at 40 MPH according to Horonjeff's findings. One important missing item from these high speed geometries was the easement or transition curve necessary to provide passenger comfort while executing the initial portion of the turnoff maneuver. Interestingly enough the International Civil Aviation Organization (ICAO) adopted the easement curves as well as the second radius of curvature suggested by the 1958 UC Berkeley team (ICAO, 1977).

Schoen et. al. [Schoen et. al., 1985] investigated the turnoff trajectory of high speed taxiing aircraft in an isolated basis. The resulting shape of the aircraft turnoff was a variable curvature geometry with a continuously decreasing radius of curvature. The end result of this research

Table 1.3 Turnoff Geometry Specification Table.

Velocity (MPH)	R_1 (ft)	L_1 (ft)	R_2 (ft)
40	1724	189	821
54	2936	236	1282
64	3138	283	1846

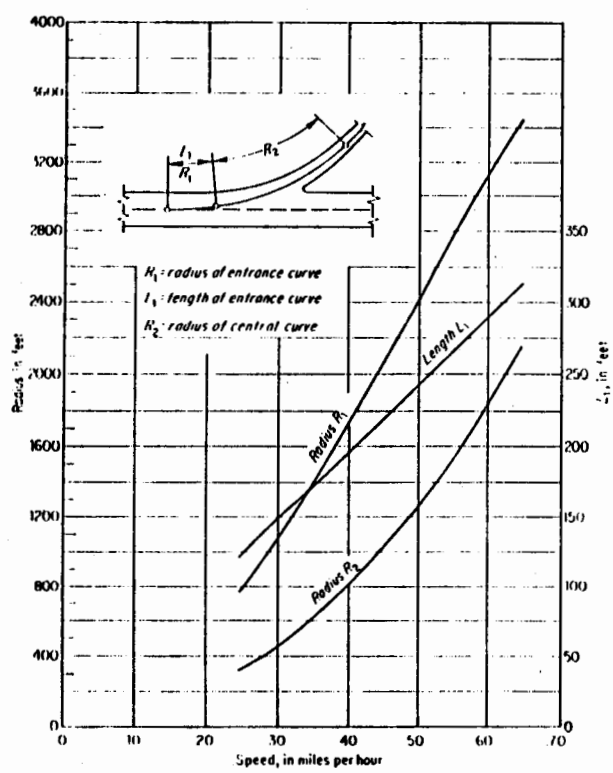

Figure 1.1 Turnoff Geometry Specification Graph [Horonjeff et. al., 1958].

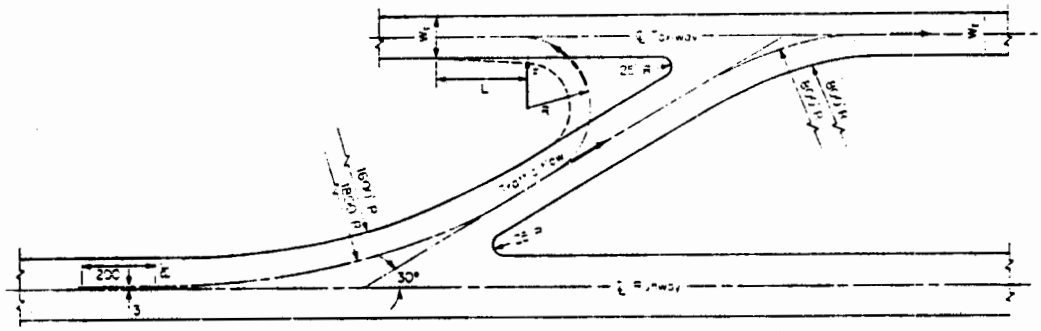

Figure 1.2 30 ° High Speed Turnoff Geometry [FAA, 1970].

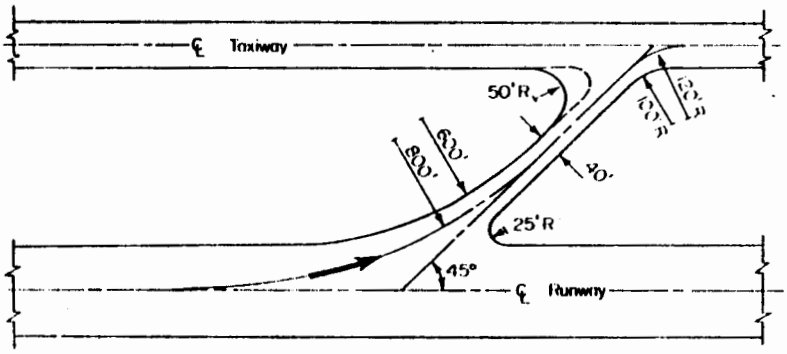

Figure 1.3 45 ° High Speed Turnoff Geometry [FAA, 1970]

was a computer program to calculate the (x, y) coordinates of the geometry, considering exit speed and aircraft turning ability. The findings of this research suggested that aircraft rotational inertia played an important factor in dictating the initial trajectory of the turnoff maneuver. This research also showed that ROT values of 30 seconds are possible at the expense of large turning radius and extremely high exit speeds (e.g., 110 MPH for a Boeing 747). Very high-speed turnoff results should, however, be treated cautiosly since at such high speeds the controllability of aircraft on the ground could become a serious operational deterrent.

The most recent research of turnoff geometry was conducted by Aviation Department staffs of Dade County, Florida (Carr et. al. , 1980, Witteveen, 1987, and Haury, 1987). They tested various types of geometry, lighting, and marking in an L1011 flight simulator. Figure 1.4 is a proposed wide entrance geometry which shows its wider throat than that of a standard FAA high-speed exit geometry. Figure 1.5 shows the difference of the standard geometry and suggested geometry. The shaded area is the standard geometry. The new geometry was implemented in Miami International Airport, Baltimore-Washington International Airport, and Orlando International Airport, and is expected to be constructed in Cincinnati International Airport and the new Denver International Airport [Witteveen, 1987 and Haury, 1987]. The wide entrance throat of this geometry is appealing in situations where lateral spacing restrictions between the runway and the nearest parallel taxiway are severe (i.e., less than 600 ft.). However, the ending radius of curvature of only 800 ft. might be a limiting factor in the operational capabilities of this exit to handle large aircraft above 50 knots in a routine basis. The FAA is currently engaged in evaluating this geometry in the Boeing 727-100 simulator and aircraft.

1.2 Mathematical Models for Optimal Turnoff Locations

The earliest effort to make a model for the optimal runway exit locating problem is also found in the pioneering work of Robert Horonjeff [Horonjeff et. al., 1959, 1960]. The objective

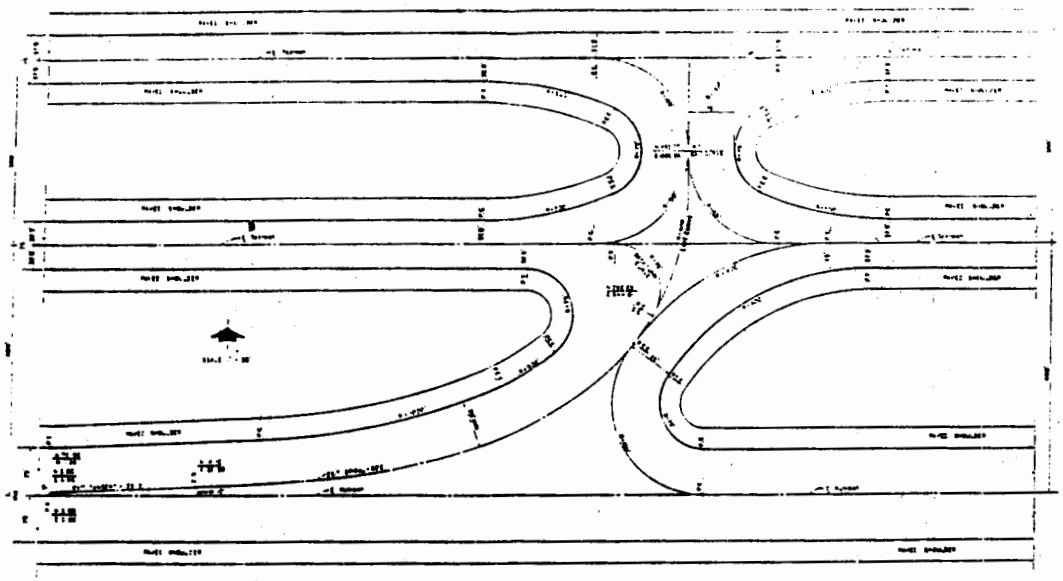

Figure 1.4 A Modified High-Speed Turnoff Geometry [Witteveen, 1987].

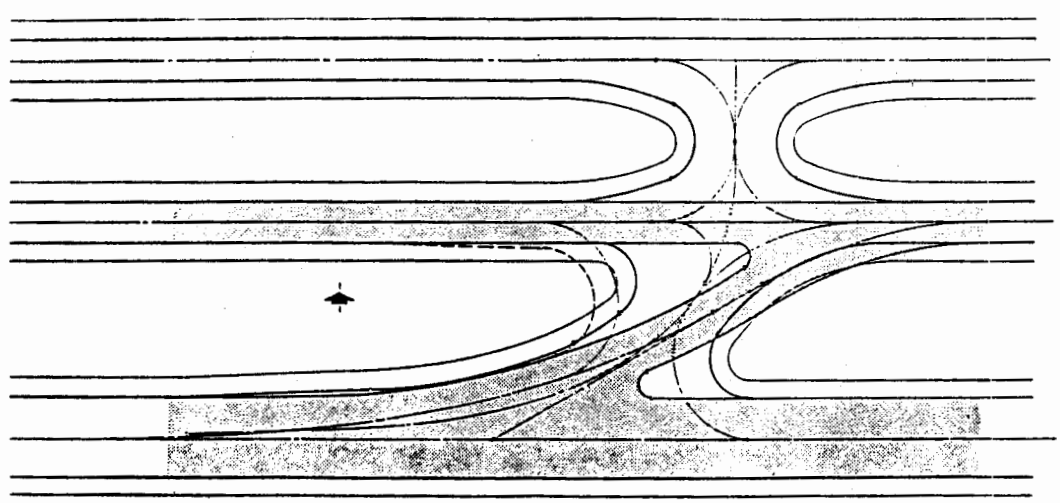

Figure 1.5 Standard and Modified Turnoff Geometries [Witteveen, 1987].

of their model was to find exit locations that maximize the landing acceptance rate of a runway in the saturated situation, assuming the aircraft arrival pattern followed a fixed time or fixed distance separation criterion. The saturated situation means that aircraft try to land continuously with a separation rule. The acceptance rate is determined by :

$$E(A_c) = \frac{1}{E(\delta)} \cdot \frac{1}{(1+q)} \qquad \{1.1\}$$

where,

$E(A_c)$ = the expected acceptance rate (aircraft/hr),
$E(\delta)$ = the expected interarrival time (hr/aircraft),
q = weighted average of 'wave off' probabilities.

Wave off occurs if the previous aircraft remains on the runway when the next aircraft reaches the runway threshold. The expected acceptance rate can be maximized by minimizing the weighted average of wave off probabilities which expressed by :

$$q = \sum_{i}^{n} p_i \cdot q_i \qquad \{1.2\}$$

where,

p_i = the proportion of aircraft type i,
q_i = the wave off probability of aircraft type i,
n = the number of aircraft types.

p_i should be provided to the model, and q_i is calculated by :

$$q_i = \Pr\{T_i > \delta\} \qquad \{1.3\}$$

where,

T_i = runway occupancy time of aircraft type i.

Since T_i is a function of exit locations ($D_1, D_2, \cdots, D_m$), q can be expressed as a function of exit locations, and thus, by calculus, the optimal exit locations, which minimize q, are found. The equation for T_i involves bivariate random variables, (d_i, t_i) which are the mean distance and time for aircraft of type i to decelerate to the predetermined exit speed, respectively. The differential equations for optimal exit locations are not simple, and can not be solved analytically. Hence, finding the optimal locations requires a numerical computation algorithm which consumes a lot of computation time.

The joint distributions of (d_i, t_i) of every aircraft type are another input data for the model. The values of d_i and t_i vary according to the operational factors such as the design exit speed and the landing weight, and environmental factors such as runway surface conditions, altitude of airport, and temperature, even though we consider only one aircraft type. Hence the parameters of the joint distribution of d_i and t_i should be estimated again if an influencing factor is changed thus posing a great computational and labor intensive challenge.

In 1974, Daellenbach [1974] developed a dynamic programming model which is equivalent to the Horonjeff's approach with some extensions. Horonjeff's model imposes a strict assumption on the aircraft arrival pattern. Daellenbach released the assumption, and permitted a generalized arrival pattern. He showed his model to be more efficient computationally and more flexible for modelling than Horonjeff's model. Daellenbach's model, however, also requires the joint distributions of (d_i, t_i) as input. The data for estimating the parameters of the joint distributions are difficult to collect and almost impossible when the influencing factors vary.

In the same year, Joline [1974] developed another dynamic programming model to find the optimal number of exits and their locations with respect to the combined objective function of ROT and exit construction cost. He incorporated the ROT gain and the exit construction cost into an objective function by equating 1 second gain in ROT with $100,000 in construction cost. While Horonjeff's model and Daellenbach's model require the joint distributions of (d_i, t_i) for each aircraft type, Joline's model needs only an univariate distribution of 'ideal exit location' for a mixed aircraft population. Joline classified aircraft into three categories based on the aircraft size, and found the distributions of ideal exit locations for these three aircraft classes based on the observations of aircraft landing operations in Chicago O'Hare Airport. The ideal exit location distribution for entire aircraft population is found by combining the three distributions according to the proportions of the three aircraft classes. As mentioned earlier, there are several factors influencing the aircraft landing distance such as the design exit speed, landing weight, etc.. Joline's model, like the previous models, makes the effects of these influencing factors hard to incorporate.

ROT consists of the time from the runway threshold to the exit location and the time from the beginning of the turn to the clearance of the runway. The second term obviously varies according to the turnoff trajectory and its magnitude varies according to the desired turnoff exit angle. None of three models above, however, takes into account the ROT variation due to the change of the turnoff trajectory. The turnoff trajectory also varies according to design exit speed, aircraft turning ability, runway surface conditions, etc.. Therefore an attempt is made in this report to bridge the gap between practical and theoretical models.

The three models above implicitly assume that an aircraft type can use more than one exit for turnoff with different ROT and exiting probability. If we want to decide separation times between the landing aircraft based on the ROT of the aircraft, it is desirable to assign an aircraft to an exit with high exiting probability, say 99%. Thereby the variation of ROT of an aircraft can be reduced. This situation is expected to occur in the near future with an improvements to aircraft traffic control (ATC) systems and better crew situational awareness provided by enhanced on-board ground navigation avionic systems. The purpose of this new research effort is to develop a more general model that will be able to predict that location of runway turnoffs in a myriad of scenarios are where changes to the aircraft population and airfield conditions can be easily defined by the user thus making it possible to be used under practical airport conditions.

1.3 Approach and Scope of the UCTR/VPI Research

The University Center for Transportation Research (UCTR) at Virginia Tech University (VPI & SU) has been asked by the FAA and NASA Langley to investigate the feasibility of implementing high-speed turnoffs at major airports to reduce the runway occupancy times. The goal of this research project is to develop a user-friendly computer simulation model to estimate the optimal location of high-speed turnoffs at an airport facility in order to reduce the runway occupancy time (ROT). The model incorporates environmental factors such as airfield elevation, runway configuration, weather conditions, etc. and operational factors such as

aircraft mix (i.e., terminal operation aircraft types) and aircraft piloting technique (i.e., aircraft touchdown speed dispersion values) to determine the potential location of high-speed turnoffs. Factors that in past studies either have been neglected or treated as externalities to the models.

A problem scenario addressed in this research can be better understood with the help of Fig. 1.6 which depicts a histogram of landing distances for a typical airport facility. It is observed that a grouping phenomena of the potential location of the runway turnoffs takes place at discrete distances from the active runway threshold as each aircraft type has unique landing rollout performance characteristics coupled with some inherent variability due to dissimilar piloting techniques. The point to be stressed here is that by **carefully** locating the runway turnoffs one could, at least in principle, reduce the ROT time for a given aircraft population and airfield conditions below a desired level (e.g., 40 seconds). Fig. 1.7 shows an example of projected turnoff locations for a hypothetical runway.

A second argument to this already complex problem is the fact that due to the unique landing characteristics of each aircraft it is also possible to determine the most efficient turnoff geometry for the same aircraft population. Fig. 1.8 depicts five different turnoff geometries for dissimilar aircraft representative of the existing Terminal Instrument Procedure categories (TERPS) using a probabilistic model developed by the McDonnell Douglas Corporation for NASA [Schoen et. al., 1985]. These results consider the aircraft landing gear friction characteristics to be the **only** source of aircraft directional control on the ground, an approximation well suited for medium to slow landing rollout speeds (e.g., 30-60 knots) where the aerodynamic efficiency of the aircraft primary control surfaces is negligible. However, the model is very restrictive as it only optimizes the geometry of a turnoff for a single aircraft with no consideration for specific environmental nor operational factors of the airfield. Again, the issue of considering the aircraft mix as part of the solution of the problem arises when one considers that the selection of a critical aircraft might not warrant the overall "best" alternative if that critical aircraft seldom operates the facility. In other words, if an optimal location is sought for a large population of aircraft it might be desirable to penalize the critical aircraft in terms of their ROT parameter if the rest of the population is large and can be

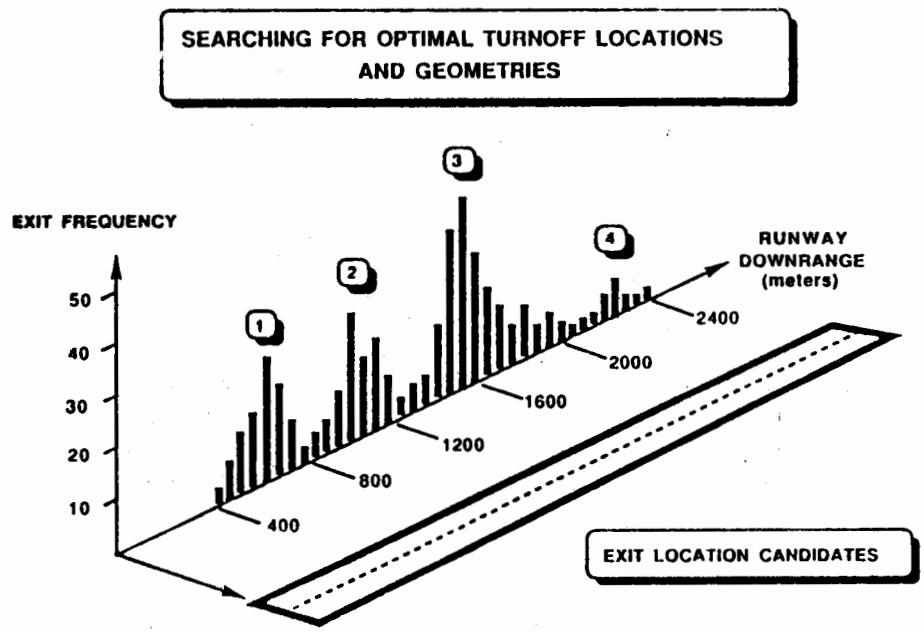

Figure 1.6 Hypothetical Aircraft Landing Distance Distribution.

accommodated in a particular geometry that reduces the overall ROT (i.e., average ROT) of the facility in question. This clearly demonstrates that an optimal solution must heavily depend upon the aircraft population mix operating in the airport environment.

From this last point an interesting question emerges regarding the applicability of an "optimal" design for current and future conditions. One might say that if a runway is at the planning stage, the planner should attempt to forecast the future aircraft population of its environment with the aid of airlines and aviation authorities, while if only improvements are sought (i.e., the runway is already in place) the use of a current aircraft population constitutes a better choice. The bottom line seems to be that the model should be flexible enough to allow the analyst to execute environmental and operational changes with a minimum of effort.

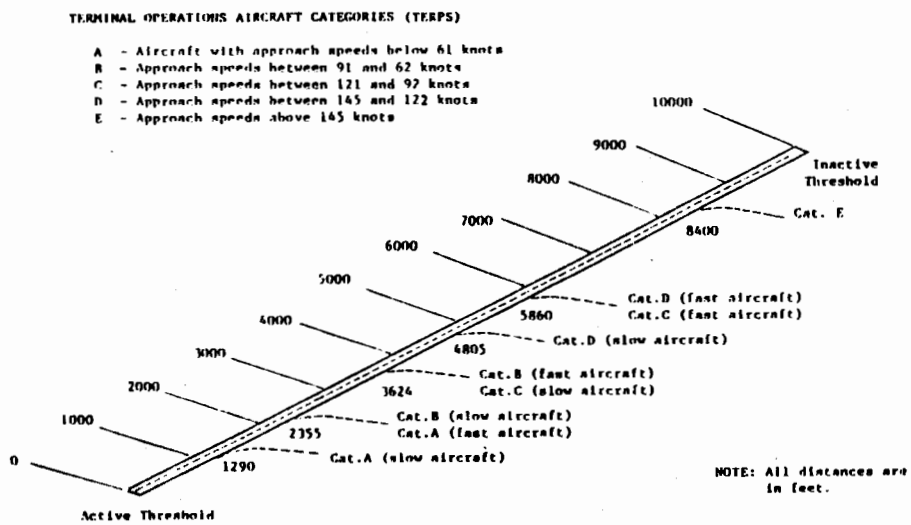

Figure 1.7 Typical Projected Turnoff Locations for a Hypothetical Runway.

The scope of the model should be viewed not as an isolated effort to address all the problems regarding runway operations, but as a novel approach to solve some of the imposed demands generated with the growth of air traffic operations and the need for using the airport infrastructure available more efficiently. The effort presented here should be integrated and coordinated with future and present complementary efforts. The main emphasis from the user's point of view will be in the general aviation area but the model avoids preferences towards a selected group of aircraft and can be expanded to suit any operating aircraft mix.

The model, once developed, should be extended and integrated to the airport capacity analysis level. At this stage the **interactions** between runway, taxiway , and apron should be studied to perceive potential problems of **integrating** variable geometry turnoffs in the airfield

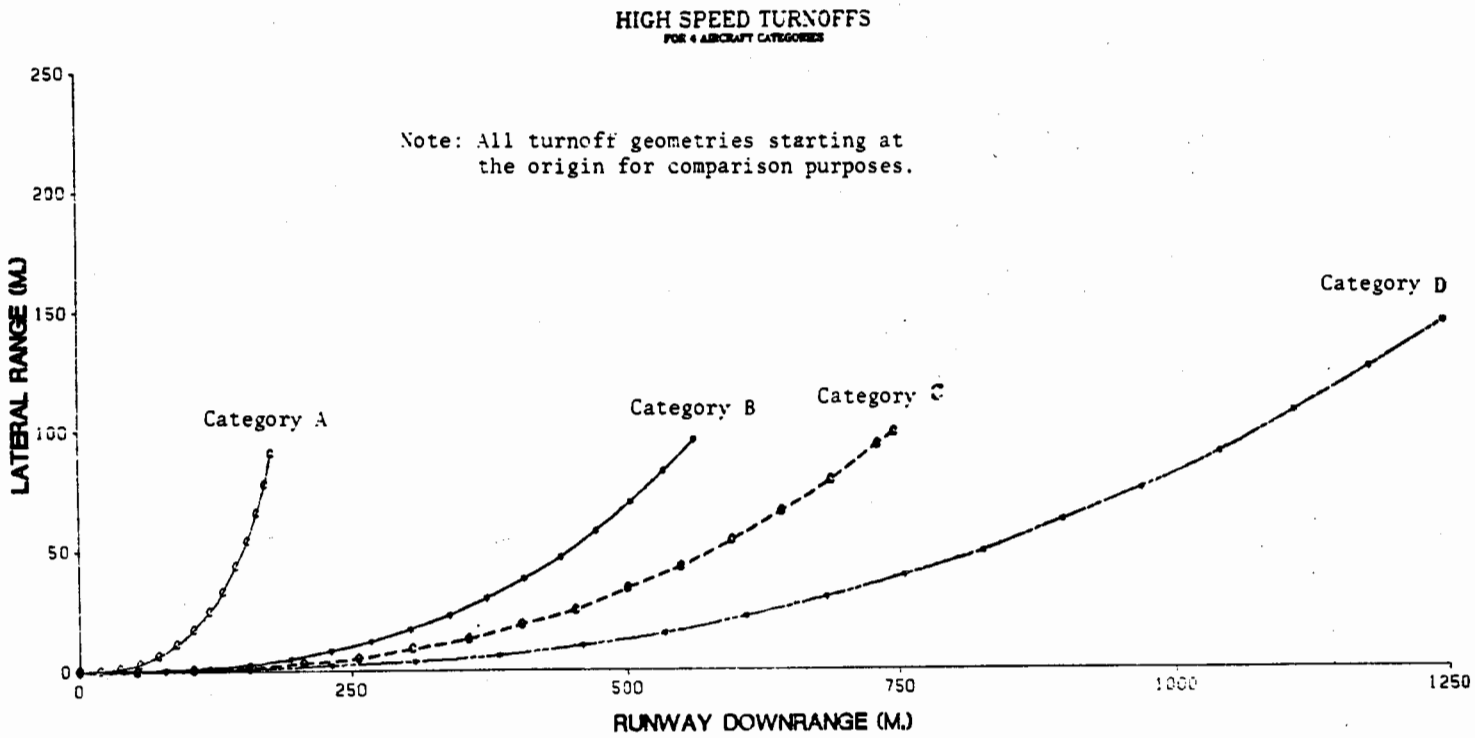

Figure 1.8 Sample Turnoff Geometries for Different Aircraft Categories.

environment. Following the implications of these results a **cost effectiveness analysis** would have to be performed in order to perceive the gains in ROT time translated into benefits to the user, and operators. Finally, the results will have to be **tested** for pilot's acceptance in terms of procedures and workload. These studies could be carried out in flight simulators and the aircraft themselves.

1.4 Model Overview

The Runway Exit Design Interactive Model (REDIM) developed in this research effort, incorporates several specific airfield variables that affect the landing performance of the aircraft as well as other important operational constraints (e.g., aircraft mix) that have a direct impact on the selection of the turnoff location and their geometry. A simplified flow diagram of the model proposed is shown in Fig. 1.9. It can be seen that five modules comprise the program: 1) an **Input module** , 2) a **dynamic simulation** module to estimate the ROT times for individual aircraft, 3) a **selection/optimization algorithm** to determine candidate turnoff locations to comply with a desired reliability threshold value and 4) an **aircraft data module** containing relevant aircraft performance and geometric parameters (also named master file in this research and 5) an **output module** to shown graphically and in tabular form the suggested runway turnoff configuration and display some measures of effectiveness desired by the analyst. Fig. 1.10 shows a typical sequence of events occuring during the flare transition and landing rollout that will be modeled explicitly in the dynamic portion of this program. The program contains a library of geometric and operational aircraft characteristics to allow the analyst to choose from a wide selection of operational airport scenarios. Obviously, the user is also capable of editing his/her own aircraft data if desired through simple steps in the input module.

The program considers three broad types of analyses: 1) evaluation of an existing runway, 2) redesign of an existing runway and 3) design of a new runway facility. In the evaluation mode REDIM estimates several measures of effectiveness indicative of the operational

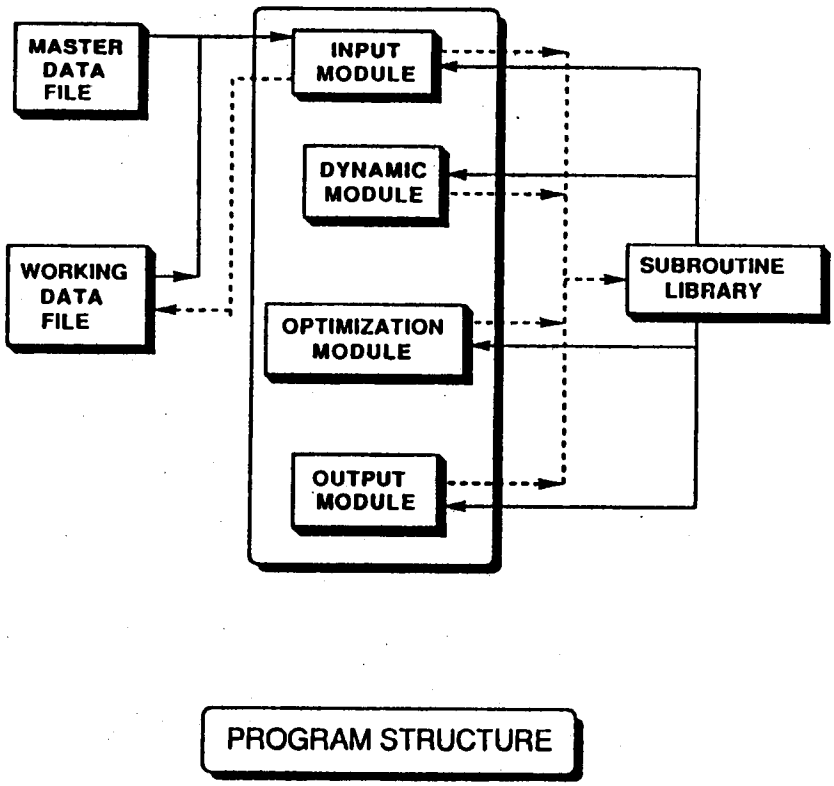

Figure 1.9 Model Flowchart Organization.

capabilities of an existing runway facility. In this mode the user inputs the number, type and location of existing turnoffs as well as the relevant aircraft population data and the model predicts the average runway occupancy time (WAROT), the particular exit(s) that an aircraft can take , and the probability of each aircraft i taking the assigned exit(s). Another potential use of this mode is to serve as a benchmark to perform valid comparisons between different runway proposals. This way the analyst can perceive the operational gains of various modification alternatives.

The second mode of operation deals with the redesign of a runway facility. In this scenario it is expected that the user might want to explore the possibility of adding new high-speed turnoffs to an existing facility and examine their impact in the operational efficiency of the

facility. Inputs in this mode are the number and type of existing turnoffs, their locations, the number of new turnoffs to be constructed and a reliability parameter. The outputs are the location and geometry of each new turnoff, the weighted average runway occupancy time, and an aircraft assignment table containing individual runway occupancy times for the desired reliability factor specified by the user.

In the third mode of operation REDIM estimates the optimal location of runway turnoffs and their corresponding geometries. An assignment table is given to the user indicating the turnoff(s) associated with each aircraft and their individual runway occupancy times. The weighted average runway occupancy time is also estimated as a global runway operational parameter and sensitivity studies can be easily be conducted by changing the number of turnoffs allocated to a specific runway. Inputs by the user in this mode are the number of exits to be constructed and the desired exit reliability parameter. More detailed descriptions of these three modes of operation will be given in the remaining chapters of this report.

REDIM blends the principles of continuous simulation with those of mathematical optimization to find the best turnoff locations and corresponding turnoff geometries for a myriad of possibilities. The program was designed to be interactive and a great effort was made to reduce the number of inputs expected from the user. A large aircraft data base is included to simplify the analyst input task but flexibility is also built-in to allow future aircraft additions. The overall effort was to make the program interactive and easy to use. Interactive input and output menus are easy to follow providing the user with graphic results on the screen or a regular line printer.

AIRCRAFT LANDING PHASES MODELED

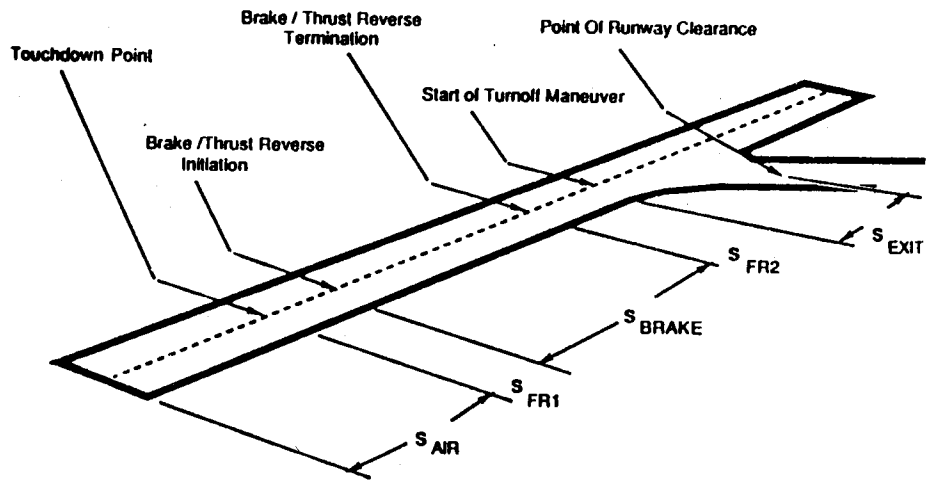

LEGEND

S_{AIR} = Air Distance to Touchdown

S_{FR1} = Free Roll Distance Between Touchdown Point and Application of Brakes / Thrust Reverse

S_{Brake} = Braking Distance

S_{FR2} = Free Roll Distance Between Brake / Thrust Reverse Termination and Exit Point

S_{EXIT} = Longitudal Distance Required to Clear the Runway from Exit Point

FUNCTIONAL FORM OF AIR AND GROUND DISTANCES

S_{AIR} = f (Aircraft Approach and Touchdown Speeds, Flight Path Angle, Threshold Height)

S_{FR1} = f (T_{FR1} , Time Delay to Applied Brakes and Thrust Reversers)

S_{Brake} = f (Runway Friction Parameters, Braking Power, Runway Gradient, Thrust Reverse Aircraft Weight)

S_{FR2} = f (T_{FR2} , Time Delay to Terminate Brake / Thrust Reverse Action)

S_{EXIT} = f (Exit Speed, Aircraft Yaw Inertia, Aircraft Weight, Lateral Comfort Factors, Tire Side Loads)

Figure 1.10 Aircraft Landing Events Modeled in the Analysis.

2.0 Input Module

The Input Module comprises a series of interactive screens that allow the user to input and edit data necessary for the analysis portion of the program (i.e., Dynamic and Optimization Modules). This module is controlled by menus or key-stroke commands such as "Esc" key. A flow chart depicting the sequence of events comprising the Input Module is shown in Fig. 2.1. As can be observed, the "Main Menu" placed at the top level of the flow chart has seven modes: 1) "Start for a New Problem," 2) "Edit Data," 3) "Begin Analysis," 4) "Edit Master File," 5) "Go To Output Module," 6) "Help" and 7) "Quit." The details of these modes are given in Section 2.4 and shown schematically in Fig. 2.1.

Input Data is classified into six broad categories: 1) analysis type and related data, 2) aircraft mix and characteristics data, 3) airport operational data, 4) airport environmental data, 5) runway gradients, and 6) weather and exit speeds. All of these are necessary for the analysis, and should be saved in a 'working data file' specified by the user with an arbitrary name. For the convenience of the user, all the aircraft characteristics are kept in a master data file named "MAST.DAT" and are transferred to a working data file automatically if necessary.

2.1 Data Classification

There are three kinds of data for analysis: 1) input data, 2) constant data, and 3) calculated data. Among these kinds of data, constant data and calculated data are determined in the Dynamic Module detailed in the next Chapter. Input data is provided by the user via the Input Module and its user-friendly screens. The input data is classified into six categories as mentioned previously. The following paragraphs define the categories in more detail.

Analysis Type and Related Data

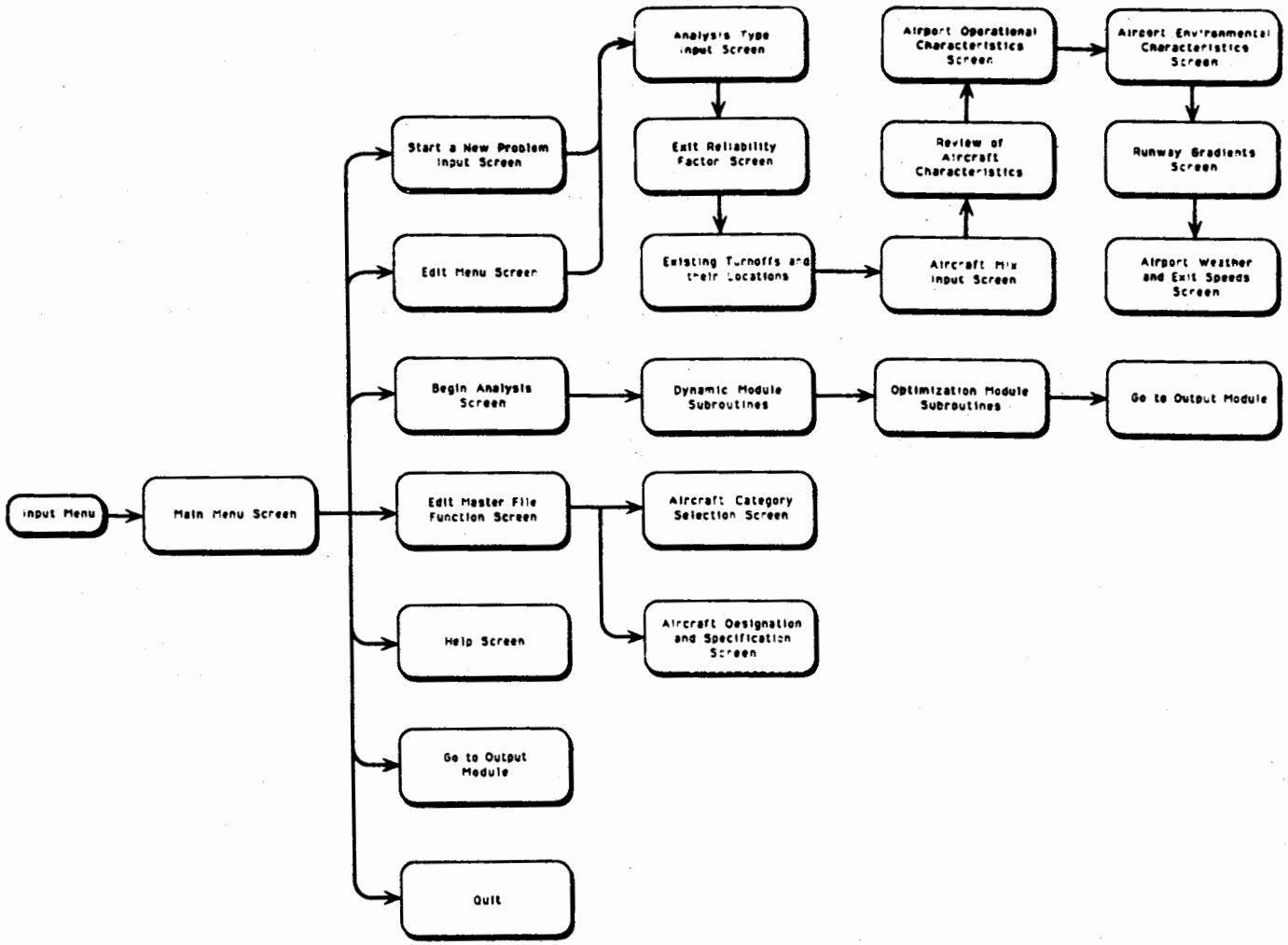

Figure 2.1 Input Module Functional Flow Chart.

The program provides the user with three choices for the type of analysis to be performed. For each type of analysis, there are some accompanying data which vary depending on the user's choice. A more detailed explanation of this is provided in Section 2.2 devoted to Input / Output relationships.

Aircraft Mix and Characteristics Data

In this category, the percentages of the aircraft comprising the airport population mix and aircraft geometric characteristics used in the program are included.

Airport Operational Data

In this category, the free roll time between the touchdown and the beginning of braking, the free roll time between the end of braking and the beginning of turn off, taxiing speed, and their standard deviations are included. A safety factor for the impending skidding condition is also part of this screen.

Airport Environmental Data

The following parameters are included in this category: wind speed, wind direction, airport elevation, airport temperature, runway orientation, visual range, runway width, and distance to the nearest taxiway.

Runway Gradient

In this category, runway length, and the effective gradient for every one tenth of runway are included.

Weather and Exit Speeds

The relative frequency of dry and wet runway surface conditions are included in this category. The desired exit speeds of each aircraft category on each surface condition are also included here.

2.2 Input/Output Relationship

As stated earlier, the user can select one of three types of analysis : 1) evaluation of an existing runway system, 2) improvement of an existing runway system, and 3) design of a new runway system.

The 'evaluation' option requires 1) the reliability parameter, 2) the number of existing exits, and 3) the types of existing exits as input data. This produces as output 1) the aircraft distribution to the existing exits with the corresponding ROT and cumulative exiting probabilities and 2) the weighted average ROT as results of analysis. When the average ROT is calculated for all the aircraft population, only one ROT is considered for each aircraft. For example, if aircraft i is able to take exit k and k+1 whose corresponding ROT's and cumulative probabilities are t_k, t_{k+1}, and $p_k p_{k+1}$, respectively. If p_k is less than the reliability specified by the user, and p_{k+1} is greater than the desired reliability, then only t_{k+1} is considered as the representative ROT for aircraft i.

The 'improvement' option assumes that a few exits would be added to an existing runway. This analysis requires 1) the reliability parameter, 2) the number of existing exits, 3) the types of existing exits, and 4) the number of new exits which will be constructed. The results are 1) optimal exit locations, 2) aircraft assignment to the existing and new exits, 3) the weighted average ROT which is minimized by the optimal exit locations, and 4) turnoff geometries of the exits.

The 'design' option assumes a hypothetical situation with no exits on the runway. The reliability parameter and the number of new exits are inputs for this type of analysis. The results are similar in nature to those of the 'improvement' option with the only difference being is that this new option takes into account the new exits for aircraft assignment, while the 'improvement' option considers both new and existing exits. I/O relationships for each analysis type are shown in Figs. 2.2 to 2.4.

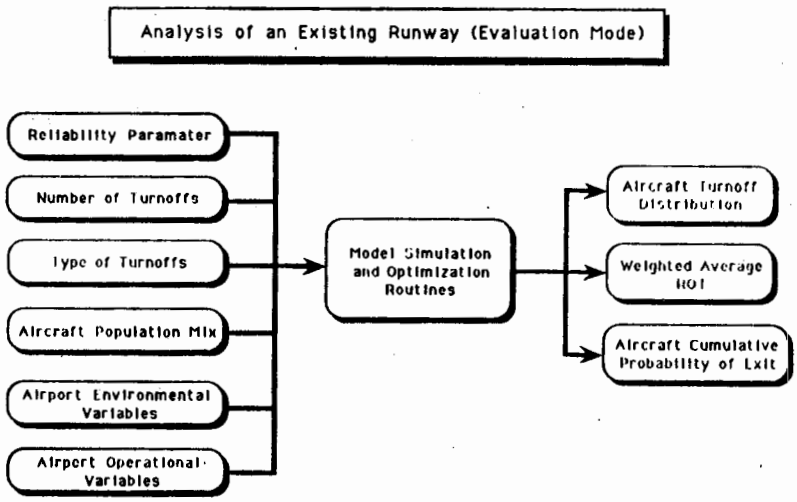

Figure 2.2 I/O Relationship for 'Evaluation' Analysis.

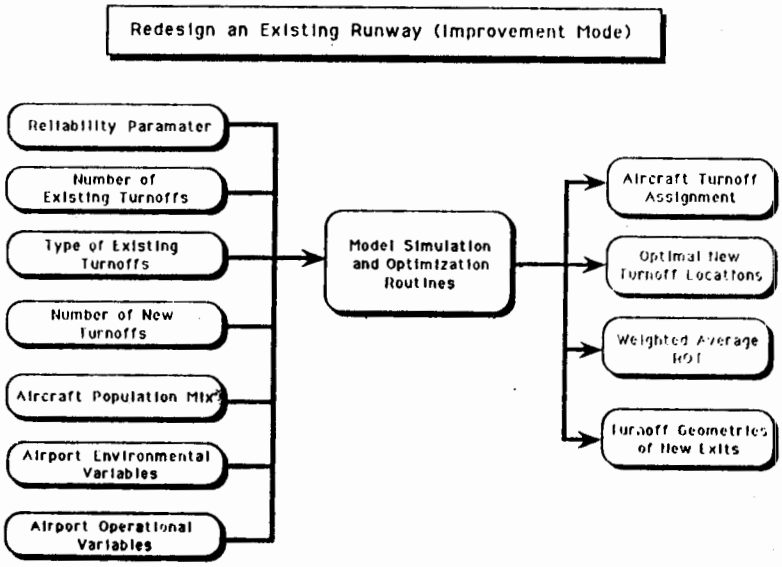

Figure 2.3 I/O Relationship for 'Improvement' Analysis.

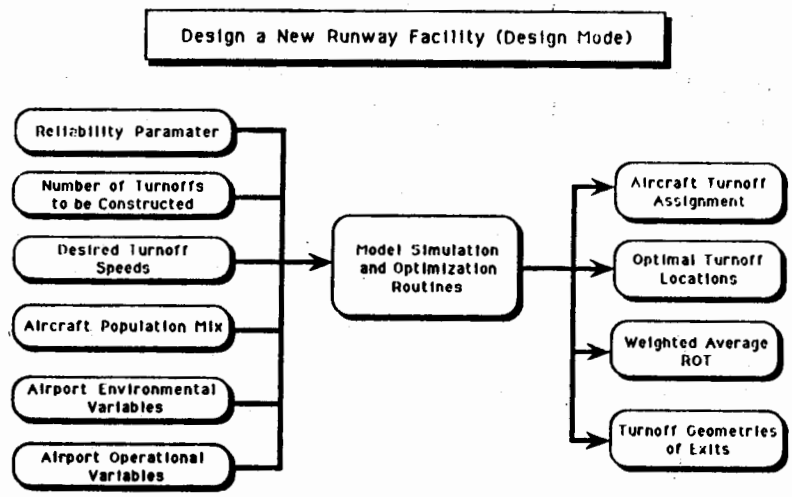

Figure 2.4 I/O Relationship for "Design' Analysis.

2.3 *Data Input Method*

In the Input Module, there are three different input methods used: 1) menu input, 2) line input, and 3) table input. Menu input arises when the user selects his choice among the list displayed on the screen using the arrow keys and enter key. The flow in the module is controlled by the menu input method. The main menu, edit menu for working data file, edit menu for master data file, selection of a analysis type, etc. are the examples of the menu input method. Line input occurs when the user puts a numerical value like runway length or a string datum like a data file name at the position specified on a screen. The user inputs file names (data and/or output file), the number of exits, the locations of exits, etc. using this method. Table input is similar to line input. However, table input is used in order to get several numerical data on the same screen, while line input is used in order to get one numerical or

string datum on a line. By the table input method the user inputs aircraft mix data, aircraft characteristics data, airport environmental data, etc.

2.4 *Procedures in Input Module*

The first screen presented to the user after the title screen is the main menu. The main menu screen gives the user a list of seven choices: 1) Start a New Problem, 2) Edit Data, 3) Begin Analysis, 4) Edit Master File, 5) Go to Output Module, 6) Help, and 7) Quit as shown in the Fig. 2.5. The functions of choices 3), 5), and 7) are used to transfer the flow control to other program modules. The purpose of choice 6) is to give a brief explanation of the screen choices to the user. Choices 1,2 and 4 invoke the procedures belonging to the Input Module.

2.4.1 Starting a New Problem

In this mode, all the data necessary for the analysis should be provided by the user. Once the user enters this mode a complete set of values is expected before completing the entire input process. The first set of data which the user needs to specify is "Analysis Type and Related Data" (refer to the Section 2.1). The type of analysis is selected through the menu input method. Fig. 2.6 shows the screen for analysis type selection, which is followed by the related data screen which might vary depending upon the analysis type selected. Fig. 2.7 is an example of such a screen. The second set of the data is "Aircraft Mix and Characteristics." The aircraft mix screen shows the names of the aircraft whose characteristics are included in master data file in table form as shown in Fig. 2.8. The user inputs the percentages of the aircraft which comprise the aircraft population, expected to operate at the runway facility.

Following the aircraft mix screen, several aircraft characteristics screens for each aircraft selected in the mix screen are displayed as shown in Fig. 2.9. All the values shown in this screen are transferred from the master data file. If the user does not want to change the

```
MAIN MENU

Use arrow (↑ or ↓) key to change your choice.
Press enter ( ↵ ) key if the choice is correct.

[illegible]

2)Edit Data

3)Begin Analysis

4)Edit Master File

5)Go To Output Module

6)Help

7)Quit
```

Figure 2.5 Main Menu Screen.

```
SELECT
Analysis
Type

Press escape (Esc) key to return to MAIN MENU.

Use arrow (↑ or ↓) key to change your choice.
Press enter ( ↵ ) key if the choice is correct.

[illegible]

2) Improve an Existing Runway

3) Design a New Runway
```

Figure 2.6 Analysis Type Menu.

values, he/she would press "Esc" key to proceed to the next step which might be another aircraft characteristics screen or airport environmental data screen.

The screens for "Airport Environmental Data" and the "Airport Operational Data" follow the "Aircraft Mix and Characteristics Data" screen. These screens having similar table formats are shown in Figs 2.10 and 2.11. The next screen deals with "Runway Gradients." At this point, the user specifies the runway length with the line input method, and inputs the gradients for every one tenth section of the runway using the table input method as depicted in Fig. 2.12. The final screen in "Start a New Problem" mode is designed for "Weather and Exit Speeds." On this screen, the relative frequencies of occurence for dry and wet conditions are specified. Also, the desired exit speeds of every aircraft category under each weather condition are selected by the table input method, as shown in Fig. 2.13.

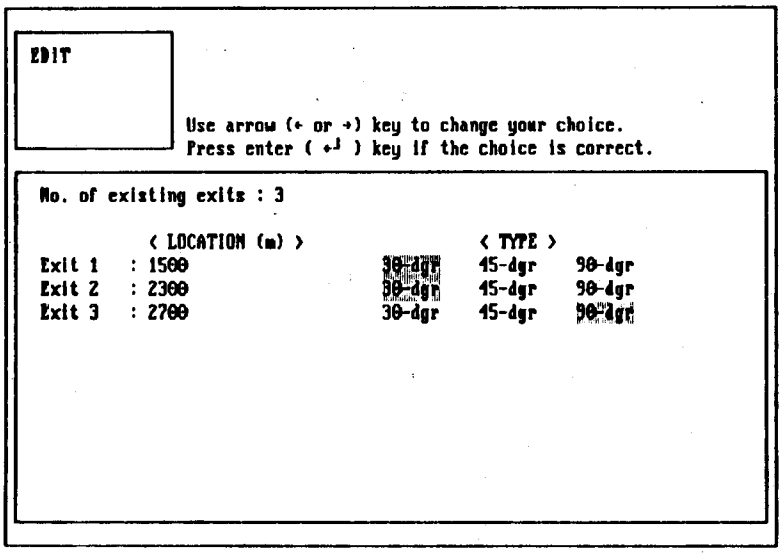

Figure 2.7 Data Related to the Type of Analysis.

```
EDIT                Press escape (Esc) key to proceed to next step.

Aircraft            Press enter ( ↵ ) key to store data.
Mix (%)             Press backspace ( ←B ) key to correct data.
                    Press arrow (←,→,↑, or ↓) key to move cursor.

TERPS A        TERPS B        TERPS C        TERPS D        TERPS E

PA-28-112 :0   BE-58     :0   A-300-600 :30  B-747-200B:0
PA-28-161 :0   BE-300    :0   A-310-300 :0   B-747-400 :0
PA-28-236 :0   CE-402C   :0   A-320-200 :0   DC-10-30  :0
PA-32-301 :0   SAAB-340  :0   B-767-300 :40  MD-11     :0
CE-172    :0   EMB-120   :0   FOKKER-100:0
BAC-733A  :0   SA-227    :0   BAe-146   :0
CE-208    :0   BE-2000   :0   B-727-200 :0
PA-46-310P:0   CE-421    :0   B-737-200 :0
CE-182    :0   CE-T406   :0   B-737-300 :0
CE-210P   :0   FA-34-200T:0   B-737-400 :0
               FA-42-1000:0   MD-83     :0
               F100      :0   MD-87     :0
               CE-550    :0   B-737-200 :0
               CE-560    :0   LEARJET-55:0
               LEARJET-31:30  G1159C    :0
               BE-400    :0   BAe-125-80:0
               FA-1125   :0   IA-1124A  :0
               BA-146    :0   CL-601-3A :0
               BA-146    :0
               BA-146    :0
```

Figure 2.8 Aircraft Mix Data Screen.

```
EDIT                Press escape (Esc) key to proceed to next step.

LEARJET-31          Press enter ( ↵ ) key to store data.
Char. Data          Press backspace ( ←B ) key to correct data.
                    Press arrow (←,→,↑, or ↓) key to move cursor.

A/C Wheelbase          (m): 6.15        A/C Wheeltrack       (m): 2.51
A/C % Load on Mains    (%): 93.42       A/C Landing Mass    (Kg): 6940
A/C Landing Distance   (m): 883.00      A/C Maximum CL          : 2.4130
A/C Wing Area       (M**2): 24.57       A/C Wing Span        (m): 13.34
A/C N.Gear to W.Tip    (m): 7.26

 Above data are transfered from MASTER FILE.
```

Figure 2.9 Aircraft Characteristics Data Screen.

2.4.2 Editing Aircraft Data

This portion of the program allows the user to modify existing data files. If user selects "2) Edit Data" mode at the main menu, the edit menu, which shows six groups of data, is displayed. In the "Edit Data" mode the user can select the group of data which he/she wants to change, while in the "Start a New Problem" mode the user should input all the data sequentially. The details for editing data are the same as in the "Start a New Problem" mode. Fig. 2.14 shows the edit menu.

2.4.3 Editing the Master File

While the function of "Edit Data" mode is editing the working data file, the function of "Edit Master File" is editing the master data file which keeps the aircraft names and their geometric characteristics. If "Edit Master File" mode is selected, the edit menu for master data file appears. In this menu, there are two choices: 1) "Add a New Aircraft" and 2) "Change some Specific Data." If the user chooses the first, he/she has to select one out of five aircraft categories (TERPS A-E) and input the new aircraft name. Then a screen for editing aircraft characteristics appears. If the user opts for the second choice, he/she has to select one aircraft category and one aircraft name included in the category selected. Then a screen for editing aircraft characteristics appears. Figs. 2.15 and 2.16 show the edit menu for master data file and the screen for adding a new aircraft, respectively.

```
EDIT                Press escape (Esc) key to return to EDIT MENU.

Airport             Press enter ( ↵ ) key to store data.
Env. Data           Press backspace ( ←B ) key to correct data.
                    Press arrow (←,→,↑, or ↓) key to move cursor.

Wind Speed      (m/s) : 0                 Wind Direction        : 0
A/P  Elevation    (m) : 500               A/P  Temperature (C) : 15
R/W  Visual Range (m): 1500               R/W  Orientation      : 0
R/W  Width        (m) : 50                Dist. to Taxiway (m) : 300
```

Figure 2.10 Airport Environmental Data Menu.

```
EDIT                Press escape (Esc) key to return to EDIT MENU.

Airport             Press enter ( ↵ ) key to store data.
Oper. Data          Press backspace ( ←B ) key to correct data.
                    Press arrow (←,→,↑, or ↓) key to move cursor.

                          AVERAGE                      STD. DEV.
Free Roll Time 1 (sec)   : 2                           .5
Free Roll Time 2 (sec)   : 1                           .2
Taxiing Speed    (m/s)   : 8                           1
Safety Fac. for Skid  (%): 50
```

Figure 2.11 Airport Operational Data Menu.

```
EDIT                Press escape (Esc) key to proceed to next step.

Gradients &         Press enter ( ↵ ) key to store data.
Friction            Press backspace ( ←B ) key to correct data.
                    Press arrow (←,→,↑, or ↓) key to move cursor.

R/W LENGTH    (m)  :  3000

GRADIENT      (%)
     0    TO  300   : 0                    300  TO  600   : 0
     600  TO  900   : 0                    900  TO  1200  : 0
     1200 TO  1500  : 0                    1500 TO  1800  : 0
     1800 TO  2100  : 0                    2100 TO  2400  : 0
     2400 TO  2700  : 0                    2700 TO  3000  : 0
```

Figure 2.12 Runway Gradients and Friction Conditions Screen.

```
EDIT                Press escape (Esc) key to return to EDIT MENU.

Weather &           Press enter ( ↵ ) key to store data.
Exit Spd            Press backspace ( ←B ) key to correct data.
                    Press arrow (←,→,↑, or ↓) key to move cursor.

                              DRY                          WET

   Percentage          (%) :  80                           20
TERPS A exit speed (m/s) :  20                           20
TERPS B exit speed (m/s) :  25                           25
TERPS C exit speed (m/s) :  30                           30
TERPS D exit speed (m/s) :  30                           30
TERPS E exit speed (m/s) :
```

Figure 2.13 Screen for Weather and Exit Speeds.

```
EDIT MENU                Press escape (Esc) key to return to MAIN MENU.

Data
File                     Use arrow (↑ or ↓) key to change your choice.
                         Press enter ( ↵ ) key if the choice is correct.

                    1)Airport Type & Related Data

                    2)Aircraft Mix & Characteristics Data

                    3)Airport Operational Data

                    4)Airport Environmental Data

                    5)Runway Gradients

                    6)Weather & Exit Speeds

                    7)Help
```

Figure 2.14 Edit Menu Screen.

```
EDIT MENU                Press escape (Esc) key to return to MAIN MENU.

Master
File                     Use arrow (↑ or ↓) key to change your choice.
                         Press enter ( ↵ ) key if the choice is correct.

                    1)Add a Set of Data for New Aircraft

                    2)Change some Specific Data
```

Figure 2.15 Edit Menu Screen for Master File.

```
SELECT                Press escape (Esc) key to return to EDIT MENU.

Aircraft
Category              Use arrow (↑ or ↓) key to change your choice.
                      Press enter ( ↵ ) key if the choice is correct.

TERPS A

TERPS B

TERPS C

TERPS D    Put your aircraft name : B-747-200

TERPS E
```

Figure 2.16 Adding a New Aircraft Menu.

3.0 Dynamic Module

The Dynamic Module comprises several computational subroutines used to evaluate the aircraft performance during the landing flare, the runway ground roll, and the turnoff maneuver. For modeling purposes, the aircraft flight and ground paths have been divided into five distinct segments as shown in Fig. 1.10: 1) an air distance, 2) a free roll distance between the air and braking segments, 3) the braking segment, 4) a second free roll distance between the braking and turnoff segments, and 5) the turnoff distance until clearing the runway for the next arrival. This segmentation eases the computational tasks in the model and also simplifies the inclusion of operational policies arising at specific points in the landing phase. The following paragraphs describe in detail the basic assumptions made in the dynamic analysis of this model. It should be understood that the purpose of the dynamic model is the identification of potential candidate solutions in search for optimal turnoff locations. This is accomplished through a pre-screening process of primary and secondary candidates as will be explained later in Chapter 5 of this report.

3.1 Air Distance

The air distance is estimated indirectly from the basic aircraft geometric and performance characteristics contained in the program Master File. The Master File contains geometric and basic performance characteristics for nearly one hundred aircraft in current use. These characteristics are used to estimate the approach (V_{AP}) and touchdown speeds (V_{TD}) for each aircraft selected by the user. Once the approach speed (or reference speed) is known, an estimation of the air distance can be made assuming a circular arc flare maneuver flown at constant load factor to transition from a constant rate of descent flown at constant descent flight angle γ on final approach to a flat flight path tangent to the the runway. An analytical expression for the air distance can be found by equating the changes in kinetic and potential

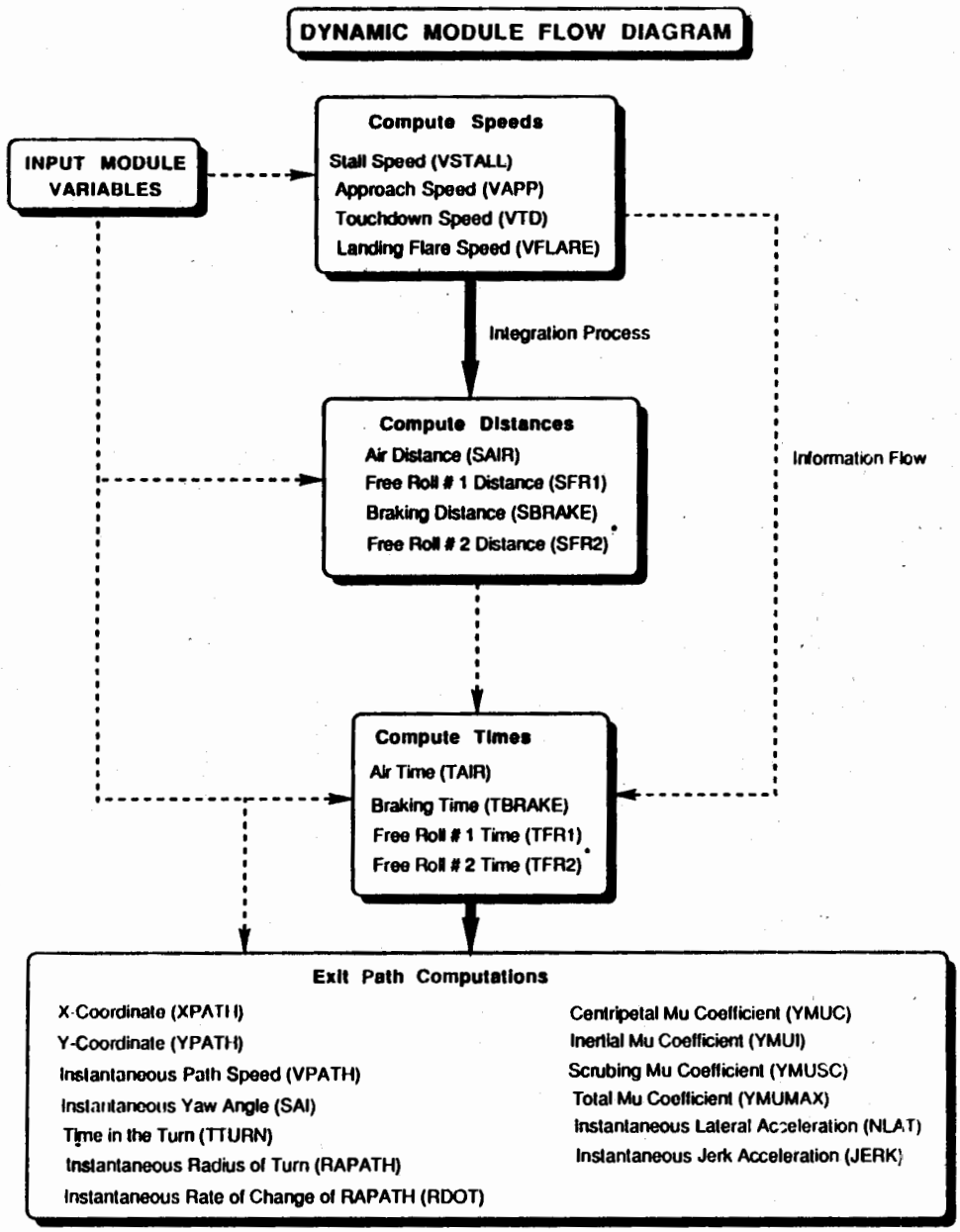

* Implies that the corresponding run option has been selected (i.e., applicable only when an existing 90 deg angle turnoff has been selected)

Figure 3.1 Dynamic Module Functional Flow Diagram.

energy of the aircraft near the ground with the product of a retarding force F_a and the air distance S_a as shown in Eq. 3.1 [Nicolai, 1976; Torenbeek, 1981; Roskam, 1986].

$$S_{air} = \frac{H_{thres}}{\gamma} + \frac{V_{flare}^2 \gamma}{2\,g\,(n_{flare} - 1)} \qquad \{3.1\}$$

where, V_{flare} is the flare speed (taken as 95% of the approach speed), γ is the effective descent flight path, H_{thres} the threshold crossing altitude. For preliminary analyses the flare load factor has been set conservatively to 1.15 g's and γ to 3 degrees to simulate a regular ILS approach flight path. Currently the dispersions in the air distance are set internally to fixed values that depend upon the aircraft category being analyzed. The aircraft categories used in this research are consistent with those implemented in the FAA Terminal Operating Procedures (TERPS) and defined in Table 3.1. The underlying assumption in this respect is that slower aircraft will usually experience smaller touchdown dispersions than those of faster aircraft in absolute distance terms (this is not in contradiction to the fact that transport-type pilots might be more accurate in terms of touchdown point standard deviations). Actual measurements of lateral and longitudinal landing dispersions for transport-type aircraft made by Hosang [Hosang, 1975] suggest that for manual control landings the average touchdown dispersion (i.e., standard deviation) is about 171 meters (560 feet). Although little data is available in actual instrument meteorological conditions (IMC) it has been found during a heads-up certification display that reduced touchdown dispersions prevail under this circumstances [Desmond, 1986].

The advantage in estimating air distances relying on information pertaining to each aircraft is two-fold: 1) frees the analyst from relying on field data for a particular aircraft that in most cases is not available or which could be implemented at a later stage for calibration of the model, 2) Introduces more realistic variabilities in the touchdown locations for the entire landing aircraft population instead of assigning a fixed touchdown location to an entire aircraft category population. The method is also sensitive to specific airfield scenarios since more parameters have been accounted for. For example, short takeoff and landing aircraft can be assigned independently different values for the flare load factor and descent flight angle as they occur in practice thus affecting accordingly the air distance values estimated internally.

Table 3.1 Aircraft Approach Category Classification (FAA, 1988).

Category	Landing Speed (1.3 V_{Stall})
A	less than 91 Knots
B	From 91 to 120 Knots inclusive
C	From 121 to 140 Knots inclusive
D	From 141 to 165 Knots inclusive
E	166 Knots and higher

The time consumed in the air phase (T_{air}) is a function of the touchdown location (S_{air}), the approach speed (V_{ap}), and the touchdown speed (V_{td}). Assuming a normal distribution for the aircraft touchdown location, T_{air} and its corresponding variance, $\sigma^2_{T_{air}}$, are given as follows:

$$T_{air} = \frac{2\ S_{air}}{V_{ap} + V_{td}} \qquad \{3.2\}$$

$$\sigma^2_{T_{air}} = \left[\frac{2}{V_{ap} + V_{td}}\right]^2 \sigma^2_{S_{air}} \qquad \{3.3\}$$

where, V_{ap} and V_{td} are the approach and touchdown speeds, respectively.

3.2 *Free Roll Distances*

Free roll distances arise in the aircraft landing operation at two different times: 1) between the air distance and the braking stage, T_{FR1} and 2) between the braking segment and the turnoff maneuver, T_{FR2}. The first free roll distance tries to simulate an inherent human delay in applying aircraft braking mechanisms such as thrust reversers, spoilers, or normal wheel braking. A conservative average value of three seconds has been allocated for this transition

stage with a typical standard deviation of one second. The corresponding free roll distance S_{FR1} and its variance $\sigma^2_{S_{FR1}}$ are as follows:

$$S_{FR1} = V_{td}\ T_{FR1} \qquad \{3.4\}$$

$$\sigma^2_{S_{FR1}} = V_{td}^{\ 2}\ \sigma^2_{T_{FR1}} \qquad \{3.5\}$$

Note that any reductions in aircraft speed during wheel spin-up have been neglected for the sake of simplicity.

The second transition segment tries to mimic a delay time arising from the proper suppression of braking action and a recognition time of the turnoff geometry prior to exiting the runway. Under all visibiltity conditions there is a delay time associated with the recognition of a high-speed turnoff and the decision of whether or not the current aircraft state (i.e., speed, braking status, etc.) is appropriate to negotiate the turn. The user has complete freedom to specify this delay time, TFR2, in the Input Menu as detailed in Chapter 3. A nominal value of 2 seconds has been allocated for this parameter as a representative value under clear air and unlimited visibility conditions (CAVU). However, the analyst could increase this value accordingly to simulate low visibility scenarios. The end result being a correspondingly higher value for the total runway occupancy time (ROT).

A complementing assumption in this analysis is that free roll time, T_{FR2} and its variance $\sigma^2_{T_{FR2}}$ are known. Then, the second free roll distance S_{FR2} and its variance $\sigma^2_{S_{FR2}}$ are,

$$S_{FR2} = V_{brake_n}\ T_{FR2} \simeq V_{exit}\, T_{FR2} \qquad \{3.6\}$$

$$\sigma^2_{S_{FR2}} = \{V_{brake_n}\}^2\ \sigma^2_{T_{FR2}} \qquad \{3.7\}$$

where, V_{brake_n} is the last braking speed integrated in the braking stage and V_{exit} is the aircraft exit speed selected by the user.

3.3 Braking Distance

Under normal landing conditions, the braking segment constitutes the largest component of the Runway Occupancy Time (ROT). As such, it becomes necessary to estimate with some accuracy the braking distance if one is to have some confidence in the total distances covered by the aircraft on the ground. The previous requirement also stems from the incorporation of airport specific variables such as local runway slope and its effect on aircraft deceleration characteristics. The problem seems to be complicated by the fact that many aircraft parameters necessary to determine the forces and moments acting on the aircraft as it brakes are not only time dependent (e.g., thrust reverse forces, braking forces, parasitic drag contributions, etc.) but also aircraft specific in most instances (e.g., small reciprocating aircraft generally do not have thrust reverse capability whereas turbofan and large turbopropeller-driven aircraft do). The dilemma is then to use a model that will provide an accurate answer without going into the sophistication and computing expense of a higher-order model (i.e., 6-DOF model).

The braking algorithm used in the model integrates the local deceleration of the aircraft, a_{acf}, as it travels along the runway (Eq. 3.8). The local deceleration is estimated from the runway initial conditions specified by the user in the Input portion of the program. At the same time a deceleration multiplier, cf_{rws}, is computed throughout the integration process in order to correct the nominal aircraft deceleration due to local variations of runway slope. This simplistic model then treats the aircraft as a second order point mass model whose resultant deceleration is integrated forward in time to obtain the velocity/distance aircraft state. The assumption of a constant uncorrected deceleration rate is justifiable if one realizes that in modern aircraft the deceleration rate is controlled by an antiskid system. The question is how can we estimate the deceleration rate for either each aircraft or for the entire aircraft population from the known runway conditions? As the reader recalls there are two different scenarios, dry and wet, defined in the runway friction characteristics as part of the Input Module. The correlation of actual aircraft data [Janes's, 1988; Aviation Week & and Space

Technology, 1988; Business and Commercial Aviation, 1989] is done backwards to estimate the necessary friction coefficient and its corresponding deceleration rate necessary to match the data published for some known conditions such as those corresponding to the aircraft maximum allowable landing mass (MALW) and dry pavement conditions. The wet condition braking analysis is performed with the introduction of a deceleration degradation multiplier, cf_{rf}, into the baseline deceleration equation (Eq. 3.9). The multiplier has been derived using NASA and ICAO empirical data [Yager and White, 1981; ICAO, 1966].

A second correction multiplier is also introduced in this analysis to modify the instantaneous deceleration due to variations in the local runway slope. The evaluation of this multiplier has been done outside the current REDIM Model using complete drag/thrust data for a Boeing 727-200 and for simplification purposes it is assumed to be constant for all the aircraft population. Equation 3.8 illustrates the approximation made of the braking distance, S_{Brake}.

$$S_{brake} = \sum_{i=1}^{n} dt\, V_{brake_i} \qquad \{3.8\}$$

Furthermore, decomposing V_{brake_i} as a function of the instantaneous aircraft deceleration (a_{acf}) and the deceleration correction factors for runway friction (cf_{rf}) and runway slope (cf_{rws}) we obtain,

$$S_{brake} = (dt)\,(n)\,(V_{td}) + (dt)^2 \sum_{i=1}^{n} (n+1-i)\; cf_{rf_i}\; cf_{rws_i}\; a_{acf} \qquad \{3.9\}$$

where, n is the number of iterations computed in the simulation of the braking process and whose numerical value is determined by the integration step size, dt, and V_{TD} is the touchdown speed. The computation of the variance of S_{brake} denoted by $\sigma^2_{S_{brake}}$ is estimated as follows,

$$\sigma^2_{S_{brake}} = \left[(dt)^2 \sum_{i=1}^{n} (n+1-i)\; cf_{rf_i}\; cf_{rws_i} \right]^2 \sigma^2_{a_{acf}} \qquad \{3.10\}$$

where, $\sigma^2_{a_{acf}}$ is the variance of the deceleration rate (another user input) and dt is the simulation step size. Note that the time consumed in the braking process and its variance are estimated according to Eq. 3.11.

$$T_{brake} = \frac{S_{brake}\ (n)}{\sum_{i=1}^{n} V_{brake_i}} \qquad \sigma^2_{T_{brake}} = \frac{\sigma^2_{S_{brake}}}{(\bar{V}_{brake})^2} \tag{3.11}$$

3.4 Turnoff Algorithm

The turnoff algorithm integrates the aircraft path throughout the exit maneuver. The exit maneuver is initiated when the aircraft reaches the user-defined exit speed and finalizes with the complete clearance of the runway by the landing aircraft as shown in Fig. 3.2. In order to simplify the number of inputs to the model it is assumed that the aircraft wingtip point controls the time to clear the runway. This is generally true for all aircraft exiting at high speed. Exceptions to this rule are small aircraft and Short Takeoff and Landing Aircraft STOL (i.e., requiring abnormally large tailplane wingspans) exiting at low speed (e.g., less than fifteen meters per second). However, since the objective of this research is the investigation of high-speed turnoffs these exceptions would seldom occur and therefore the prediction of the clearing point can be done adequately with a single aircraft control point.

The characteristic motion of an aircraft turning at speeds where insignificant aerodynamic control can be exerted by conventional primary aerodynamic surfaces is simplified to the forces acting on the nose landing gear. An algorithm developed by Schoen et al [Schoen et al, 1985] and used in a previous NASA research effort on this topic considers three side force contributions acting on the aircraft nose landing: 1) the centripetal force, 2) the aircraft inertia, and 3) the tire scrubbing resistance to the turn. Mathematically, the nondimensional contributions to the nose gear are,

$$\mu_{skid} = \mu_{I_{zz}} + \mu_c + \mu_{sc} \tag{3.12}$$

where, μ_{skid} is the nose gear tire skidding friction coefficient, $\mu_{I_{zz}}$ is the aircraft inertia contribution term to the nose gear side load, μ_c is the centripetal acceleration contribution, and μ_{sc} is the tire scrubing resistance. These contributions are calculated in Eqs. 3.13 to 3.15.

$$\mu_{I_{zz}} = \frac{I_{zz}\ \alpha}{m\ g\ wb\ lm/100\ (1 - lm/100)} \qquad \{3.13\}$$

it is noted from this equation that the term $m\ g\ (1 - lm/100)$ represents the aircraft weight supported by the nose gear whereas $wb\ (lm/100)$ is the moment arm from the aircraft center of mass to the nose gear.

$$\mu_c = \frac{V^2}{g\ R} \qquad \{3.14\}$$

$$\mu_{sc} = f(R, m) \qquad \{3.15\}$$

where, I_{zz} is aircraft moment of inertia about the vertical axis, in Kg-m-m, α is the angular acceleration (rad/sec,) of the aircraft fuselage as it executes the turning maneuver, wb is the aircraft wheelbase (meters), lm is the aircraft mass supported by the main gear (in percent), g is the gravitational constant (m/sec-sec), m is the total aircraft mass (Kg.), V is the instantaneous speed (m./sec.) of the nose gear, and R is the instantaneous radius of the curve (m.). Further breakdown of the angular acceleration yields for Eq. 3.13 the following,

$$\mu_{I_{zz}} = \frac{I_{zz}\ \left(\frac{\dot{V}\ R - V\ \dot{R}}{R^2}\right)}{m\ g\ wb\ lm/100\ (1 - lm/100)} \qquad \{3.16\}$$

where, $\dot{R}$ represents the rate of change of the turning radius of curvature, $\dot{V}$ if the instantaneous velocity rate of change of the nose gear, and R and V are the state variables of our system. A further simplification can be introduced if the term $\dot{V}\ R$ is neglected on the grounds of very small values for the deceleration rate through the turnoff maneuver. Fact that has been found true in the empirical studies of Horonjeff and Hosang [Horonjeff et. al., 1958; Hosang, 1975]. The new expression becomes,

$$\mu_{I_{zz}} = \frac{I_{zz}\,[-V\,\dot{R}]}{R^2\;m\;g\;wb\;lm/100\;(1-lm/100)} \qquad \{3.17\}$$

solving for the rate variable, $\dot{R}$ and integrating over time it is possible to estimate the state variables of the motion,

$$\dot{R} = \frac{\mu_{I_{zz}}\,R^2}{I_{zz}\,V}\;m\;g\;wb\;lm/100\;(1-lm/100) \qquad \{3.18\}$$

$$R_t = \int_0^t \dot{R}\;dt \qquad \{3.19\}$$

$$X_t = \int_0^t V\cos(\psi)\;dt \qquad \{3.20\}$$

$$Y_t = \int_0^t V\sin(\psi)\;dt \qquad \{3.21\}$$

where, X and Y are the position coordinates of the vehicle as it progresses into the turn and ψ is the heading angle that the nose gear makes with a global axis system centered about initial position of the turnoff path (Fig. 3.2). Eqn. 3.18 is further restricted by passenger comfort factor limitations as will be explained in Section 3.5 of this Chapter.

The neglect of aerodynamic effects in this analysis might be realistic for up to about two thirds of the landing speed (V_{lan}) as this is known to be the threshold for significant aerodynamic control for conventional aircraft [Miller, 1967]. Even with this restriction, the evaluation of runway turnoffs can be accomplished for a large range of aircraft speed values ranging from 10 to 45 m/sec. (22.3-100.4 MPH) for transport-type category aircraft. As will become evident during the discussion of results of this research turnoff designs above 45 m/sec. (100.4 MPH) are probably unlikely due to lateral space limitations following the turn. This topic is currently being investigated in a continuous research carried by the Center for Transportation Research with the FAA and NASA.

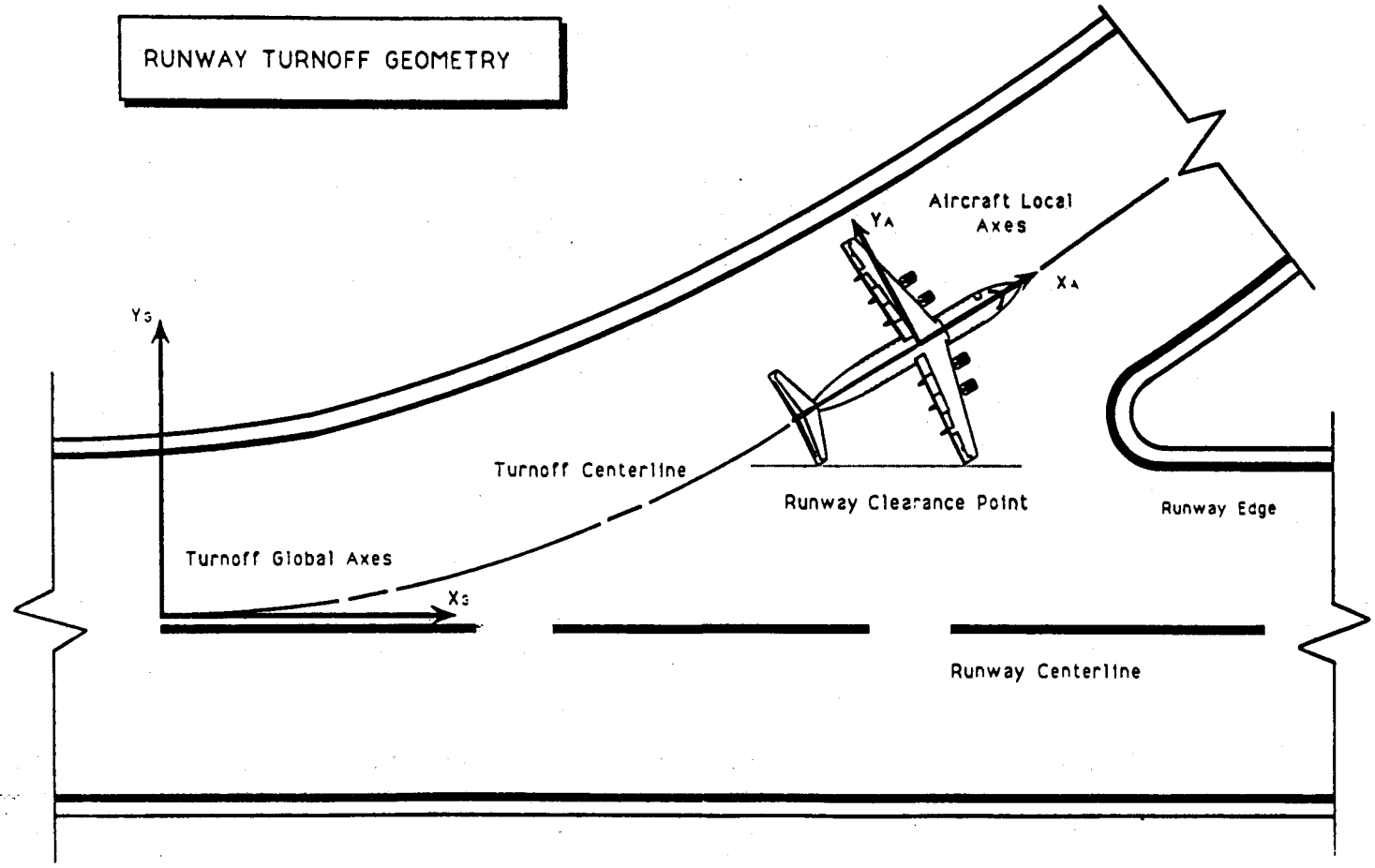

Figure 3.2 Runway Clearance Point Nomenclature.

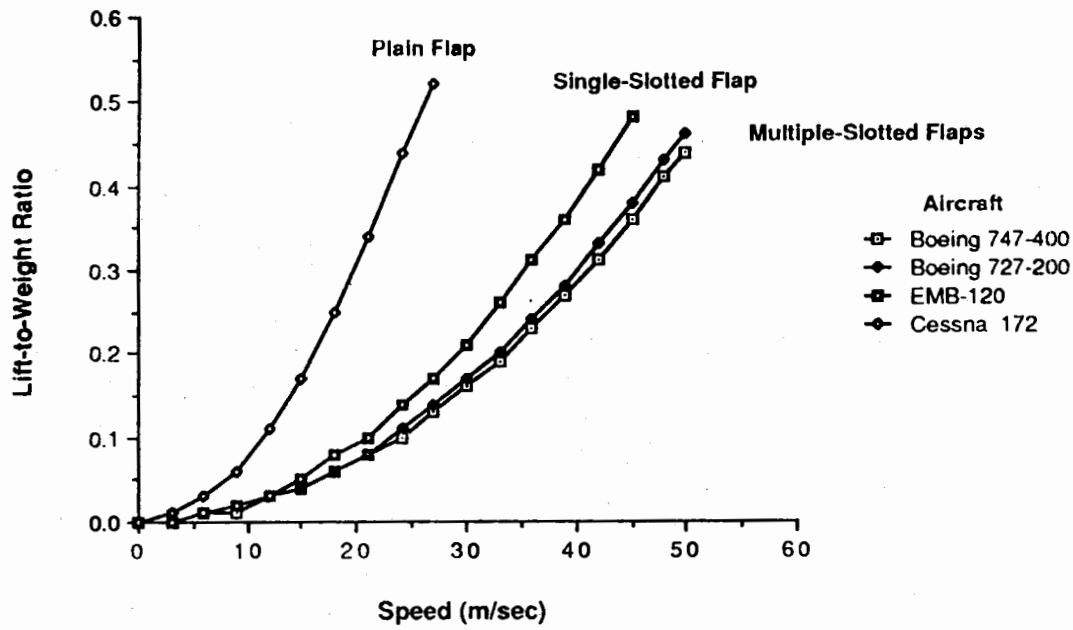

Figure 3.3 Comparative Lift-to-Weight Ratios for High-Speed Taxiing Aircraft (Low α).

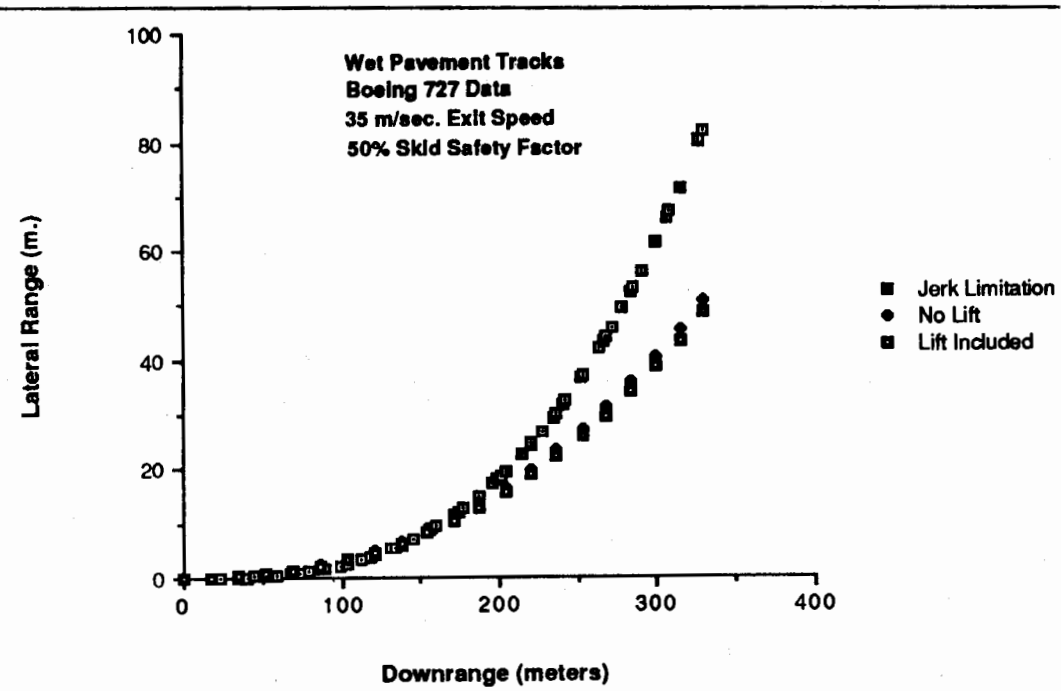

Figure 3.4 Aircraft Turnoff Tracks with and without Lifting Forces (Boeing 727-200).

The inclusion of the lifting forces acting on the aircraft at high speed can be added to Eqn. 3.18 replacing the *mass* term by an equivalent force that accounts for the potentially large lifting forces experienced at high speeds.

$$\dot{R} = \frac{\mu_{I_{zz}} R^2}{I_{zz} V} \quad (m - .5\,\rho\, V^2\, S\, C_L)\, g \;\; wb \;\; lm/100 \;\; (1 - lm/100) \qquad \{3.22\}$$

where, ρ is the air density, C_L is the aircraft lift coefficient in ground effect and the landing flap configuration, S is the wing area and V is the aircraft speed. Fig. 3.3 depicts the lift-to-weight ratio for three types of aircraft. The significance of this plot is that it allows us to establish desired exit speed boundaries for each TERP aircraft category. It can be seen from this plot that for a typical single-engine aircraft the L/W ratio below 15 m/sec. can be practically ignored. Similarly, for medium sized and heavy transport aircraft the lift effects become noticeable after 25 m/sec. (56 MPH) but for all practical purposes the turnoff trajectories are

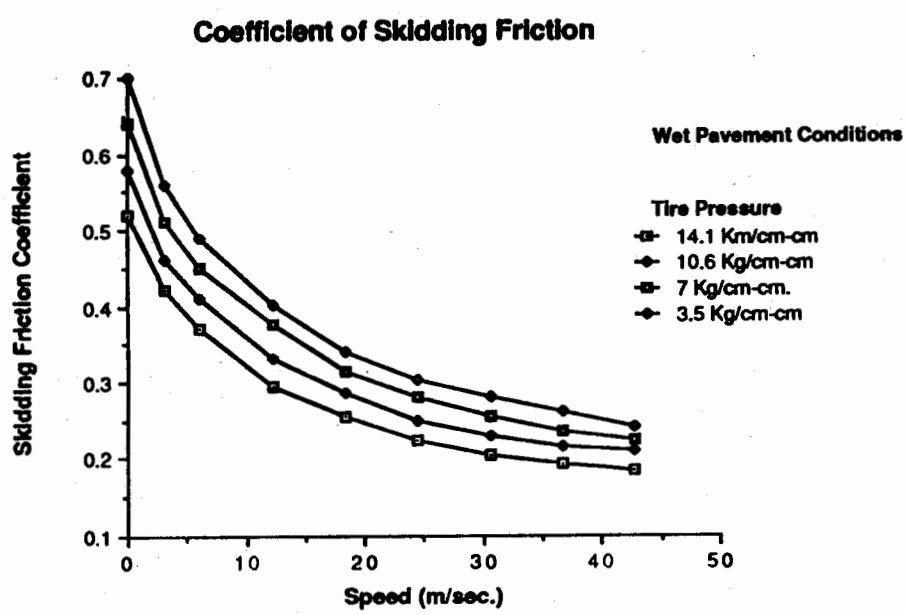

Figure 3.5 Skid Friction Variations with Tire Pressure and Speed.

not significantly altered but after 45 m./sec. or more as depicted in Fig. 3.4. The reader is warned that these results were derived under the assumption that the lift contribution acts near the aircraft center of gravity and therefore no significant pitching moment is induced to load the nose gear. In practice pilots can modify the nose gear load distribution by deflection of the aircraft elevator surfaces once these become effective (about two thirds of the liftoff speed) thus making more difficult the task of arriving at a unique conclusion.

Equally important is the fact that Fig. 3.3 depicts the lift generated by an aircraft at small angles of attack and flaps down (i.e., rolling on a high-speed turnoff). However, the potential lifting force capable of being generated is much larger if the angle of attack is increased through the use of elevator power. This is a fact of fundamental importance if one is to restrict aircraft from turning at excessive speeds where the aircraft might actually be flying! Taking as example a light single-engine aircraft such as the Cessna 172 it is seen from Fig. 3.3 that at 25 m./sec. the lift-to-weight ratio is about .42 for low angles of attack (i.e., 2-3 degrees) in the landing configuration (i.e., flaps fully down). However, this happens to be the stalling speed for this aircraft in the landing configuration (for an angle of attack of about 16 degrees) and therefore it would be unreasonable to turn this aircraft at such high speeds. REDIM currently has a high speed threshold limiter to overcome this complication by announcing the potential input error and suggesting upper and lower bounds for the aircraft exit speeds. A more sophisticated model including the aerodynamic terms in the aircraft equations of motion would necessitate the knowledge of several important aerodynamic derivatives, geometric parameters, and reference areas for every aircraft considered imposing a large computational burden for the optimization procedure and necessitating a more complete input data set from the user. This approach was then ruled out due to the complexity of the input data needed.

The aforementioned algorithm has been modified in order to account for the large variations in skidding friction coefficients observed for a large aircraft population. It is well documented in the literature that the skidding friction coefficient is a function of aircraft tire pressure and aircraft speed, among other variables [NASA TN 4418, 1966; Wong, 1978]. A summary of this functional relationship is depicted graphically in Fig. 3.5 where four aircraft tire pressures are represented in this figure and they correlate well with the four different

aircraft categories modeled in this research. The upper curve corresponds to a tire pressure of 50 PSI (pounds per square inch) and is representative of the characteristics of TERP A category aircraft. Similarly, the lower curve represents a 200 PSI tire pressure typical of current heavy aircraft (i.e., Boeing 747, DC-10, L-1011, etc.).

Complementing this algorithm a small forward deceleration can be introduced in order to account for the small speed losses expected while turning. The rolling friction opposing the motion of the aircraft on the ground introduces a deceleration rate proportional to the product of g and f_{roll} where this last term is the coefficient of rolling friction. For the sake of simplicity f_{roll} is taken constant with speed although it is known to vary with tire speed as well. A typical value of .03 is used for f_{roll} for the base model.

$$a_{roll} = g \ f_{roll} \qquad \{3.23\}$$

An Euler first-order integrating scheme is used to solve numerically the aircraft equations of motion through the turnoff maneuver. The time spent on the turn, T_{path} is considered to be deterministic in nature. A baseline step size of one hundredth of second was found to offer accurate results within the desired computational time limitations for the program. The accuracy of the method is evident from Fig. 3.6 where the first-order solution is compared with an equivalent Runge-Kutta fourth-order scheme (notice that both curves overlap). These solutions were obtained using the geometric and performance parameters of a Boeing 727-200 and as can be seen from the turnoff paths generated the results are within one half of a percent of each other (i.e., less than half a meter difference between both solutions at the end of a high-speed turnoff). Another justification for the Euler algorithm was the desired accuracy in stopping the simulation as closely as possible to the runway clearance point (Fig. 3.2). With the current step size it is possible to ascertain the turnoff time (TOT) and the lateral range distance within very small windows, .01 seconds or .15 meters, for an aircraft traveling at 30 m/sec. (67.2 MPH) and reaching the runway clearance point with up to 30 degrees of total heading change.

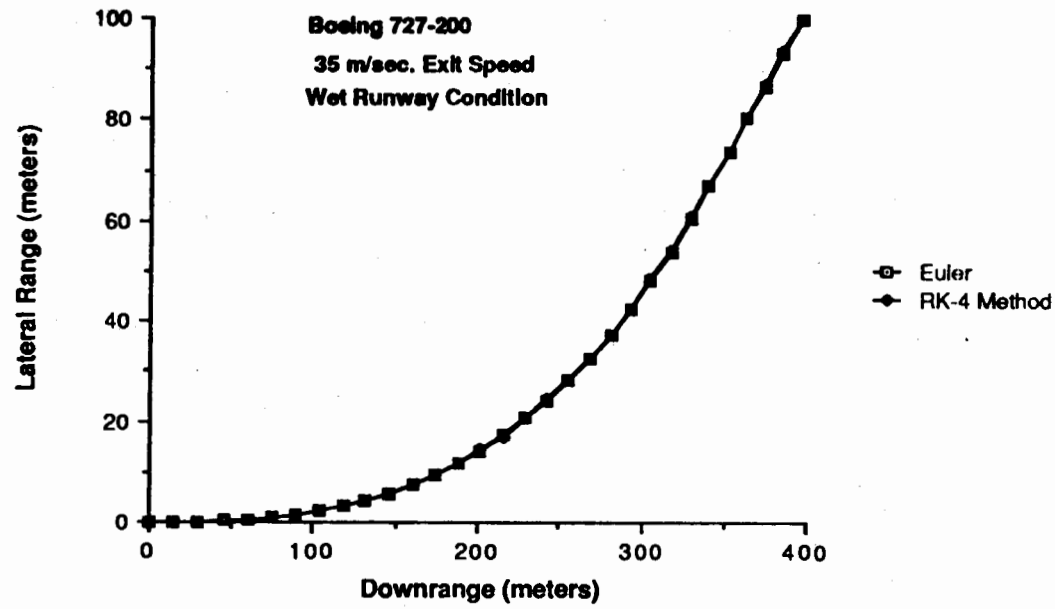

Figure 3.6 Comparison of Track Simulation Results Using two Integrating Methods.

The aircraft position coordinates in the turn (X_{path}, and (Y_{path}), the aircraft speed (V_{path}), and the aircraft instantaneous heading (ψ) constitute state variables through the turnoff maneuver (Eqns. 3.20-22). These states are integrated forward in time to assess the instantaneous turning radius (R_{path}) and ultimately estimate the position changes experienced by an aircraft as a high-speed turnoff is negotiated. The aircraft is considered to have cleared the runway when its right wingtip has traveled the lateral distance necessary to cross the runway edge imaginary plane. Once the turnoff path and times are estimated it is possible to ascertain the time from threshold crossing to the end of the turnoff maneuver. Since some of the distances and times involved in the process are random variables the net effect is that runway occupancy time (ROT) and the total distance to initiate the turnoff are both probabilistic in nature.

$$S_{turn} = S_{air} + S_{FR1} + S_{brake} + S_{FR2} \qquad \{3.24\}$$

$$\sigma^2_{S_{turn}} = \sigma^2_{S_{air}} + \sigma^2_{S_{FR1}} + \sigma^2_{S_{brake}} + \sigma^2_{S_{FR2}} \quad \{3.25\}$$

$$T_{turn} = T_{air} + T_{FR1} + T_{brake} + T_{FR2} \quad \{3.26\}$$

$$\sigma^2_{T_{turn}} = \sigma^2_{T_{air}} + \sigma^2_{T_{FR1}} + \sigma^2_{T_{brake}} + \sigma^2_{T_{FR2}} \quad \{3.27\}$$

$$ROT = T_{turn} + T_{path} \quad \{3.28\}$$

$$\sigma^2_{ROT} \simeq \sigma^2_{T_{turn}} \quad \{3.29\}$$

where, S_{turn} is the distance from the threshold to the initiation of the turnoff (i.e., exit location distance), $\sigma^2_{S_{turn}}$ is the variance of this previous parameter, T_{turn} and $\sigma^2_{T_{turn}}$ are the time consumed from threshold to the initiation of the turnoff and its corresponding variance, T_{path} is the time in the turnoff and ROT is the total runway occupancy time for a single aircraft with variance σ^2_{ROT}.

3.5 Comfort Factor Considerations

At this point it is important to introduce and discuss the vehicle limitations due to the passenger comfort factor. The measures of effectiveness used to estimate passenger comfort in a turning vehicle have traditionally been the normal acceleration, a_n and the two vectorial components of the jerk usually defined in the literature as the normal and tangential jerk, J_n and J_t, respectively. There seems to be little information in the literature regarding the human comfort "thresholds" to lateral accelerations and jerks. Most of the data seems to have concentrated around motions in the plane of symmetry of transportation vehicles (i.e., pitch rate and vertical accelerations). Data from the railroad industry seems to offer the only tractable guidelines for both lateral acceleration and jerk (Hulbert, 1979 and Wright, 1989). Average accepted limitations for normal jerk oscillates between 0.055 to 0.065 g's (i.e., 0.54-64 m/sec-sec.) whereas that for lateral acceleration is about 0.12-0.15 g's (i.e., 1.18-1.47 m/sec-sec). It is however important to understand that these represent train threshold values

which might be overly conservative when applied to aircraft passengers. Aircraft pilots can adjust laterally the trajectory of the vehicle on the ground and consequently have a large influence in the lateral acceleration and jerk perceived by a passenger. Also, the suspension system found in typical aircraft is better suited to absorb rolling and yawing motions than those found in trains and this should favor the ground riding qualities of air vehicles. Finally, aircraft seats are usually designed with more lateral and longitudinal restraints than those found in trains thus hiding the passenger perception of uncomfortable motions. These facts need further research to assess their validity and should be interpreted as tentative.

Schoen et. al. [Schoen et. al., 1985] used a combined performance measure to relate the upper limits of the normal acceleration and the jerk. The suggested relationship is given in Eq. 3.30 and shown graphically in Fig. 3.7. It must be pointed out that this comfort factor modeling has been suggested in the literature but has not been correlated with experimental data validating the results. It seems possible that this method might be too restrictive when applied to aircraft ground motion due to the larger lateral restraint mechanisms offered by aircraft seats when compared with their train counterparts. Also the reader should recall that normal acceleration and normal jerk are related according to the functional form shown in Eqn. 3.31.

$$\frac{a_n}{a_{max}} + \frac{J_n}{J_{max}} < 1.00 \qquad \{3.30\}$$

$$a_n = \frac{J_n\, l}{V_e} \qquad \{3.31\}$$

where, a_n is the normal acceleration, V_e is the entry exit speed (i.e., assumed constant throughout the turnoff for the transition curve practical analysis), a_{max} is the maximum permissible normal acceleration, J_n is the normal jerk and J_{max} is the maximum tolerated normal jerk value.

The kinematic equations of motion defining a turning vehicle through a transition spiral are shown in Eqns. 3.32 and 3.33 (in cartesian coordinates). The approximation represents a truncation of the Taylor series expansion up to the third term. Note that an iterative solution

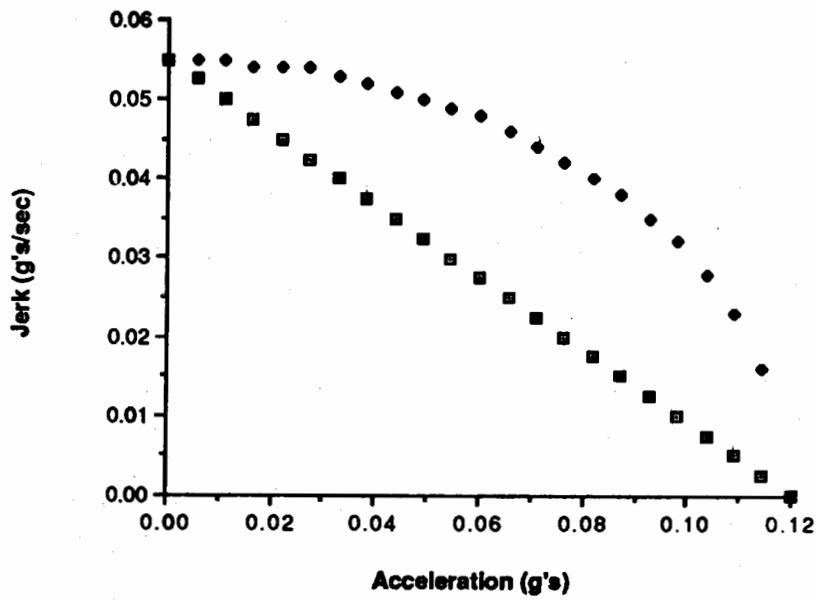

Figure 3.7 Possible Passenger Comfort Indifference Curves.

to find x and y can easily be implemented if a first estimate is made with the first order term of Eqns. 3.32 and 3.33 without a great loss in accuracy [Anderson, 1979].

$$x = l - \frac{1}{80}\frac{J_n^2\, l^5}{V_e^6} + \frac{1}{3465}\frac{J_n^4\, l^9}{V_e^{12}} \qquad \{3.32\}$$

$$y = \frac{1}{6}\frac{J_n\, l^3}{V_e^3} - \frac{1}{336}\frac{J_n^3\, l^7}{V_e^9} + \frac{1}{42240}\frac{J_n^5\, l^{11}}{V_e^{15}} \qquad \{3.33\}$$

where, x and y are the coordinates of the turnoff, J_n is the normal jerk, l is the curve length and V_e is the aircraft speed at the entrance of the turnoff.

Figure 3.8 compares two high-speed turnoff tracks for two transport-type aircraft and two different speeds with their corresponding jerk-limited turnoff tracks. The threshold jerk value used for this figure was 0.55 $m/\sec^3$ which has been accepted by many researchers in the

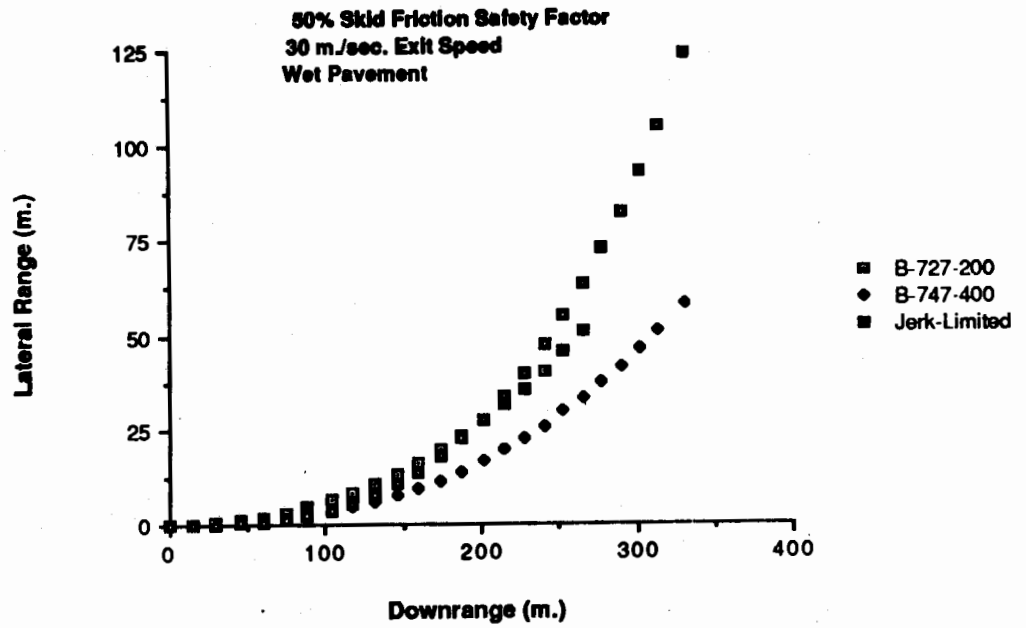

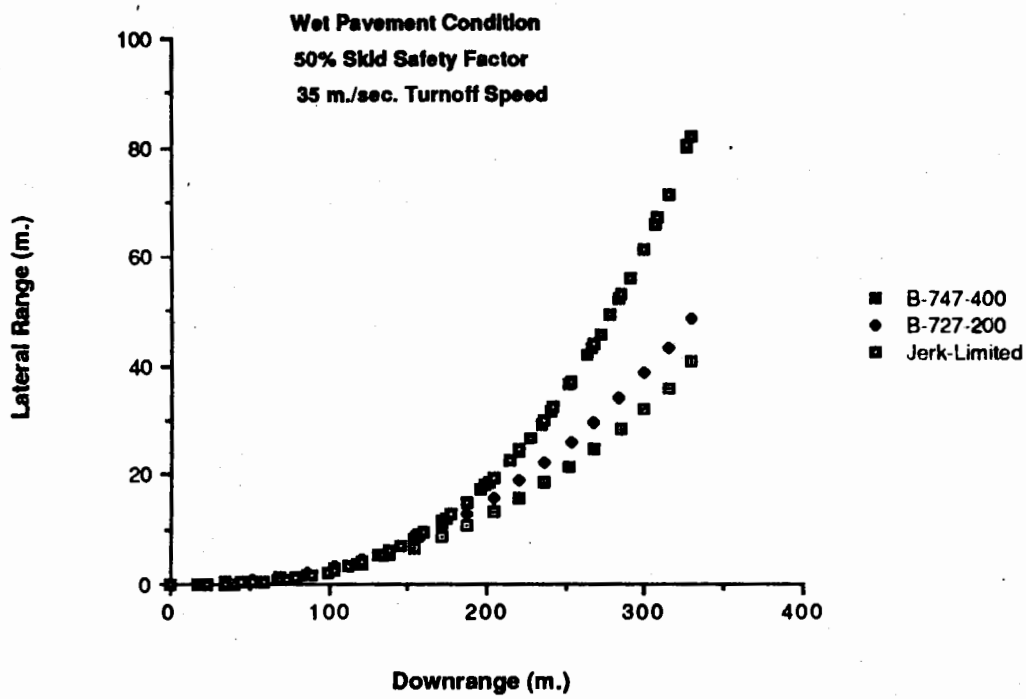

Figure 3.8 Comparison of High-Speed Turnoff Tracks for Various Aircraft.

train industry. It should be pointed out that both paths are very close to each other in the first one hundred meters into the turnoff maneuver. The jerk-limited track quickly ceases to be of concern once this point is reached. A magnification of these results of these results during the first one hundred meters reveals that the jerk-limited transition curve slightly dominates the turnoff geometry and thus an enlargement of the local radius of curvature might be desirable. It should be pointed out , however, that the differences in both curves are so small that the resulting practical geometry remains almost unaffected. The conclusion of this discussion seems to suggest that further investigation needs to be carried out in actual vehicles in order to determine if these differences are really important from a practical point of view. Also, it is suggested that more research needs to be carried out in the area of aircraft ground ride qualities and human comfort factors to lateral accelerations. The data and models reviewed in our research are inconclusive in terms of well defined thresholds of comfort. It is possible that the normal acceleration and jerk tolerances accepted by train passengers could in fact be overly conservative when applied to aircraft ground scenarios. It is time to fill this void in aerospace research.

The equations of motion of the point mass vehicle can then be effectively modified to account for the comfort limitations. The main effect of restricting the turnoff geometry to comply with a minimum jerk-limitation threshold is to restrict the rate of change in the turnoff curvature. For a constant speed transition spiral the first order differential equation defining the rate of change of the heading angle with respect to time is,

$$\frac{d\psi}{dt} = \frac{d\psi}{dl}\,\frac{dl}{dt} \qquad \{3.34\}$$

$$\frac{d\psi}{dt} = \frac{d\psi}{dl}\,V = \frac{V}{R} \qquad \{3.35\}$$

where, ψ is the instantaneous heading angle, l is turnoff curve length, V is the aircraft turnoff speed, R is the instantaneous turning radius and t is the time in the turnoff maneuver. Differentiating Eqn. 3.34 with respect to time and knowing the value of the second derivative of ψ with respect to time and neglecting for a moment the deceleration term the limiting expression of $\dot{R}$ limited by jerk constraints is shown in Eq. 3.36.

$$\frac{d^2\psi}{dt^2} = \frac{d^2\psi}{dl^2} V^2 = \frac{J_n}{V^3} = -\frac{V\dot{R}}{R^2} \qquad \{3.36\}$$

$$\dot{R} = -\frac{J_n R^2}{V^2} = \frac{J_n R}{a_n} \qquad \{3.37\}$$

Equation 3.37 can then be used to restrict the value of $\dot{R}$ for any limiting values of J_n and a_n (i.e., for values previously defined as a_{max} and J_{max}). It is interesting to note that although previous research has tried to justify a combined passenger comfort performance index in terms of these two parameters they arise naturally in the geometric definition of a spiral curve and are in fact related as seen in Eqn. 3.37. Consequently, a linear combination of the two parameters is very unlikely to dictate passenger a comfort indifference curve. In these author's opinion the indifference curve could probably resemble a quarter of an ellipse rather than being linear although further research will ultimately dictate these thresholds. Careful examination of Eqns. 3.34 through 3.37 indicates that jerk limitations dominate the initial portion of a constant speed transition spiral whereas the upper value of normal acceleration takes precedence as the turnoff geometry progresses in time as the result of a decreasing turnoff curvature over time.

3.6 Exit Assignment Algorithm

The exit assignment algorithm, as its name implies estimates the probable exit that an aircraft would take under a given set of operating conditions. The algorithm is used in all of REDIM run options and assigns either existing or potential turnoffs to every aircraft according to their landing performance characteristics. In the design and redesign running modes the algorithm assigns all exits downrange of the primary candidate generated by the *i th* aircraft in question. This is necessary as every other exit downrange constitutes a potential optimal solution for the optimization routine. This will become more evident in Section 4.3.2 of this report where the dynamic programming formulation is explained in detail.

3.7 Airport Environmental Variables

It was said in Chapter 2 that the airport environmental variables were defined in a single screen bearing a similar name. The environmental characteristics of interest are: 1) wind speed (WSPEED), 2) wind direction (WDIR), 3) airport elevation (AIRELV), 4) airport temperature (AIRTEMP), 5) runway orientation (RUNOR), 6) runway visual range (RVR), 7) runway width (RUNWID), and 8) distance to nearest taxiway (DISTT).

The wind vector is used in conjunction with the runway orientation to estimate the longitudinal and lateral wind components affecting aircraft operations. The longitudinal wind component affects the landing speeds of the aircraft population and as such has a direct impact in the runway occupancy time and turnoff locations. Regarding the use of a single wind vector as input to the model, the the user is urged to execute the baseline program under the average prevailing wind conditions at the airport facility just as he/she would do under the average prevailing temperature.

Temperature and airfield elevation have a direct impact in the performance of the aircraft in the air and on the ground. Changes to the aircraft equivalent airspeed (EAS) due to temperature and field elevation can have large impact in the ROT and the turnoff location parameters as will be seen in Chapter 6 of this report. The model converts equivalent speeds (EAS) to true air speeds (TAS) to estimate the stalling (V_{Stall}) and approach speeds and ultimately predict the aircraft landing roll performance. The runway width and runway distance to nearest taxiway are included in this set of parameters in order to estimate the time spent on the turnoff maneuver by each aircraft.

3.8 Aircraft Characteristics

The aircraft characteristics used in the model are shown in Table 3.2. These are necessary to estimate the aircraft performance on the ground as well as in the flare maneuver. The aircraft mass, wing area, and the maximum landing lift coefficient dictate the approach speed and hence affect the ROT and exit location. It is also used to estimate the second moment of inertia of the aircraft around the vertical axis (I_{zz}) ultimately influencing the turning aircraft capabilities through an exit. Roskam [Roskam, 1985] suggests a logarithmic relationship between these two parameters which seems to correlate very well for all aircraft TERP categories. The regression equation in metric units is shown in Eq. 3.29 where the aircraft mass is given in kilograms and the moment of inertia in kg-m-m.

The aircraft wheeltrack (ACFWT) is used to estimate the maximum track-in distance present during the turnoff maneuver. The track-in distance is defined as the perpendicular distance measured from the geometric center of the aircraft main gears to the imaginary path followed by the nose gear. Track-in distances are used to assure a sound geometric design of the high-speed turnoff. It should be pointed out that in general track-in distances tend to be relatively small for very high speeds (i.e., > 30 m/sec.) However, for large aircraft and medium speeds they should be considered in the geometric design. Fig. 3.9 shows graphically the nomenclature used to model the aircraft kinematic behavior including the estimation of the track-in distance. As the dynamic simulation executes a sample record of the main gear position (X_{ml}, Y_{ml}) is kept and the track-in distance is evaluated. A simple sorting routine searches for the largest value of track-in and this is later transfered to the output module to calculate the corresponding turnoff geometry that satisfies the kinematic constraints of the turnoff track. As usual, a safety distance is selectively used to estimate the distance from the centerline of the the turnoff track to the edge of the pavement. No judgemental oversteering is assumed in the program as this is certainly not recommended for an aircraft traveling at high-speed on the ground.

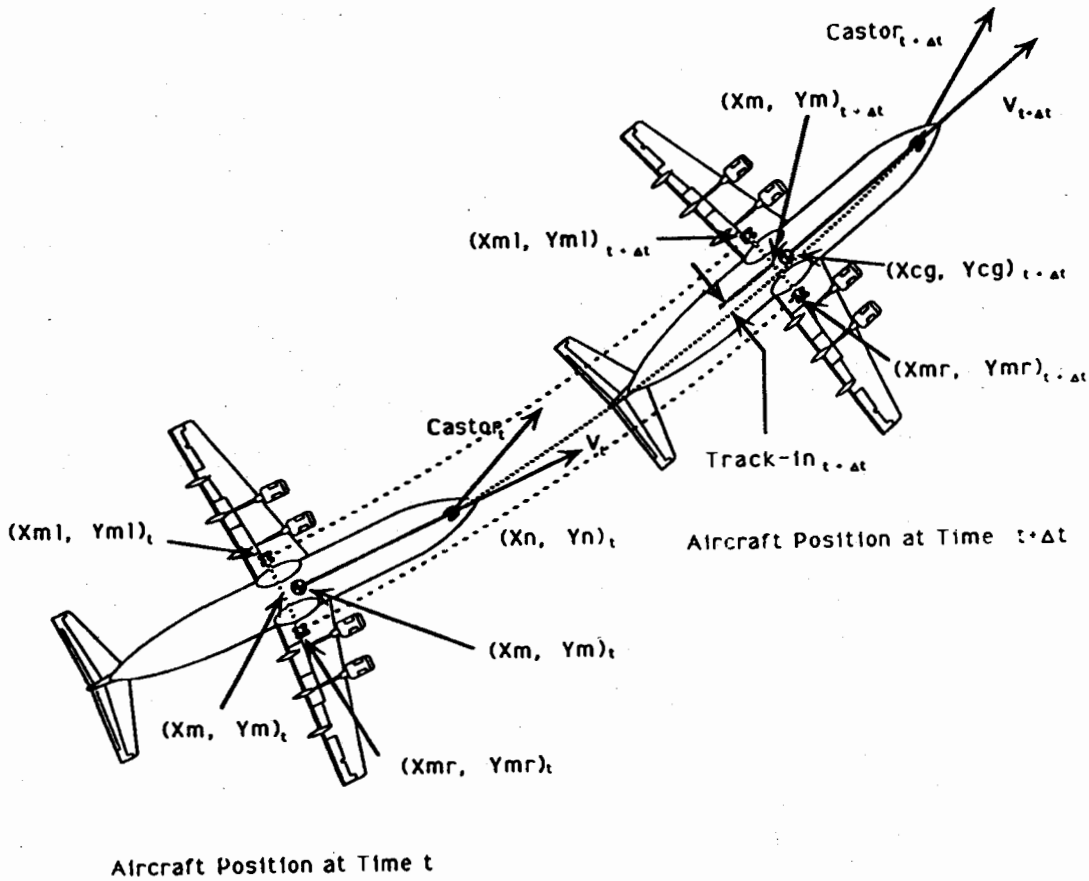

Nomenclature

(Xcg, Ycg)	Aircraft Center of Gravity Coordinates
(Xm, Ym)	Coordinates of Main Landing Gear Geometric Center
(Xml, Yml)	Left Main Landing Gear Position Coordinates
(Xmr, Ymr)	Right Main Landing Gear Position Coordinates
Castor	Castor Angle
V	Aircraft Velocity Vector (at Center of Gravity)
Track-in	Track-in Distance (from Nose Gear to Main Gear Geometric Center)

Figure 3.9 Aircraft Kinematic Behavior Nomenclature.

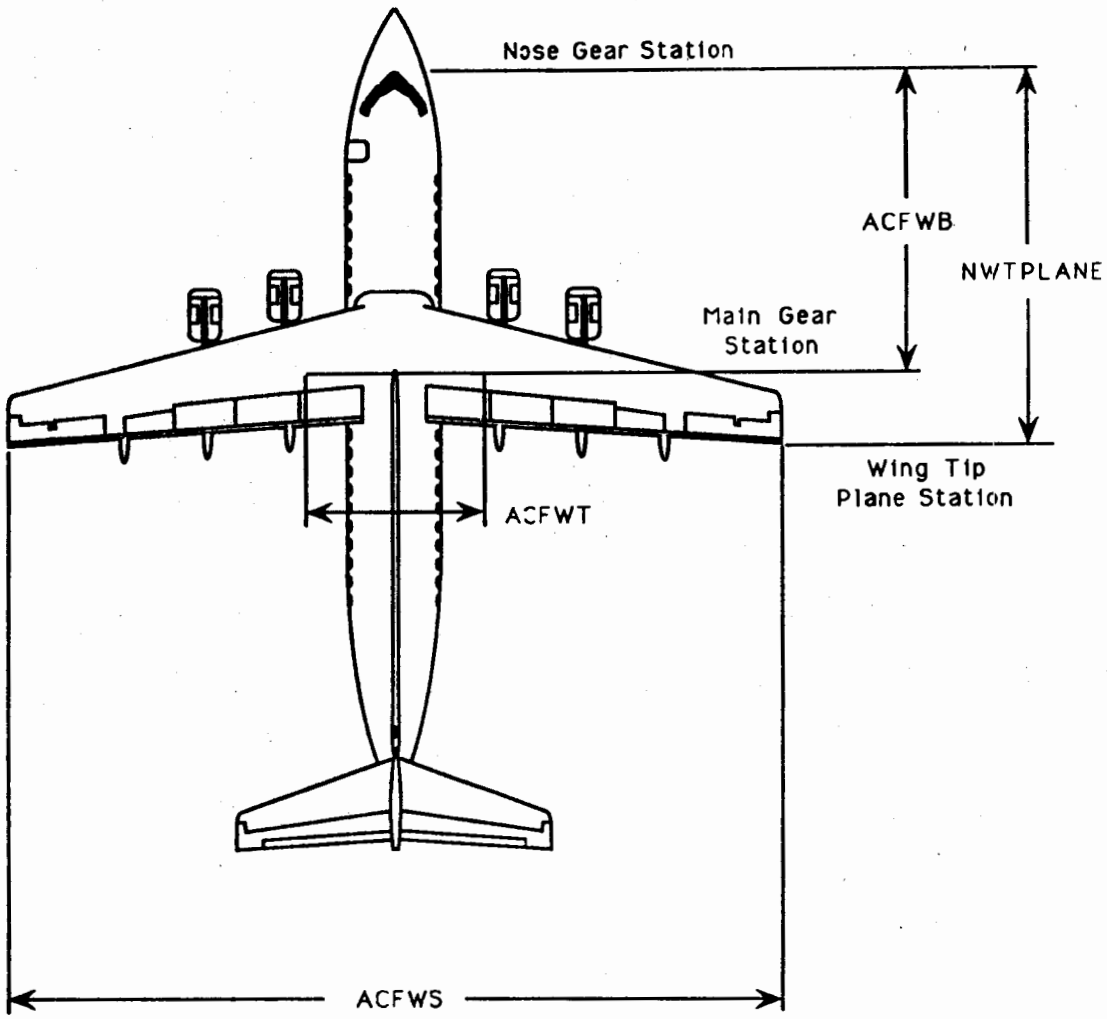

ACFWS	Aircraft Wing Span
ACFWB	Aircraft Wheel Base
NWTPLANE	Distance from Nose Gear to Wing Tip Plane
ACFWT	Aircraft Wheel Track

Figure 3.10 Aircraft Geometric Characteristics.

Another geometric parameter included here is the distance from the aircraft nose gear to the imaginary plane passing through the airplane wingtips. This distance is used as the controlling point to ascertain whether or not the aircraft has cleared the runway. A graphical description of some of these parameters is seen in Fig. 3.10.

$$I_{zz} = Antilog_{10}\ \{1.7215\ \log_{10}\ (m) - 1.6730\} \qquad \{3.29\}$$

Table 3.2 Aircraft Characteristics.

Name	Variable	Remarks
Aircraft Mass	ACFMASS	Max. Landing Mass (Kg.)
Aircraft Wheelbase	ACFWB	in meters
Aircraft Wheeltrack	ACFWT	in meters
Aircraft Load on Main Landing Gear	ACFLM	At aft C.G. (%)
Aircraft Wing Area	ACFWA	Gross wing area (sq. m.)
Aircraft Maximum Lift Coefficient	ACFCL	At max. flap setting (dim.)
Distance from Nose Gear to Wingtip	NWTIP	in meters

4.0 Optimization Module

The dynamic simulations of aircraft landing movements calculate the best turnoff locations for each aircraft in both dry and wet runway surface conditions. The best turnoff location is defined as the nearest location from the runway threshold where the aircraft decelerates to the pre-specified desirable exit speed with the pre-specified reliability. If the aircraft reduces its speed to the pre-specified exit speed before reaching the assigned turnoff location, the aircraft will be considered to exit the runway successfully. Reliability is defined as the probability that the aircraft exits the runway successfully. For example, if the reliability is specified as 90%, 90 aircraft out of 100 landing attempts will exit the runway successfully.

If an exit is constructed at the best turnoff location for an aircraft, the runway occupancy time (ROT) of the aircraft will be minimized without sacrificing the reliability. Though some exits constructed ahead of the best turnoff location can produce less ROT, it is not permissible to assign the aircraft to these exits, since reliability must be sacrificed.

Suppose there are five aircraft in consideration, the simulations of the aircraft landing movements will provide ten different turnoff locations for each aircraft and two runway surface conditions. The goal of an optimization algorithm is to find a few locations (e.g. 2 or 3) at which all the aircraft in consideration can exit the runway with the minimum weighted sum of ROT. Since each aircraft and each surface condition can have different relative frequency, the weighted sum of ROT should be minimized instead of total ROT. Figure 4.1 illustrates the best turnoff locations and their relative frequencies. Let l_{ij} and w_{ij} represent the best turnoff location and relative frequency for aircraft i and surface condition j.

The optimization procedure in REDIM conducted with the following steps:

1. Generate the complete set of candidate locations.
2. Calculate the ROT of every aircraft for each candidate locations.
3. Find the optimal location(s) out of the candidates.
4. Assign aircraft to the optimal locations

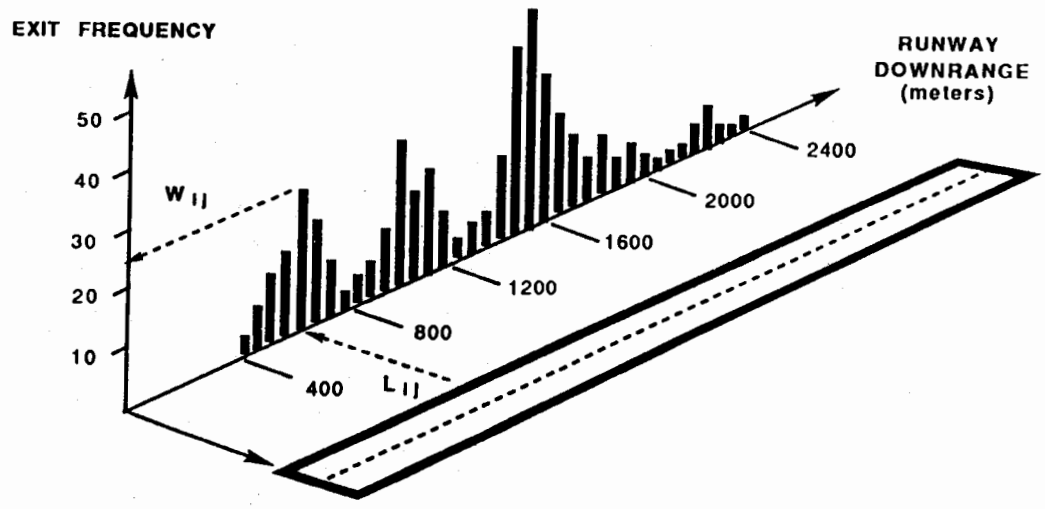

Figure 4.1 The Best Turnoff Locations and Their Weights.

Steps 1 and 2 are the data preparation for step 3 which is the mathematical optimization. The optimization in step 3 employs a dynamic programming technique. Step 4 is the interpretation of the optimization results into a practical solution. A flow chart of the optimization is depicted in Figure 4.2. The notations used in the flow chart are explained in the following sections.

4.1 Generation of a Complete Set of Candidates

Finding optimal turnoff locations is a continuous optimization problem. That is, an optimal turnoff location can be at any place on the runway. Fortunately, theorem 1 of Appendix B shows that the optimal solutions can be found by searching through a finite set of potential turnoff locations. This set of potential solutions consists of two types of candidates : 1) primary and 2) secondary candidates. Primary candidates are the best exit locations for each aircraft,

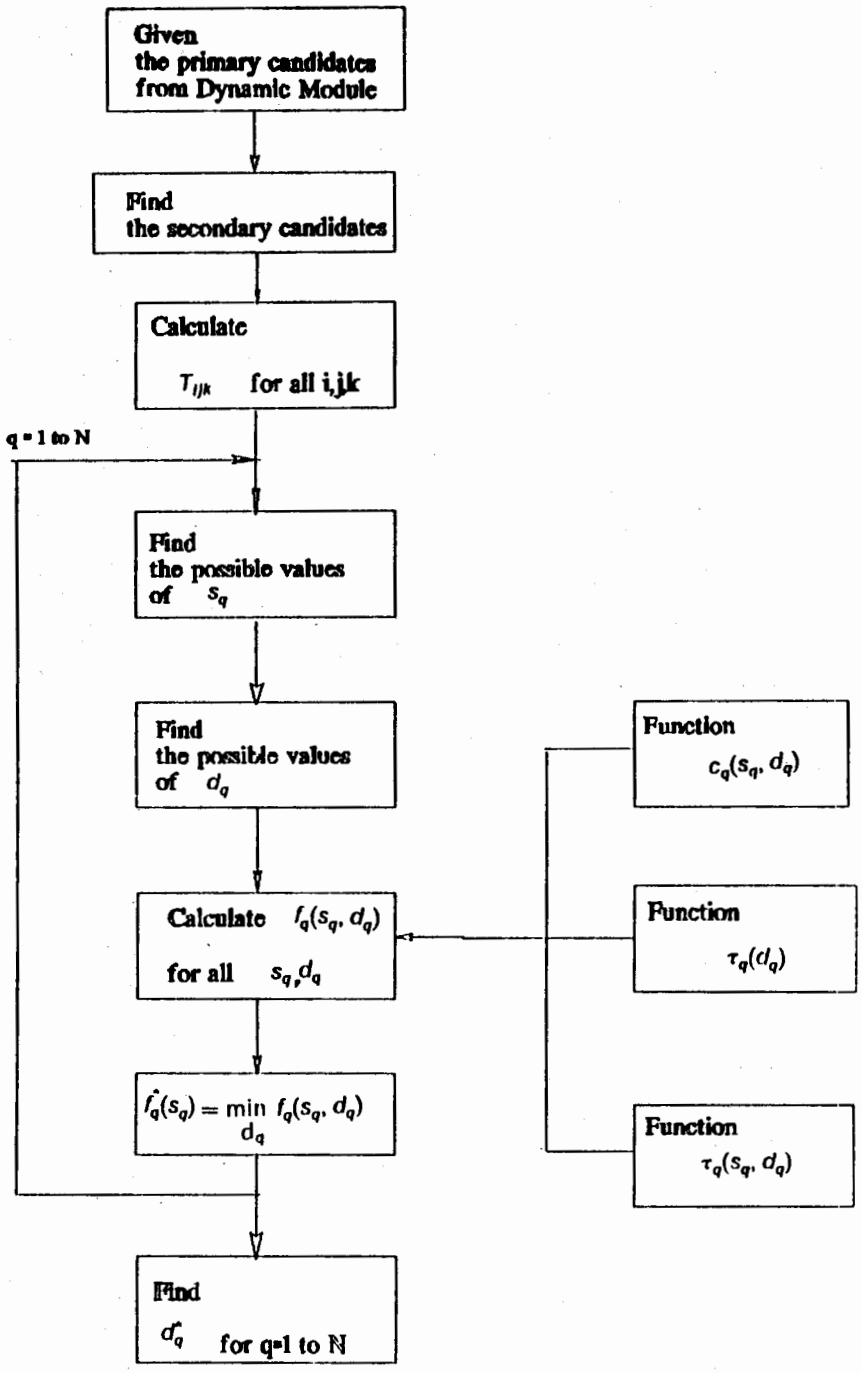

Figure 4.2 Optimization Procedure Flow Chart.

which are found during the simulations of individual aircraft landings. Secondary candidates are exit locations for each aircraft i and surface condition j located at discrete distance, D_{min}, away from a primary candidate. Secondary candidates are generated as follows :

$$l_{ij} + k \times D_{min},$$

where l_{ij} is the primary candidate for aircraft i, surface condition j.

$k = 1, 2, \cdots$

Under current FAA runway turnoff standards [FAA, 1985] two adjacent turnoffs do not affect the runway exit index unless they are separated by at least 750 ft. (229 m.) from each other. In REDIM we have added more flexibility by allowing the user to define the desired minimum distance D_{min} between adjacent exits. The primary and secondary candidates comprise the complete candidate set. Suppose a runway scenario with three aircraft in consideration, and the best locations for each aircraft and two pavement conditions are (1000, 1100, 1300,1400, 1600, 1700). In this example, the complete candidate set would be (1000, 1100, 1229, 1300, 1329, 1400, 1458, 1529, 1558, 1600, 1629, 1687, 1700). Theorem 1 of Appendix A guarantees that the optimal locations should be some of the candidate set. Thus we need to examine only the candidate set to find optimal locations instead of examining infinite points on the runway.

4.2 Estimation of Runway Occupancy Times

The simulations of landing movements provided the best exit locations for each aircraft and the corresponding times required to reach those exit locations. The complete candidates were enumerated. The next step is to find out the time required to clear runway for every aircraft for every candidate. The time is denoted as T_{ijk}. That is, T_{ijk} is defined as the runway occupancy time when aircraft i takes turnoff candidate k on surface condition j. Every T_{ijk} has three components, which are : 1) time to reach the best exit location (T_b), 2) time to travel from the best location to the candidate (T_{fr} : subscript 'fr' stands for 'free roll'.), and 3) time to clear the runway after the beginning of the turnoff (T_{off}). Figure 4.3 illustrates the components of the T_{ijk}.

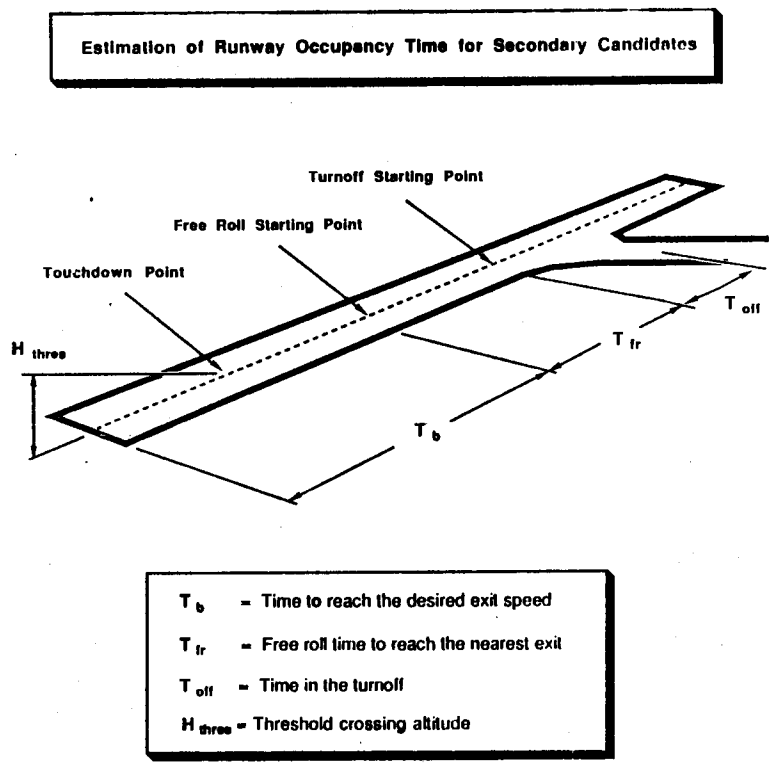

Figure 4.3 The Components of T_{ijk} Time.

If the best location of aircraft i is farther downrange than turnoff candidate k from the runway threshold, T_{ijk} would be set as 0, which means aircraft i is not able to take turnoff candidate k. Otherwise, T_{ijk} would be calculated as the sum of T_b, T_{fr}, and T_{off}. T_b is calculated during the simulations. T_{fr} is calculated assuming that the aircraft coasts on the runway 'without braking' until the speed of the aircraft is reduced to the taxiing speed which is specified by the user. 'Without braking' implies the rolling friction coefficient , f, is equal to 0.03 (i.e. deceleration rate is 9.81 m/s ^{2} (g) * 0.03 (f) = 0.2943 m/s ^{2}). Once taxiing speed is reached, the aircraft is assumed to travel on the runway with constant speed which is same as taxiing speed.

Suppose the best turnoff location of aircraft i and T_b are calculated as 1000 m and 35 seconds, respectively with the following input parameters :

- Desired exit speed = 30 m/s
- Taxiing speed = 7 m/s.

The distance to reach taxiing speed would be :

$D = (30^2 - 7^2) / (2 \times g \times f)$, where $g=9.81$, $f=0.03$

$= 1445$ m.

If another candidate k is located 1300 m downrange from the runway threshold, , then T_{fr}, the travel time to reach the new candidate would be :

$$T_{fr} = \frac{(2 \times D_{fr})}{(V_i + V_t)},$$

where D_{fr} is free roll distance (300 m),

V_i is initial speed (30 m/s),

V_t is terminal speed ($\sqrt{V_i^2 - 2gfD_{fr}} = 26.9$ m/s)

$= 10.5$ seconds.

The calculation of T_{off} is closely related to the turnoff geometry . That is, T_{off} is the travel time along the turnoff geometry from the beginning of the turn to the clearance of the runway. For the exact calculation, a numerical integration requiring large computational times is needed. Moreover, this integration should be executed for every T_{ijk}, unless T_{ijk} is set as 0. T_{off} is therefore approximated by the method described in Appendix B, to reduce the computation time. T_{off} usually ranges from 8 seconds to 13 seconds according to the size and exit speed of the aircraft (for moderate exit angles).

4.3 Finding Optimal Locations

In this section, a technique to find optimal turnoff locations is described. The final goal is to find a given number of turnoff locations which minimize the total weighted sum of ROT from the set of candidates. The number of turnoff is provided by the user. The optimization task can be modeled as a specific linear programming model. A dynamic programming algorithm is

applied to find the solution, since the dynamic programming algorithm is more efficient than the ordinary linear programming algorithm for our case.

4.3.1 Mathematical Model

Suppose M different types of aircraft use a runway, then 2 M different turnoff locations would be calculated for every aircraft and two runway surface conditions (dry and wet) during the simulation of landing movements. A complete set of exit candidates, which is indexed k = 1 to K, is generated based on the 2 M initial locations. It is not always permissible to assign aircraft i on surface condition j to candidate k. Let us define A(i,j) as a set of feasible candidates for aircraft i on the surface condition j, for i=1 to M, j=1 to 2. If candidate k is nearer from the threshold than the primary candidate for aircraft i and surface condition j, the candidate k does not belong to A(i,j).

If exit candidate k is selected to be built, the candidates which are within D_{min} (229 m or 750 ft) from the candidate k can not be constructed. Let us define S(k) as the mutually exclusive set of candidates in which at most one candidate can be selected to be built, for k = 1 to K.

In order to the minimize the weighted sum of ROT, information about weights should be provided by the user. Let a_i be the proportion of aircraft i for i = 1 to M, and let p_j be the probability of occurrence of the surface condition for j = 1 to 2 (if j=1, surface condition is dry, otherwise, surface condition is wet).

Suppose the number of exits to be built is set as N. The binary decision variables are defined as follows:

$$x_k = \begin{cases} 1, & \text{if exit candidate k is selected} \\ 0, & \text{otherwise,} \end{cases} \qquad \text{for } k = 1 \text{ to } K$$

$$y_{ijk} = \begin{cases} 1, \text{ if aircraft i is assigned to the exit candidates k on surface condition j} \\ 0, \text{ otherwise,} \qquad \text{for } i = 1 \text{ to } M,\ j = 1 \text{ to } 2,\ k \in A(i,j) \end{cases}$$

Then, the model which attempts to design a feasible runway with the least total weighted runway occupancy time may be formulated as follows:

$$\textit{Minimize} \quad \sum_{i=1}^{M} \sum_{j=1}^{2} \sum_{k \in A(i,j)} a_i \, p_j \, T_{ijk} \, y_{ijk} \tag{4.1}$$

$$\textit{subject to} \quad \sum_{k \in A(i,j)} y_{ijk} = 1 \qquad \textit{for} \quad i = 1,2,\ldots,M;\ j = 1,2 \tag{4.2}$$

$$\sum_{k \in S(k)} x_k \leq 1 \qquad \textit{for} \quad k = 1,2,\ldots,K \tag{4.3}$$

$$\sum_{k=1}^{K} x_k \leq N \tag{4.4}$$

$$y_{ikj} \leq x_k \qquad \textit{for} \quad i = 1,2,\ldots,M;\ j = 1,2;\ k \in A(i,j) \tag{4.5}$$

$$\bar{x}, \bar{y} \qquad \textit{binary} \tag{4.6}$$

The objective function (Eq. 4.1) represents the aggregate expected runway occupancy time. Constraint (Eq. 4.2) requires that each aircraft type should be assigned to one (available) exit under each surface condition. Constraint (Eq. 4.3) ensures a feasible mix of exits, while constraint (Eq. 4.4) enforces a maximum limit to the total number of exits constructed. The fourth constraint (Eq. 4.5) asserts that only the constructed exits must be used, and lastly, Eq. 4.6 enforces the logical restrictions on the variables.

The same formulation given above may be used to model the problem of re-designing or modifying existing runways, by simply fixing the appropriate variables x_k to be one. This option can also be adopted for a priority enforcing choice of certain exits.

4.3.2 Dynamic Programming Formulation

Suppose the number of exits to be built is N, the number of candidates is K, and the candidates are sorted based on the distance from the threshold. For the dynamic programming (DP) formulation, one imaginary candidate need to be introduced. This imaginary candidate is indexed 0, and is located 229 m. ahead of the first candidate. The corresponding T_{ij0} is set as 0, for all (i,j). This means no aircraft can take exit 0. With the imaginary candidate, we can observe the following characteristics of T_{ijk} :

1) There exists at least one $T_{ijk} = 0$ for all (i,j).
2) If $T_{ijk_0} > 0$, then $T_{ijk} > 0$, for $k \geq k_0$, for all (i,j).
3) $T_{ijk} \leq T_{ij(k+1)}$, *for* $k \in A(i,j)$, for all (i,j).

D(k) is defined as the distance from candidate k to candidate 1. Thus D(0) = -229 m., and D(1) = 0 m. Let us define another variable, which is denoted as K_0, a candidate index beyond which at least one exit should be constructed. K_0 is determined by :

$$K_0 = \text{Max } \{ \text{ k ; } T_{ij(k-1)} = 0 \text{ for some (i,j) } \} \leq \text{K}$$

K_0 ensures that each aircraft will be assigned to an exit, even if it is the largest aircraft. With the variables defined in the previous section and above, the DP formulation is as follows :

Stages ; Stage q corresponds to a situation in which up to q exits can be located to the right of the the last exit already located. q ranges from 1 to N. For $1 \leq q \leq N$, (N-q) exits are assumed to have been constructed.

States ; The state s_q at stage q is a candidate index, and corresponds to the right most exit currently located. For $1 \leq q \leq N-1$, the possible values of s_q are l_q, • • • , K, where l_q is the smallest exit candidate index such that it is possible to

construct (N-q) exits in candidate 1, • • • , l_q subject to the D_{min} separation restriction. That is, l_q is determined by :

l_q = Min { k ; D(k) $\geq$ $(N-q) \times D_{min}$ }, and

If q = N, s_N = 0.

Decisions ; Decision d_q is another candidate index. Given stage q and state s_q, the decision, d_q , corresponds to the next exit to be constructed to the right of s_q. Let 'd_q = 0' mean that no more exits are constructed. Then the possible values of d_q are 0, and L_q, •••, K, *for* $1 \leq q \leq N-1$, where L_q is the smallest exit index such that D(L_q) - D(l_q) $\geq$ D_{min}, if it exists, for q = N, L_N = 1.

Given any stage q and state s_q, all aircraft-surface condition combinations (i,j) for which T_{ijs_q} > 0 would have been assigned to some existing exit, due to the characteristics of T_{ijk}. Hence, the problem decomposes into locating up to q more exits to the right of s_q with the minimum separation constraint, considering only (i,j) combinations whose T_{ijs_q} = 0. which implies that (i,j) is not yet assigned. Since the optimum of this decomposed problem is independent of the previous decision, and depends only on q and s_q, Bellman's principle of optimality holds, and thus, the DP application is valid.

With the stage, the state, and the decision defined above, some functions need to be defined for the complete DP formulation. These are :

Immediate return function

The return function $c_q(s_q, d_q)$ is the 'immediate' stage cost incurred by making decision, d_q, at stage q in state s_q. This cost corresponds to the additional (i,j) assignments which can be made with a given d_q. Hence,

$$\infty, \qquad \text{if } D(d_q) - D(s_q) < D_{\min}, \text{ and } d_q \neq 0$$

$$c_q(s_q, d_q) = \sum_{\{(i,j):\, T_{ijs_q} = 0,\ \text{but } T_{ijd_q} > 0\}} a_i p_j T_{ijd_q}, \qquad \text{if } D(d_q) - D(s_q) \geq D_{\min}, \text{ and } d_q \neq 0 \qquad \{4.7\}$$

$$0, \qquad \text{if } d_q = 0$$

Stage transition function

$$\tau_q(d_q) \begin{cases} q - 1, & \text{if } d_q \neq 0 \\ 0, & \text{if } d_q = 0 \end{cases} \qquad \{4.8\}$$

State transition function

$$\tau_q(s_q, d_q) \begin{cases} d_q, & \text{if } d_q \neq 0 \\ s_q, & \text{if } d_q = 0 \end{cases} \qquad \{4.9\}$$

Recursive formula

Defining $f_q^*(s_q)$ to be the optimal accumulated return function with given input state s_q at stage q, the recursive formula would be:

$$f_q^*(s_q) = \underset{d_q}{\text{minimum}} \{ c_q(s_q, d_q) + f^*_{\tau_q(d_q)}(\tau_q(s_q, d_q)) \}, \qquad \{4.10\}$$

where the final condition is

$$f_0^*(s_0) = \begin{cases} \infty, & \text{if } s_0 < K_0 \\ 0, & \text{otherwise} \end{cases} \qquad \{4.11\}$$

By iterating the recursive formula (4.10) with q from 1 to (N-1), we can find the optimal accumulated return (minimum weighted sum of ROT) for all possible states for each stage. At the final iteration, or the last stage (q = N), the overall weighted sum of ROT is minimized, and then a sequence of optimal decisions, d_q^* (q = 1, • • , N), which minimizes the overall

weighted sum of ROT is revealed. These d_q^*'s are the optimal exit candidate indices which we are looking for.

4.4 Aircraft Exit Assignment

By the DP technique, the optimal exit locations are found. The final step in the optimization sequence is to assign every aircraft-surface condition combination, (i,j), to an appropriate exit. This step is performed by making (i,j) to take the exit which is permissible and requires minimum ROT.

4.5 A Simple Example

In this section, a simple example is discussed to illustrate the optimization procedure developed previously. Suppose three aircraft use a single runway, where two exits will be constructed. The aircraft types and the relative frequncies of operation are : 1) Learjet-31 (30%), 2) Airbus A300-600 (30%), and 3) Boeing B767-300 (40%). The desired exit speed for all the three aircraft is 30 m/s (67 MPH). The exit reliability factor is 90%. The chances of dry and wet conditions occcuring are same (i.e., 50% each). With these data, the simulation of landing movement calculates six primary exit candidates for three aircraft and two runway surface conditions. That is, the best exit location for the Learjet-31 on dry surface is 906 m, and on wet surface is 968 m. 1546 m is the best location for the A300-600 on dry surface, and 1711 m is the best location under wet condition. The best location for B767-300 is 1638 m on dry surface, and 1816 m on wet surface. The corresponding ROT's are 26.9, 28.5, 40.8, 44.6, 42.3, 46.4 seconds, respectively, as seen on Table 4.1.

Based on the primary candidates and assuming an arbitrary minimum separation distance (D_{min}) of 213 m. (700 ft.), eight more secondary candidates are found to comprise the complete candidate set. These fourteen exit candidates are : are 906m, 968m, 1119m, 1181m,

1332m, 1394m, 1545m, 1546m, 1607m, 1638m, 1711m, 1758m, 1795m, and 1816m (**STEP 1**). A T_{ijk} matrix is calculated as shown in Table 4.1 (**STEP 2**). The optimization is performed with the T_{ijk} data, and then 968m and 1816m are selected as optimal exit locations (**STEP 3**). Finally, the aircraft are assigned to the selected exit locations as shown in Table 4.2, the weighted average ROT is calculated as 43.2 seconds.

4.6 Modified Algorithm for 'Improvement' Analysis

The optimization algorithm described in section 4.1 to 4.4 was developed for design analysis which assumed no exits were available on the runway. With some modifications, this algorithm can be applied to an improvement analysis scenario in which some exits already exist on the runway and a few more exits will be added to reduce the ROT.

In this new procedure, the existing exit locations as well as the best locations are considered as primary candidates. The complete candidates are generated with the same principles used in design analysis, and then the candidates which are located within the $\pm D_{min}$ range from the existing exits are eliminated. Stages, states, and decisions of DP formulation are same as those of the design analysis. The immediate return function should be changed to consider the effect of the existing exits. Suppose the ROT of aircraft i should be accumulated as an immediate return of a decision, d_q, associated with a state, s_q. If there are some existing exits in the region of (s_q, d_q), and a existing exit requires less ROT than d_q does, then the less ROT required by the existing exit is considered as an immediate return.

Table 4.1 T_{ijk} Data for Three Aircraft.

EXIT #		1	2	3	4	5	6	7	8	9	10	11	12	13	14
LOCATION	(m)	906	968	1119	1181	1332	1394	1545	1546	1607	1638	1711	1758	1759	1816
Learjet-31	dry	27.00	29.36	35.05	37.49	43.77	46.49	53.58	55.37	58.49	60.11	64.66	67.50	67.58	71.19
	wet	0.00	28.62	34.17	36.55	42.64	45.27	52.09	53.82	56.80	58.35	62.66	65.32	65.34	68.77
Airbus 300	dry	0.00	0.00	0.00	0.00	0.00	0.00	0.00	41.01	43.27	44.43	47.67	49.57	49.62	51.96
	wet	0.00	0.00	0.00	0.00	0.00	0.00	0.00	0.00	0.00	0.00	44.89	46.66	46.71	48.88
Boeing 767	dry	0.00	0.00	0.00	0.00	0.00	0.00	0.00	0.00	0.00	42.77	45.9	47.73	47.78	50.03
	wet	0.00	0.00	0.00	0.00	0.00	0.00	0.00	0.00	0.00	0.00	0.00	0.00	0.00	46.91

Table 4.2 Aircraft Assignments

ROT / RELIABILITY TABLE
(This is for Designing a New Runway)

Exit #	1	2
Location (m)	968.6	1816.8
Exit Type	New	New
LEARJET-31		
DRY ROT (20.0%)	29.36	
WET ROT (20.0%)	28.62	
A-300-600		
DRY ROT (20.0%)		51.96
WET ROT (20.0%)		48.88
B-767-300		
DRY ROT (20.0%)		50.03
WET ROT (20.0%)		46.91

ROT - Runway Occupancy Time in Secs
Reliability in % = 90
Average ROT = 43.21

5.0 Output Module

The Output Module plays a very significant role in the program. REDIM is structured so that at each stage the user is prompted with specific questions and guidelines that are to be followed in order to view the appropriate results. A significant feature in this module is that in each of the runmodes, all the screens clearly display information regarding the aircraft and the airport data. This information provided at the top of each of the screens, will be of great use to the user as (s)he will be presented with the general information pertaining to that type of analysis. The Output Structure is shown in terms of a Output functional flow diagram in Fig. 5.1.

After defining the variables in the Input Module, the user may go back to the Main Menu. From this menu, the user has the option to go to the Output Menu among other options. When the user chooses to go to the Output Menu, (s)he is provided with four options. The options being: (1) View the Output (2) Print the Report (3) Help and (4) Go to Main Menu. Fig. 5.2 clearly depicts the Output Menu on the screen. In the following paragraphs, all the options that are provided to the user in the Output Menu will be discussed in detail.

5.1 View the Output

When the user selects this option, the program automatically goes into the runmode variable that was previously specified by the user in the Input Module and present the View Menu screen which corresponds to the aforesaid option. For each of the runmode variable options, the program presents different screens which prominently display the results in color, while at the same time guiding the user. Each screen also displays the general input variables that were initially provided by the user in the Input Module. The user at any stage in the Output Module is allowed to go back to the Main Menu, through which a wide range of options can be chosen. Now we will go into each of the runmode variable option and see

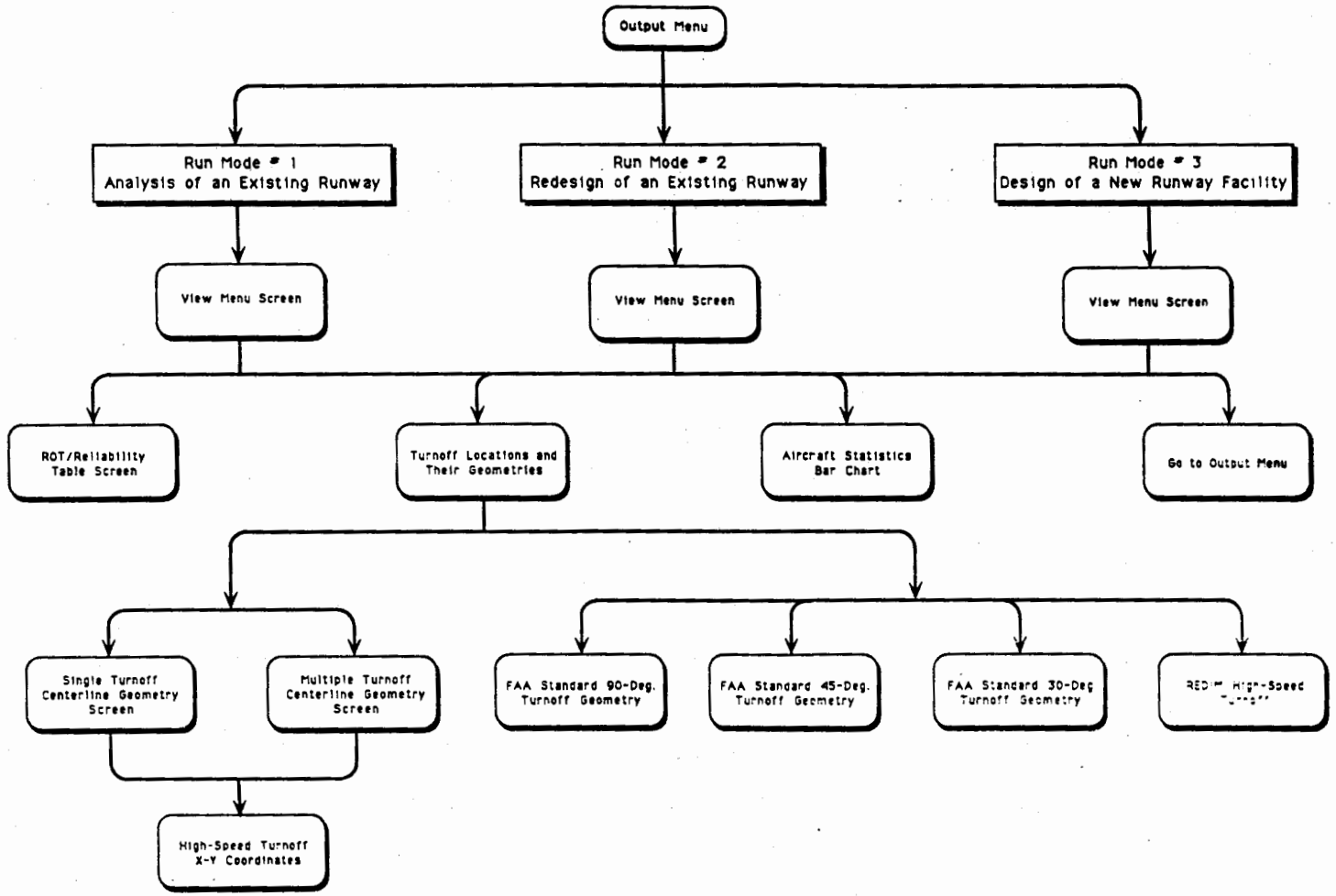

Figure 5.1 Output Functional Flow Diagram.

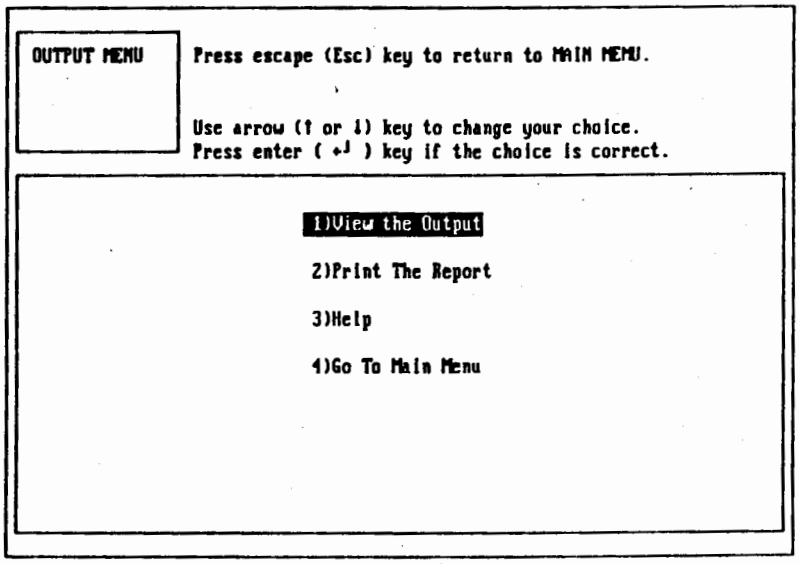

Figure 5.2 Output Menu.

explicitly as to what is presented, and also the extent of flexibility that is made available to the user.

5.1.1 Evaluate an Existing Runway

This runmode is specifically designed to evaluate and existing runway. The data required to evaluate an existing runway is entered by the user in the Input Module. As the user selects to view the Output from the Output Menu (Fig. 5.2), (s)he is provided with a different screen which displays the View Menu (Fig. 5.4). This View Menu corresponds to the runmode option which is used to evaluate an existing runway. Three options are provided in this menu. The options being (1) ROT / REL Table of Results (2) Turnoff locations and their Geometries and (3) Go to Output Menu. The flow pattern for this runmode option is shown in Fig. 5.3 and the View Menu screen is illustrated in Fig. 5.4. In the following paragraphs, we will discuss in detail these options.

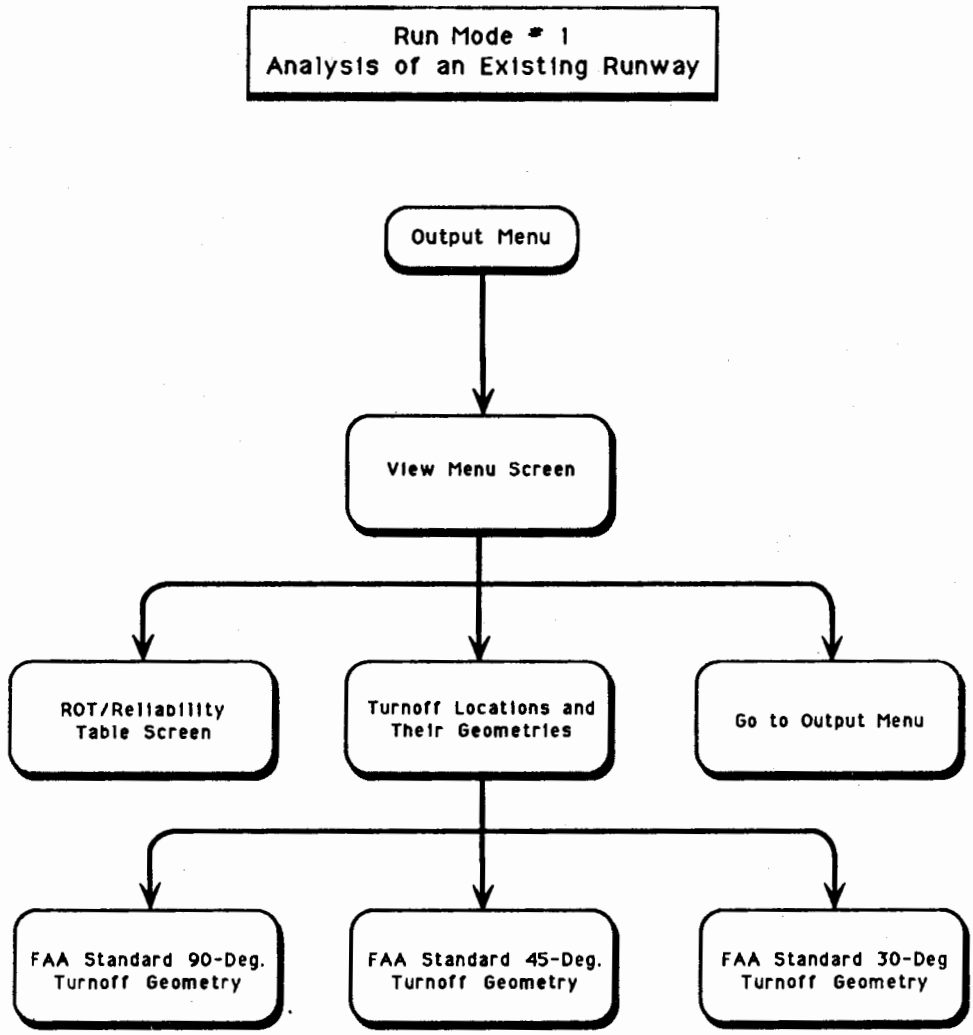

Figure 5.3 Functional Flow Diagram for the Evaluation Mode (Runmode 1).

```
VIEW MENU        Press escape (Esc) key to return to OUTPUT MENU.

                 Use arrow (↑ or ↓) key to change your choice.
                 Press enter ( ↵ ) key if the choice is correct.

                 1)View ROT Table

                 2)View Turnoff Locations And Their Geometries

                 3)Go To Output Menu
```

Figure 5.4 View Menu for 'Runmode 1'.

ROT / RELIABILITY TABLE
(This is for Evaluating an Existing Runway)

Exit # / Location (m) / Exit Type	1 1000 30-Deg	2 2000 45-Deg	3 3000 30-Deg
PA-38-112			
DRY ROT	42.53	125.21	225.21
(12.5%) REL	1.00	0.00	0.00
WET ROT	42.41	124.73	224.73
(12.5%) REL	1.00	0.00	0.00
BE-300			
DRY ROT	29.02	87.11	188.13
(12.5%) REL	0.84	0.16	0.00
WET ROT	29.43	83.24	183.61
(12.5%) REL	0.74	0.26	0.00
A-320-200			
DRY ROT	30.93	51.52	128.17
(12.5%) REL	0.00	0.99	0.01
WET ROT	32.11	47.58	113.72
(12.5%) REL	0.00	0.93	0.07
MD-11			
DRY ROT	34.78	48.44	83.77
(12.5%) REL	0.00	0.22	0.78
WET ROT	36.54	50.30	73.64
(12.5%) REL	0.00	0.02	0.98

ROT - Runway Occupancy Time in Secs
REL - Reliability
Average ROT = 63.97

Press any key to continue

Figure 5.5 ROT / Reliability Table of Results.

ROT / Reliability Table of Results: This screen, shown in Fig. 5.5, displays the number of turnoffs, their location, and the type of turnoffs. The FAA standard turnoffs, 30 degree, 45 degree and 90 degree are illustrated in Figs. 5.7, 5.8 and 5.9, respectively. For each of the aircraft selected earlier in the Input Module, the corresponding runway occupancy time and the reliability associated with each of the turnoffs is displayed. These help the user in judging the appropriate turnoff for that particular aircraft. One more significant feature in this table is the separation of the values for wet and dry airport conditions. The user is also in a position to view the changes in runway occupancy time and the reliability associated with each of the turnoffs when two runway conditions (wet or dry) are present. In addition to these, the relative frequency of occurrence for every aircraft under every runway scenario is specified as a percentage of all the aircraft occurrences. This table is shown in Fig. 5.5.

In each screen as only four aircraft are shown, it is necessary to press 'F' key (for forward) to view additional aircraft and 'B' key (for backward) to view the previous screen. In each of the screens the viewer is presented with the average runway occupancy time which encompasses the whole population of aircraft selected by the user. These include dry and wet conditions at the airport. An option is provided to print the table by just pressing the 'P' key (for print). The user is also allowed to go back to the View Menu at any stage by entering 'V' key (for View Menu).

Turnoff Locations and their Geometries: In this screen, shown in Fig. 5.6, t the user is presented with the display of turnoff locations along with other pertinent airport data. The turnoff locations along the runway downrange are shown in Fig. 5.6. An added feature is the presentation of exit numbers and their location in a tabular form. An option to view the standard FAA geometry for each of the turnoffs is also provided. The user is prompted to enter the exit number to view the standard FAA geometry. Each of the turnoffs may represent any of the standard FAA geometries viz., 30 degree or 45 degree or 90 degree. Only one exit number is to be entered to view the complete turnoff geometry. As the exit number is entered, the program determines the type of turnoff for the exit number from the Input Module. Earlier, in the Input Module, the user selected the type of turnoff geometry for a particular exit number. This turnoff geometry may represent any of the three standard FAA turnoff geometries shown

in Figs. 5.7, 5.8 and 5.9 respectively. After viewing the standard FAA turnoff geometry for the specified turnoff, the user is returned to the first screen where a choice for a different exit can be made. This screen would appear as shown in Fig. 5.5. The user may exit from this screen by entering '0' (zero).

When the user selects to view the standard turnoff geometry for a particular turnoff, the program automatically takes in the values of runway width, taxiway width, the distance between the runway and taxiway and the type of turnoff. This data was earlier supplied by the user in the Input Module. In the standard FAA turnoff geometry display, the specifications are prominently shown for the benefit of the user. Although, the Metric system is mainly used for computations in the program, the units for specifications are also displayed in the English system. This helps the user who might be still using the FAA standards in the English system.

Go to Output Menu: This option is provided to enable the user to go back to the Output Menu from the View Menu. The user may also exercise this option by pressing the escape 'Esc' key.

5.1.2 Improve an Existing Runway

This runmode option is made available to the user to improve or modify an existing runway. The required data of the airport facility that needs to be improved is entered in the model through the Input Module. The user after entering the data may go to the Output Menu through the Main Menu. The Output Menu screen is as shown in Fig. 5.2. and the flow pattern for this runmode option is shown in Fig. 5.10. As the user selects to view the output from the Output Menu, he or she is presented with the View Menu screen. This View Menu screen corresponds to the runmode option which is to improve an existing facility. The View Menu screen is provided with four options: (1) ROT Table of Results, (2) Turnoff Locations and their Turnoff Geometries, (3) Aircraft Statistics and their ROT's, and (4) Go to Output Menu. The view menu screen is shown in Fig. 5.11. In the following paragraphs, we will discuss in detail each one of the above said options.

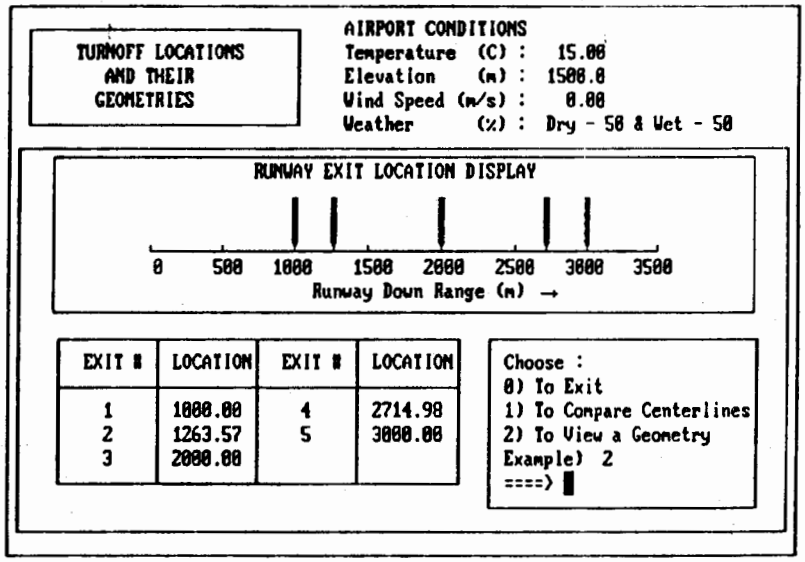

Figure 5.6 Turnoff Locations along the Runway Downrange.

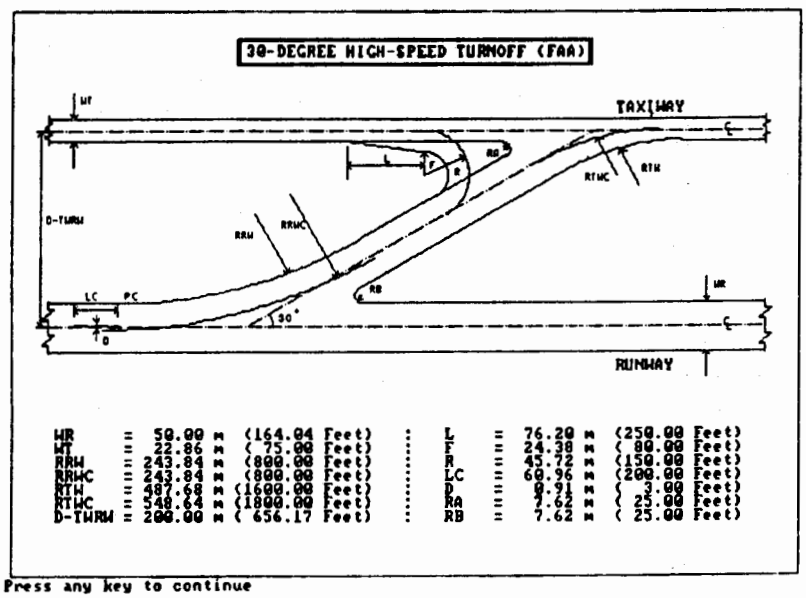

Figure 5.7 Standard FAA 30-Degree Turnoff Geometry (REDIM Depiction).

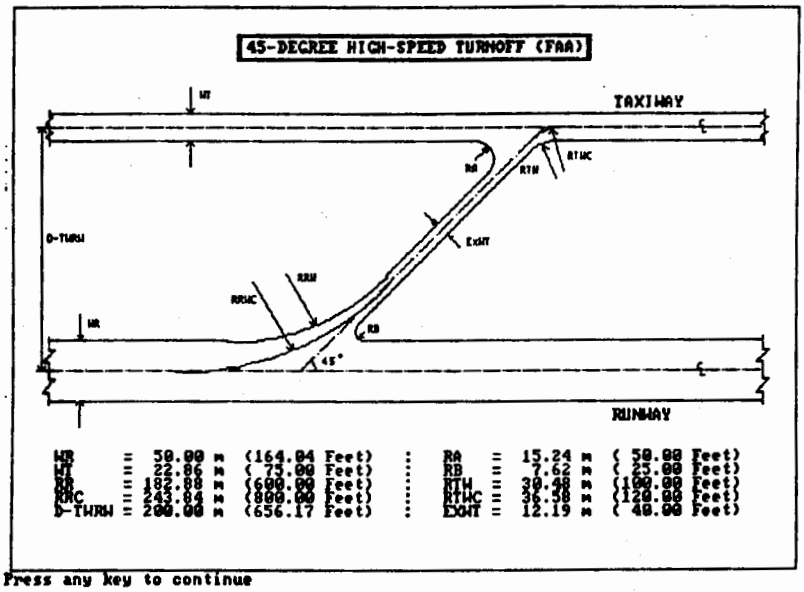

Press any key to continue

Figure 5.8 Standard FAA 45-Degree Turnoff Geometry (REDIM Depiction).

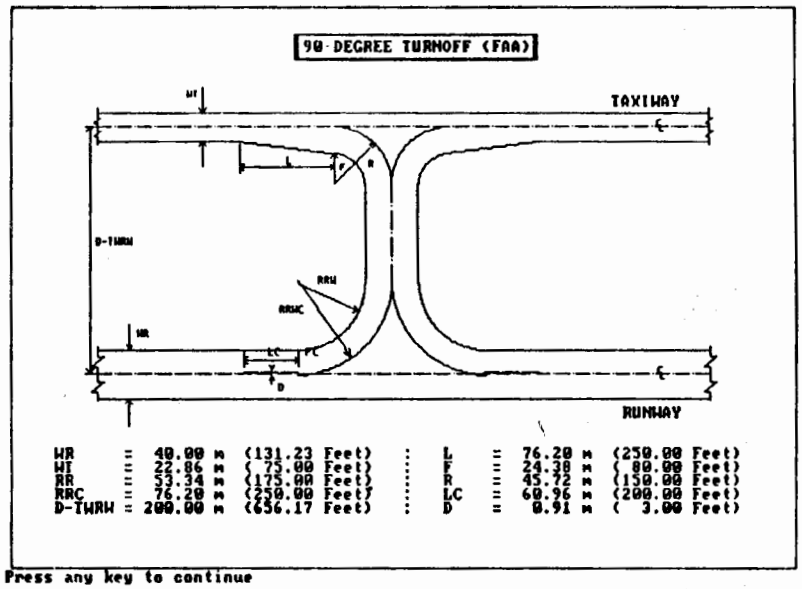

Press any key to continue

Figure 5.9 Standard FAA 90-Degree Turnoff Geometry (REDIM Depiction).

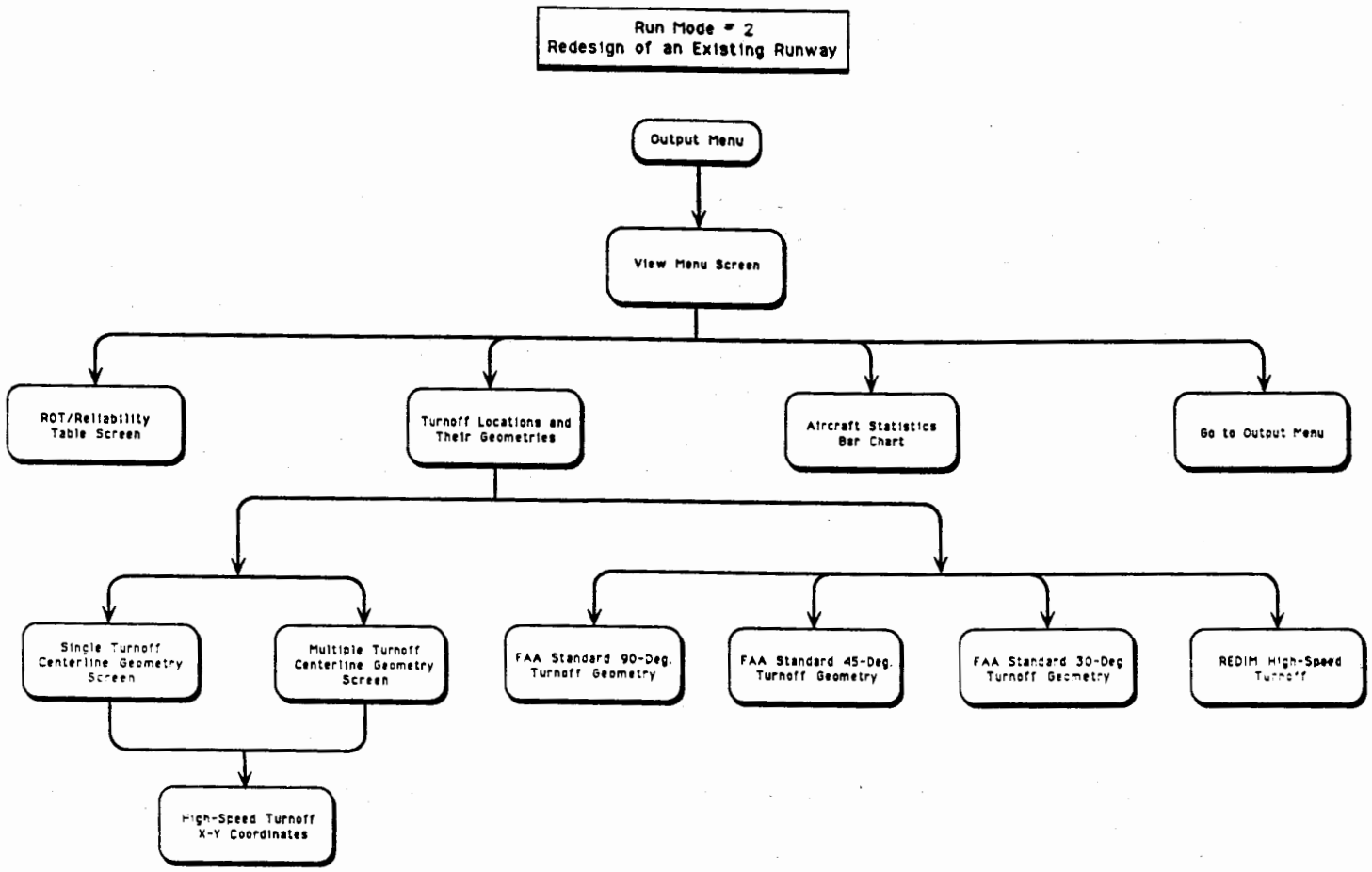

Figure 5.10 Functional Flow Diagram for Runmode '2'.

ROT Table of Results: This table displays the number of turnoffs, the existing and the proposed ones, and their locations in a format similar to that of Fig. 5.12. The type of turnoff geometry is also displayed in the third row of the table. The type of turnoff geometry either could be of standard FAA turnoff geometry viz., 30 degree or 45 degree or 90 degree, for the existing ones or a new turnoff geometry developed by the model for the proposed new ones. The new turnoffs are differentiated from the existing ones through color coding. This helps in knowing the location of new turnoffs at a simple glance. For each of the aircraft selected earlier in the Input Module, the corresponding runway occupancy time associated with the appropriate turnoff is displayed. The relevant values for both the airport conditions, wet and dry are displayed. The user is also in a position to view the change in runway occupancy time associated with appropriate turnoff when the airport conditions (wet or dry) are changed. In addition to these, the relative frequency of occurrence of this aircraft, for a particular scenario (wet or dry conditions) is specified as a percentage of all the aircraft occurrences. The empty boxes in the table imply that the aircraft in question cannot negotiate that particular turnoff. The reliability associated with the aircraft and turnoff, which was earlier provided by the user in the Input Module, is displayed at the bottom of the table.

In each screen, as only four aircraft are shown in the table, it is necessary to press 'F' key (for forward) to view additional aircraft and 'B' key (for backward) to view the previous screen. In each of the screens the user is presented with the average runway occupancy time which encompasses the whole population of aircraft selected by the user. These include dry and wet conditions at the airport. The user is provided with an option to print the table by just pressing the 'P' key (for print). The user is also allowed to go back to the View Menu at any stage by entering 'V' key (for View Menu). Figure 5.12 illustrates and ROT table with four aircraft.

Turnoff Locations and their Geometries: In this screen (Fig. 5.5), the user is presented with a graphical display of turnoff locations along the runway downrange. In the display, the existing turnoffs as well as the proposed turnoffs are shown. The new turnoffs are differentiated from the existing ones through color coding. This enables the user in noticing the location of new

```
VIEW MENU        Press escape (Esc) key to return to OUTPUT MENU.

                 Use arrow (↑ or ↓) key to change your choice.
                 Press enter ( ↵ ) key if the choice is correct.

                 1)View ROT/REL Table

                 2)View Turnoff Locations And Their Geometries

                 3)View Aircraft Statistics

                 4)Go To Output Menu
```

Figure 5.11 View Menu for Runmodes '2' & '3'.

ROT / RELIABILITY TABLE
(This is for Designing a New Runway)

Exit # / Location (m) / Exit Type	1 / 1110.8 / New	2 / 1964.2 / New	3 / 2715.0 / New
PA-38-112			
DRY ROT (12.5%)	46.88		
WET ROT (12.5%)	46.74		
BE-300			
DRY ROT (12.5%)	31.39		
WET ROT (12.5%)	30.46		
A-320-200			
DRY ROT (12.5%)		49.63	
WET ROT (12.5%)		45.98	
MD-11			
DRY ROT (12.5%)			67.36
WET ROT (12.5%)			60.87

ROT - Runway Occupancy Time in Secs
Reliability in % = 90
Average ROT = 47.41

Figure 5.12 ROT Table of Results.

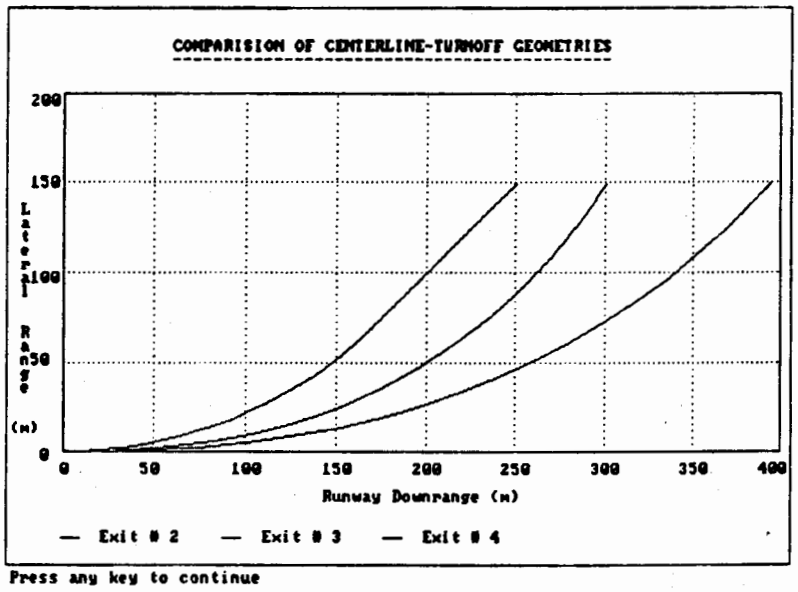

Figure 5.13 Comparison of Centerline Turnoff Geometries.

turnoffs along the runway downrange. An added feature in this screen is the presentation of exit numbers and their location in a tabular form.

On the same screen, depicted in Fig. 5.5, a small menu screen is provided with options to view the complete turnoff geometry or to compare the centerline geometries. For the latter option, the user needs to input the exit number(s). The user has the flexibility to select any combination of exit numbers for comparing the geometry of different turnoffs or may even select only one exit number to view the centerline geometry of a particular turnoff. Fig. 5.13 illustrates the output screen for the comparison of turnoff geometries. It should, however, be noted that all the requested turnoff geometries start at a common point for comparison purposes. Also, as can be seen from Fig. 5.15, the user has the benefit to view the centerline turnoff geometry coordinates in a tabular form for each of the turnoffs. The user needs to press 'T' to view the table with coordinates of centerline turnoff geometry from the screen which displays the centerline turnoff geometry. If the user does not intend to view the coordinates, (s)he may press 'E' (for exit location) to return to the turnoff locations screen.

The user after returning to the previous screen, which depicts the small menu, may now view the centerline turnoff geometry or the complete turnoff geometry. The user may either select to view the complete turnoff geometry or may even again choose to view the centerline turnoff geometry for a different combination of turnoffs. When the user selects to view the complete turnoff geometry, the program requests the user to enter the exit number to be displayed. Here, the user needs to input only one exit number and not any combination of exit numbers. The program displays the complete turnoff geometry of that specific exit number entered by the user. For the exit number entered by the user, the program internally determines the type of turnoff geometry. The type of turnoff geometry can be either of the 30 degree or 45 degree or 90 degree standard FAA turnoff for the existing turnoffs or can be a new turnoff geometry developed by the model for the proposed new turnoff(s). The FAA standard 30 degree, 45 degree and 90 degree are best illustrated in Figs. 5.7, 5.8 and 5.9 respectively. The new turnoff geometry developed by the model for the proposed new turnoff is shown in Fig. 5.16. The user after viewing the complete turnoff geometry of the turnoff requested, may return back to the turnoff location and their geometries screen where (s)he may again enter a different turnoff to view its complete turnoff geometry.

When the user selects to view the standard turnoff geometry for a particular turnoff, the program automatically takes in the values of runway width, taxiway width, the distance between the runway and taxiway, the type of turnoff and other data supplied in the Input Module. In the standard FAA turnoff geometry display, the specifications are prominently shown, and the units are displayed in both English and Metric systems for the benefit of the user.

Aircraft Statistics and their ROT's: This screen displays the runway occupancy time of each of the aircraft in the form of a bar chart. At the top edge of each of the bars, the aircraft number is displayed. For each of the aircraft, selected by the user in the Input Module, the runway occupancy time is separately displayed for wet and dry runway surface conditions. For the benefit of user, the bars representing the aircraft and its name are of the same color. On the bar chart, a straight line is drawn across the bars to portray the average ROT.

In each screen a maximum of six aircraft are shown, each with two bars, one for wet condition and the other for dry condition. It is necessary to press 'F' key (for forward) to view additional aircraft and 'B' key (for backward) to view the previous screen. In each of the screens, the average runway occupancy time which encompasses the whole population of aircraft selected by the user is shown. This includes dry and wet conditions at the airport. An option is provided to print the table by just pressing the 'P' key (for print). The user is also allowed to go back to the View Menu at any stage by entering 'V' key (for View Menu). The bar chart is illustrated in Fig. 5.17.

Go to Output Menu: This option is provided to enable the user to go back to the Output Menu from the View Menu. The user may also exercise this option by pressing the escape 'Esc' key.

5.1.3 Design of a New Runway

This runmode deals with the design of a new runway facility. The user is requested to enter the relevant data in the Input Module for the design of a new runway facility. The user after entering the data in the Input Module is returned to the Main Module. The user at this point may go to the Output Menu to view the results. The Output Menu is as shown in Fig. 5.2. and the flow pattern corresponding to this runmode option is shown in Fig. 5.15. As the user selects to view the output from the Output Menu, he or she is presented with a new screen which displays the View Menu screen. This View Menu screen corresponds to the runmode option which is to design a new runway facility. Four options are provided in the View Menu. The options are (1) ROT Table of Results (2) Turnoff Location and their Geometries (3) Aircraft Statistics and their ROT's, and (4) Go to Output Menu. The View Menu screen is best illustrated in Fig. 5.11. In the following paragraphs, we will discuss in detail each of these options.

ROT Table of Results: This table displays the number of new turnoffs for the proposed new runway facility and their locations. As none of the standard FAA turncffs are proposed in the new runway, the type of turnoff geometry is described as a new turnoff geometry developed

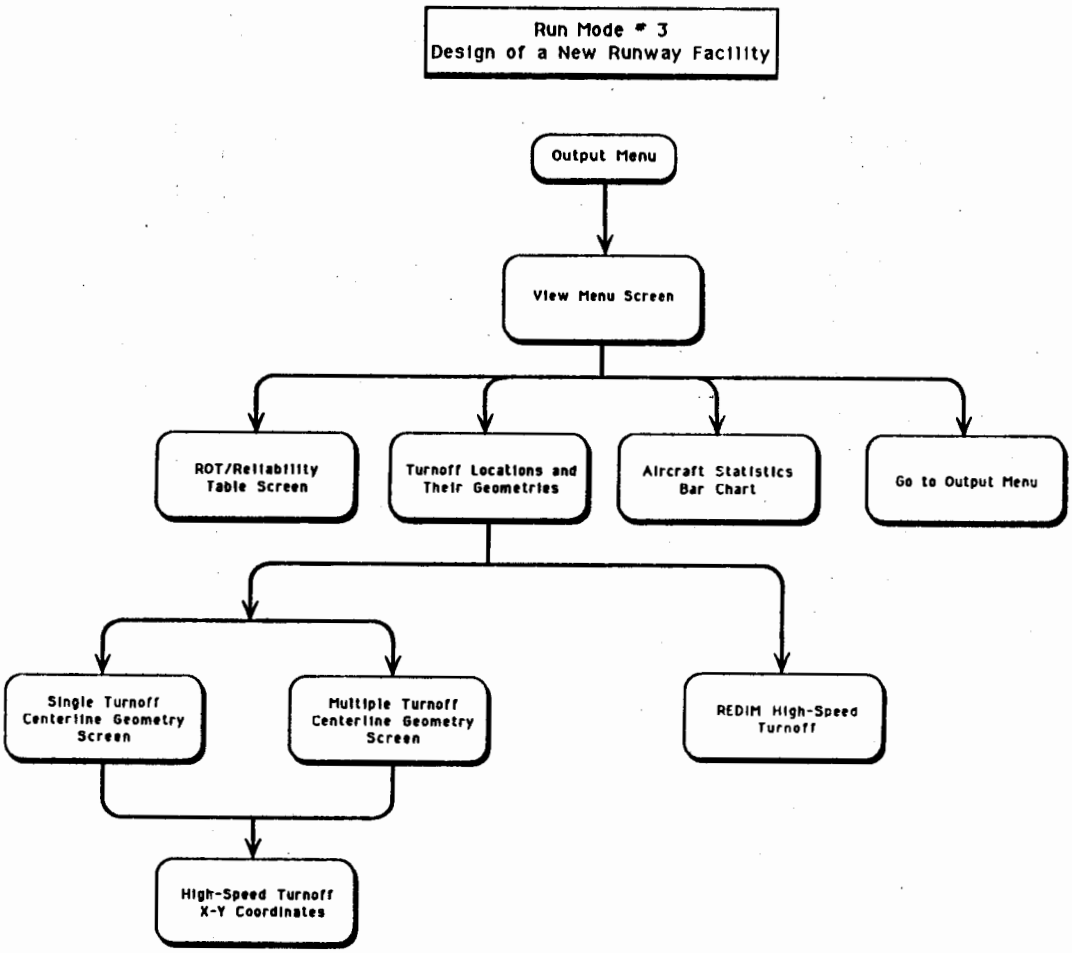

Figure 5.14 Functional Flow Diagram for Runmode '3'.

AIRPORT CONDITIONS			AIRCRAFT POPULATION		
Temperature	(C)	: 15.00	TERP A	:	25.00
Elevation	(m)	: 1500.0	TERP B	:	30.00
Wind Speed	(m/s)	: 0.00	TERP C	:	30.00
			TERP D	:	15.00

RUNWAY TURNOFF GEOMETRY COORDINATES FOR EXIT # 2

X	Y	X	Y	X	Y
27.500	0.009	97.306	4.723	165.897	18.416
44.994	0.508	114.620	7.259	182.696	23.316
52.472	1.377	131.838	10.385	199.313	28.801
79.916	2.769	148.937	14.104		

Press any key to continue

Figure 5.15 Table of Turnoff Geometry Coordinates.

by the model. For each of the aircraft selected earlier in the Input Module by the user, the corresponding runway occupancy time associated with the appropriate turnoff is displayed. These values, for both wet and dry airport conditions, are displayed separately in the table. In addition to these, the relative frequency of occurrence of this aircraft, for a particular scenario (wet or dry conditions) is specified as a percentage of all the aircraft occurrences. The empty boxes in the table imply that the aircraft in question cannot negotiate that particular turnoff. The reliability associated with each aircraft and turnoff(s), which was earlier provided by the user in the Input Module, is displayed at the bottom of the table.

In each screen, as only four aircraft are shown in the table, it is necessary to press 'F' key (for forward) to view additional aircraft and 'B' key (for backward) to view the previous screen. In each of the screens the average ROT which encompasses the whole population of aircraft selected by the user is shown. This includes dry and wet conditions at the airport. An option to print the table by just pressing the 'P' key (for print) is also provided. The user

is also allowed to go back to the View Menu at any stage by entering 'V' key (for View Menu). This table is illustrated in Fig. 5.12.

Turnoff Locations and their Geometries: This screen presents the user with a graphical display of optimal turnoff locations along the runway downrange. These optimally located turnoffs are all proposed by the model for the new runway facility. A table with the exit numbers and their location is also presented on the same screen. The output screen is similar to that shown in Fig. 5.5.

On the same screen, depicted in Fig. 5.5, a small menu screen is provided with options to view the complete turnoff geometry or to compare the centerline geometries. For the comparison of centerline geometries, the user needs to input the exit number(s). This provides flexibility to select any combination of exit numbers for comparing the geometry of different turnoffs or may even select only one exit number to view the centerline geometry of a particular turnoff. Fig. 5.11 illustrates the output screen for the comparison of turnoff geometries. It should, however, be noted that all the turnoff geometries start at a common point for comparison purposes. Also, as can be seen from Fig. 5.15, the user has the benefit to view the centerline turnoff geometry coordinates in a tabular form for each of the turnoffs. The user needs to press 'T' to view the table with coordinates of centerline turnoff geometry from the screen which displays the centerline turnoff geometry. If the user does not intend to view the coordinates, (s)he may press 'E' (for exit location) to return to the turnoff locations screen.

The user after returning to the previous screen, which depicts the small menu, may now view the centerline turnoff geometry or the complete turnoff geometry. The user may either select to view the complete turnoff geometry or may even again choose to view the centerline turnoff geometry for a different combination of turnoffs. When the user selects to view the complete turnoff geometry, the program requests the user to enter the exit number to be displayed. Here, the user needs to input only one exit number and not any combination of exit numbers. The program displays the complete turnoff geometry of that specific exit number entered by the user. This high speed turnoff geometry is developed by the model for

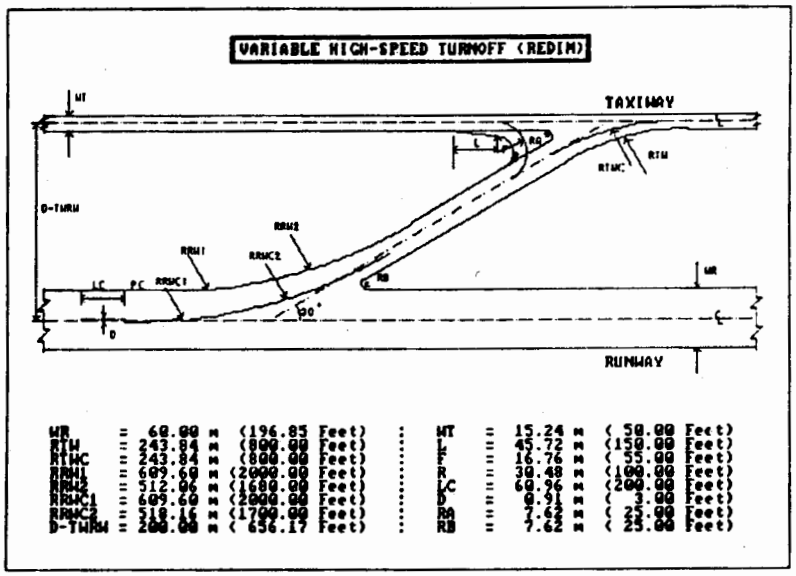

Figure 5.16 Variable Turnoff Geometry (Developed by REDIM).

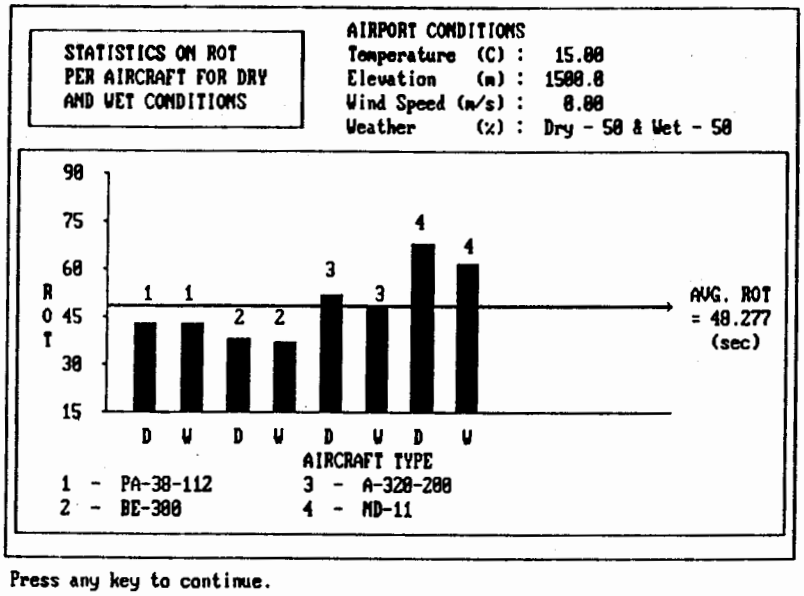

Press any key to continue.

Figure 5.17 Aircraft Statistics and their ROT's.

the proposed new turnoff(s) and is shown in Fig. 5.16. The user after viewing the complete turnoff geometry of the turnoff requested, may return back to the turnoff location and their geometries screen where (s)he may again enter a different turnoff to view its complete turnoff geometry.

When the user selects to view the standard turnoff geometry for a particular turnoff, the program automatically takes in the values of runway width, taxiway width, the distance between the runway and taxiway, the type of turnoff and other data supplied in the Input Module.

Aircraft Statistics and their ROT's: This screen displays the runway occupancy time for each of the aircraft in the form of a bar chart. At the top edge of each of the bars, the aircraft number is displayed. Each aircraft is represented by two bars. The first one represents ROT for dry condition whereas the second one represents ROT for wet runway surface condition. For the benefit of user, the bars representing the aircraft and its name are of the same color. On the bar chart, a straight line is drawn across the bars to portray the weighted average ROT.

Each screen accommodates six aircraft, each with two bars, one for wet condition and the other for dry condition. The user needs to press 'F' key (for forward) to view additional aircraft and 'B' key (for backward) to view the previous screen. In each of the screens the user is presented with the average ROT, which encompasses the whole population of aircraft selected by the user. This includes dry and wet conditions at the airport. The user is provided with an option to print the table by just pressing the 'P' key (for print). An option is provided to go back to the View Menu at any stage by entering 'V' key (for View Menu). The bar chart is illustrated in Fig. 5.15.

Go to Output Menu: This option is provided to enable the user to go back to the Output Menu from the View Menu. The user may also exercise this option by pressing the escape 'Esc' key.

5.2 *Print the Report*

This option provides a hard-copy report which is a complete report of the "Runway Exit Design Interactive Model". The report is divided into two sections. The first one deals with the summary of input data where as the second one concentrates on the results of the analysis.

The input data summary is subdivided into five categories, as done earlier in the Input Module. Category (1) 'Analysis Type and Existing Exits' gives the type of analysis selected and the number of exits, their type and their location. Category (2) 'Aircraft Mix and Characteristics' provides a table with the names of the aircraft selected and their characteristics. The characteristics of the aircraft include: wheelbase, wheeltrack, landing mass, wing area, landing run distance, load on main gear, distance of nose gear to wingtip, and the maximum clearance distance. Category (3) 'Operational Data' provides free roll times, taxiing speed and their standard deviations, and the safety factor for skid. Category (4) 'Envirionmental Data' provides the wind speed, wind direction, airport elevation, temperature, runway visual range, runway orientation, runway width and the distance to the runway. Category (5) 'Runway Gradients' provides the runway length and the gradients for every one-tenth of the runway length specified. Category (6) 'Weather and Exit Speeds' provides the weather conditions (probability of dry and wet condition) in percentage and the speeds for each of the TERP categories, both for dry and wet conditions. A sample output report is shown in Figs. 6.24 and 6.25 of this report.

In the results of the analysis section, the weighted average runway occupancy time (ROT) and a table with the number of exits, their location and their type is provided. For runmode '1', ie., for the analysis of an existing runway, the reliability associated with each of the aircraft and exit, for both dry and wet runway surface conditions is provided along with the corresponding ROT's. For runmodes '2' and '3', ie., for the improvement of an existing runway or for designing a new runway, the reliability associated with all the turnoffs is given separately. The table also provides the turnoff assignment to each of the aircraft. Another

portion of the results pertaining to runmodes '2' and '3', provides the coordinates of the centerline for each of the turnoffs.

5.3 Help

The main prupose of this option is to help the user by explaining each of the options that are made available in the Output Module. The help screen explains briefly the first option, 'View the Output' which displays the output on the screen and the second option, 'Print the Report', which gives the hard-copy of the complete report. The user may press any key to exit from this screen and return to the 'Output Menu' screen.

'Go to Main Menu' is the last option that is provided in the Output Menu. This allows the user to go back to the Main Menu from the Output Menu. The user may also exercise this option by pressing the escape 'Esc' key.

6.0 Use of the Model

The purpose of this chapter is to illustrate the use of the REDIM model and to justify the validity of the results obtained throughout the report. Perhaps one of the most important issues behind this model is the capability for the user to perform sensitivity analyses for a wide range of airfield environmental, operational, and aircraft dependent variables. As it was pointed out in Section 2.1 the model incorporates all these variables in a very interactive format to the user thus minimizing the rerun effort. Fig. 6.1 illustrates the sensitivity of the model to airfield elevation and exit speed (i.e., maintaining a constant exit probability). The results shown apply to a short-haul transport aircraft (i.e., BAe 146-200) and depict graphically the increases in runway occupancy time (ROT) as the exit speed is reduced and the airfield elevation is increased. Note that the increase in ROT with decreasing exit speed is nearly linear for the speed ranges tested (10-40 m/sec., 19.4-77.7 knots). The changes due to airfield elevation stem from the larger equivalent airspeeds (EAS) during landings at higher elevations. The magnitude of change in these results is proportional to square root the atmospheric density ratio. Following a similar treatment Fig. 6.2 shows the variations in ROT for several exit speeds and airfield temperatures for a typical short-haul transport aircraft (i.e., Bae 146-200). The sensitivity of ROT with temperatures is again deduced from the changes to the aircraft EAS as the temperature is changed. Computations are done in the model to estimate an equivalent atmosphere under the user-defined conditions and then estimate the aircraft equivalent airspeed during the landing phase.

Fig. 6.3 illustrates the sensitivities of ROT and the turnoff location parameters with changing aircraft mass. The same short-haul, turbofan engined transport aircraft (BAe 146-200) operating at a desired exit speed of 15 m/sec. is used for illustrative purposes. The values for aircraft landing mass cover the entire allowable landing mass envelope for this aircraft. It is observed that the variations in the location of the turnoff could be significant (230 meters between end points). The reader should realize, however, that in practice a large percentage of aircraft are operated in the middle of the region shown in this figure (i.e.,

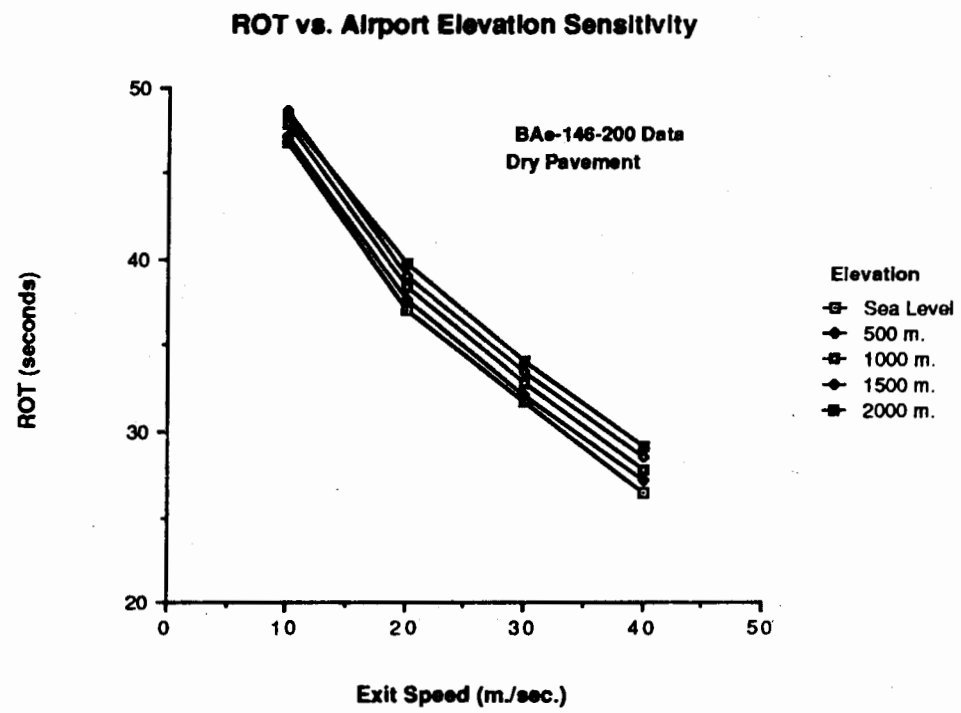

Figure 6.1 ROT Parameter vs. Exit Speed and Airfield Elevation for the BAe-146-200.

80-85% of the maximum allowable landing mass) and thus the changes to ROT and turnoff location parameters might be more constrained than those shown. These results capture the many landing performance variations observed in aircraft flight manuals in a systematic way.

6.1 *Example 1 (Evaluating a Runway Facility)*

The first example to be discussed here illustrates the use of REDIM to analyze an **existing** single-runway airport facility serving a mix of general aviation (GA), commuter and small transport aircraft. The first decision faced by the user is to select the type of analysis required

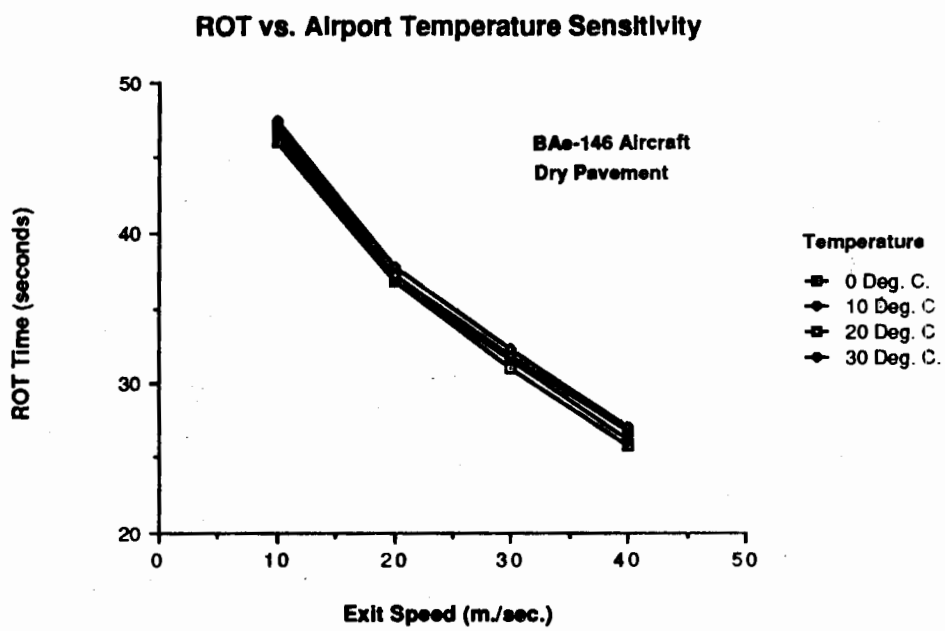

Figure 6.2 ROT Parameter vs. Exit Speed and Airfield Temperature.

for this example. Fig. 6.4 illustrates the main menu screen where the 'Start a New Problem' option is selected to initiate the user input sequence. Shortly thereafter REDIM prompts the user to name his working file. This file will be created automatically and additions will be made as the input sequence progresses. The model will ask the user to answer yes or no after every input screen to save new information. Fig 6.5 selects the type of analysis wanted which in this case corresponds to 'Evaluation of an Existing Facility'. Next in the sequence of user inputs is the definition of the physical characteristics of the existing scenario. Lets assume that the existing runway has three right-angled (i.e., 90-degree angle turnoffs) located at both ends of the runway and half the way downrange. For a 2000 meter long runway (another assumption in the problem) the locations will be at 0, 1000, and 2000 meters from the active

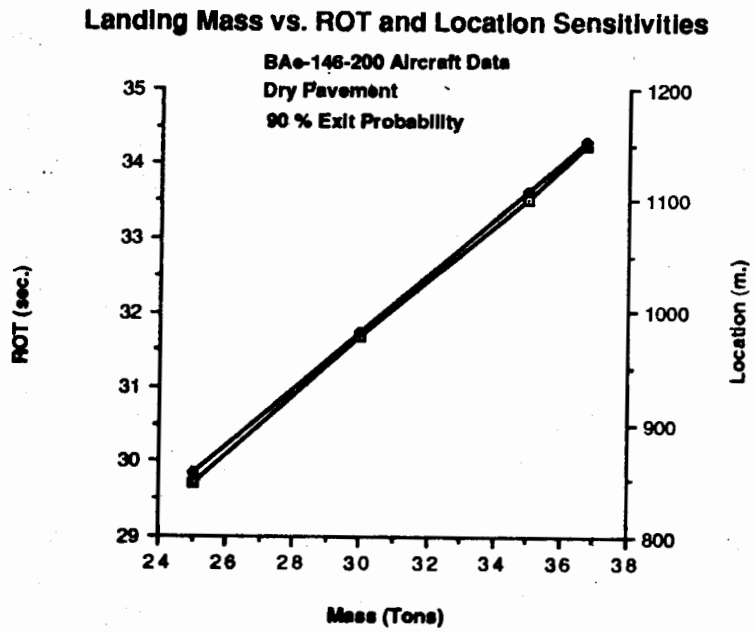

Figure 6.3 ROT and Exit Location Sensitivities to Aircraft Landing Mass (BAe 146-200).

threshold. Fig. 6.6 illustrates the procedure to build this scenario using the 'Edit' menu screen containing definitions for the number and type of existing runway exits.

Nine representative aircraft spanning three different TERP categories, A, B and C were selected from REDIM aircraft master file for this example. Fig. 6.7 illustrates the aircraft mix distribution corresponding to an **equivalent mix index** of 30%. After the user has decided the complete aircraft population operating in the facility pressing the 'Esc' key reviews the aircraft characteristics for all the population selected. This is done to provide the user with some familiarization of the aircraft selected and to allow any operational changes if necessary. The analyst might, for example, reduce the aircraft landing masses by a specified amount. After

```
MAIN MENU

Use arrow (↑ or ↓) key to change your choice.
Press enter ( ↵ ) key if the choice is correct.

1)Start A New Problem
2)Edit Data
3)Begin Analysis
4)Edit Master File
5)Go To Output Module
6)Help
7)Quit
```

Figure 6.4 Main Menu to Start Example 1.

```
SELECT
Analysis
Type

Press escape (Esc) key to return to EDIT MENU.

Use arrow (↑ or ↓) key to change your choice.
Press enter ( ↵ ) key if the choice is correct.

1) Evaluate an Existing Runway
2) Improve an Existing Runway
3) Design a New Runway
```

Figure 6.5 Evaluation Mode for Example 1.

```
EDIT

Use arrow (← or →) key to change your choice.
Press enter ( ↵ ) key if the choice is correct.

No. of existing exits : 3

          < LOCATION (m) >                    < TYPE >
Exit 1   : 0                    30-dgr    45-dgr    90-dgr
Exit 2   : 1000                 30-dgr    45-dgr    90-dgr
Exit 3   : 2000                 30-dgr    45-dgr    90-dgr
```

Figure 6.6 Selecting Existing Turnoffs and Their Type for Example 1.

```
EDIT                Press escape (Esc) key to proceed to next step.

Aircraft            Press enter ( ↵ ) key to store data.
Mix (%)             Press backspace ( ←B ) key to correct data.
                    Press arrow (←,→,↑, or ↓) key to move cursor.

TERPS A          TERPS B          TERPS C          TERPS D          TERPS E

PA-38-112 :10    BE-58     :10    A-300-600 :0     B-747-200B:0
PA-28-161 :10    BE-300    :10    A-310-300 :0     B-747-400 :0
PA-28-236 :0     CE-402C   :10    A-320-200 :0     DC-10-30  :0
PA-32-301 :0     SAAB-340  :10    B-767-300 :0     MD-11     :0
CE-172    :0     EMB-120   :10    FOKKER-100:15
BE-733A   :0     SA-227    :0     BAe-146   :15
CR-208    :0     BE-2000   :0     B-727-200 :0
PA-46-310P:0     CE-421    :0     B-737-300 :0
CE-182    :0     CE-F406   :0     B-737-400 :0
CE-210P   :0     PA-34-220T:0     MD-83     :0
                 PA-42-1000:0     MD-87     :0
                 P180      :0     B-757-200 :0
                 CE-550    :0     LEARJET-55:0
                 CE-650    :0     CL159C    :0
                 LEARJET-31:0     BAe-125-80:0
                 BE-400    :0     IA-1124A  :0
                 IA-1125   :0     CL-601-3A :0
                 DA-100    :0
                 DA-200    :0
                 DA-30     :0
```

Figure 6.7 Aircraft Mix Editor Screen for Example 1.

the verification of the aircraft data is done the user is prompted to save the new values in the user's current file.

The next input screen deals with the airport operational data values to be used in this example. Fig. 6.8 displays the baseline values used by REDIM for the analysis. The user is free to change any one of these values by typing the desired values over the existing ones. A parameter of significant importance in this screen is the safety factor for skidding coefficient to be used. A 50% safety factor has proven to correlate well with existing empirical turnoff data [Horonjeff, 1959] and it is highly recommended for a broad range of analyses. More conservative designs might opt for higher safety factor values thus increasing the radius of curvature of the proposed optimal turnoffs and also increasing the resulting weighted average ROT for the runway. For this example the use of the baseline values seems appropriate and hence Fig. 6.8 depicts the actual values used for this analysis.

The airport environmental conditions used for this example are shown in Fig. 6.9. Salient features include: 1) calm winds, 2) sea level runway location, 3) 25 C° as the average temperature of the hottest month, 4) 0-18 runway orientation and 5) a distance of 280 m. (918 ft.) from runway to taxiway centerlines. This latter parameter will be used in the output module to construct a complete high-speed geometry to the nearest taxiway using a terminal exit angle of 30 degrees. However, this topic is currently being studied to investigate various extended turnoff configurations that will be used selectively according to several runway-taxiway configurations. For more information regarding the sensitivity of the 'terminal' turnoff angle used refer to Section 6.3 of this document. The penultimate input screen in the 'Evaluation Mode' prompts the user to select the local runway gradients in tenth's of the total runway length. This is shown in Fig. 6.10. In this scenario, a 2000 meter runway is readily divided into ten 200 meter segments to which a local gradient value is associated. For the purpose of this example we use a constant -.5 % gradient (downslope) throughout the complete runway length. Note that the notation used in the program is consistent with that familiar to airport and highway engineers. Also, REDIM has a a built-in check routine to verify that local gradients will not exceed the maximum allowable by FAA standards. This verification is accomplished prior to the actual simulation and optimization procedures. But

```
EDIT                Press escape (Esc) key to return to EDIT MENU.

Airport             Press enter ( ↵ ) key to store data.
Oper. Data          Press backspace ( ←B ) key to correct data.
                    Press arrow (←,→,↑, or ↓) key to move cursor.

                              AVERAGE                        STD. DEV.
Free Roll Time 1 (sec)   : 2                                 .5
Free Roll Time 2 (sec)   : 1                                 .2
Taxiing Speed    (m/s)   : 8                                 1
Safety Fac. for Skid  (%): 50
```

Figure 6.8 Airport Operational Values for Example 1.

```
EDIT                Press escape (Esc) key to return to EDIT MENU.

Airport             Press enter ( ↵ ) key to store data.
Env. Data           Press backspace ( ←B ) key to correct data.
                    Press arrow (←,→,↑, or ↓) key to move cursor.

Wind Speed      (m/s) : 0                 Wind Direction       : 0
A/P  Elevation    (m) : 0                 A/P  Temperature (C) : 25
Min.Exit Interval (m): 200                R/W  Orientation     : 0
R/W  Width        (m) : 45                Dist. to Taxiway (m) : 280
```

Figure 6.9 Airport Environmental Values for Example 1.

```
EDIT                Press escape (Esc) key to proceed to next step.

Gradients           Press enter ( ↵ ) key to store data.
                    Press backspace ( ←B ) key to correct data.
                    Press arrow (←,→,↑, or ↓) key to move cursor.

R/W LENGTH    (m)  :  2000

GRADIENT      (%)
     0    TO  200   : -.5                 200  TO  400   : -.5
     400  TO  600   : -.5                 600  TO  800   : -.5
     800  TO  1000  : -.5                 1000 TO  1200  : -.5
     1200 TO  1400  : -.5                 1400 TO  1600  : -.5
     1600 TO  1800  : -.5                 1800 TO  2000  : -.5
```

Figure 6.10 Runway Gradients for Example 1.

```
EDIT                Press escape (Esc) key to return to EDIT MENU.

Weather &           Press enter ( ↵ ) key to store data.
Exit Spd            Press backspace ( ←B ) key to correct data.
                    Press arrow (←,→,↑, or ↓) key to move cursor.

                                DRY                     WET

   Percentage          (%) :  50                       50
TERPS A exit speed (m/s) :  15                       15
TERPS B exit speed (m/s) :  15                       15
TERPS C exit speed (m/s) :  20                       20
TERPS D exit speed (m/s) :  25                       25
TERPS E exit speed (m/s) :  25                       25
```

Figure 6.11 Weather Characteristics and Exit Speeds for Example 1.

the user can correct the error interactively by means of the 'Main Menu' which is always within reach through the 'Esc' key.

Finally, in the 'Weather and Exit Speeds' screen (Fig. 6.11) the user enters the relative frequency of occurence of weather conditions to be factored in the analysis. Two weather conditions are modeled in the current program, wet and dry runways, allowing more flexibility from an operational point of view. In general terms, wet scenarios will result in larger values of weighted average ROT times. However, this might be deemed necessary by the user in order to account for airport specific conditions at the location being analyzed. Overall, the runway turnoff designs will also be more conservative with larger radii of curvature and further downrange turnoff locations. In this case equal weights, 50% probabilities, are given to both runway conditions.

This concludes the input set for this first example. At this point, the analyst is expected to return to the 'Main Menu' through the 'Esc' key from where the model analysis routines (i.e., simulation and optimization) are invoked selecting 'Begin Analysis' from this menu. This starts the landing simulation of every aircraft subjected to the operational parameters input by the user to find candidate exit locations, their geometries, and finally to select those considered optimal according to a minimum weighted ROT performance index criterion. The execution of the simulations and optimization routines can take anywhere from 10 seconds to a few minutes depending upon the number of aircraft selected. In order to provide some visual feedback to the user through the simulation process the user is exposed to relevant statistics for each aircraft simulated. The statistics include: 1) the aircraft type designator, 2) the individual runway occupancy time, and the 3) exit location used. For this nine aircraft example the computation time is about 10 seconds for the dynamic simulation. In this case no optimization is necessary as only the 'Evaluation Mode' subroutines are invoked.

The results of this single-runway scenario are shown interactively in Figs. 6.12 to 6.15 which are part of the Output Module routines. Fig. 6.12 illustrates the main 'Output Menu' screen shown to the user where 'View the Output' and 'Print the Report' constitute the two alternatives to obtain screen and printed output, respectively. Selecting the first option, 'View

```
OUTPUT MENU      Press escape (Esc) key to return to MAIN MENU.

                 Use arrow (↑ or ↓) key to change your choice.
                 Press enter ( ↵ ) key if the choice is correct.

                      1)View the Output

                      2)Print The Report

                      3)Help

                      4)Go To Main Menu
```

Figure 6.12 Main 'Output Menu' for Example 1.

```
VIEW MENU        Press escape (Esc) key to return to OUTPUT MENU.

                 Use arrow (↑ or ↓) key to change your choice.
                 Press enter ( ↵ ) key if the choice is correct.

                      1)View ROT Table

                      2)View Turnoff Locations And Their Geometries

                      3)Go To Output Menu
```

Figure 6.13 'View Menu' for Example 1.

the Output' the analyst is exposed to Fig. 6.13 where a triple selection screen directs the user to the runway occupancy table (ROT Table), the turnoff locations and their geometries or back to the output menu. The ROT table depicted in Fig. 6.14 shows a partial view of the ROT Table where individual ROT times and the complete aircraft assignment is made for to the three existing exits. Notice that exit number, location and exit type are clearly identified in the first row of the table. Thereafter, every aircraft is identified by its program designator (i.e., see Appendix A for more details on designators and aircraft representation). As detailed in Chapter 5 of this document, two scenario conditions are analyzed by REDIM, wet and dry runway conditions with relative frequencies of occurence specified by the user (see Fig. 6.11). The interpretation of the ROT table results is as follows: every aircraft is assigned to one or several turnoffs where potentially a successful exit maneuver can be executed. Taken as example the swedish made commuter aircraft SAAB 340 the runway occupancy time for the dry scenario is 44.2 seconds taking the second turnoff (Exit # 2), located 1000 meters from the active runway threshold. The probability for this aircraft taking this middle exit is only 7.9 % suggesting average landing rolls greater than 1000 meters. Notice that if the third exit is used to clear the runway the remaining percent of the population, 92.1%, is able to exit at the expense of a large ROT value (138.6 sec.) as the aircraft is required to travel at near taxiing speed for the remaining portion of runway. This value should be viewed only as an upper limit since, ground operations permitting, the SAAB-340 will probably execute a 180-degree turn and still take the second exit. Under this new set of conjectures an estimated ROT time closer to 95 seconds is more realistic. Following the same aircraft it is noted that wet conditions lower the ROT time through the third exit since the aircraft requires longer braking distances with the corresponding reduction in the ROT devoted to taxi to the next turnoff. Note, however, that the percent of the SAAB-340 population taking the second exit is only 8% implying that a small percentage of the operations will be able to use this exit.

Table 6.1 provides the baseline exit speed values used in REDIM to predict the turnoff location and reliability parameter for individual aircraft using three FAA standard turnoff geometries. Note that for the 90-Degree angle turnoff the entry speed is defined by the user as a taxiing speed. This speed represents the safe value at which a pilot will comfortably

maneuver his airplane on the ground to reach the nearest turnoff location once a predetermined exit threshold value has been reached.

Table 6.1 REDIM Baseline Exit Speeds for Standard FAA Turnoffs.

Turnoff Type	Turnoff Entry Speed
90-Degree	Taxiing Speed (User Defined) Typically 8 m./sec. (18 MPH)
45-Degree	17.9 m./sec. (40 MPH)
30-Degree	26.9 m./sec. (60 MPH)

In Fig. 6.14 the weighted average runway occupancy time (WAROT) is also indicated for the complete population analyzed. In this case 102.94 seconds represents a large WAROT value for this simple example. According to this result a maximum of 34 landings per hour would be the upper limit for this single runway under the given conditions. For mixed operations this value could increase by another 10% or so. The question is how much can this facility be improved by adding more turnoffs? The answer to this is the subject of Example 2 to be discussed in the next section.

6.2 *Example 2 (Improving a Runway Facility)*

This problem is an extension to the previous one as it was observed that the existing turnoff locations were 'inefficient' to handle the hypothesized aircraft population resulting in large ROT times. The idea behind this second example is to improve the existing single runway design through the incorporation of additional high-speed turnoffs. The location and geometry of these will be found by REDIM's dynamic-optimization algorithms. Since it is pressumed that the analyst has created a file with the airport specifications in the previous

ROT / RELIABILITY TABLE
(This is for Evaluating an Existing Runway)

Exit #	1	2	3
Location (m)	0	1000	2000
Exit Type	90-Deg	90-Deg	90-Deg
CE-402C			
DRY ROT		64.19	
(7.5%) REL		1.00	
WET ROT		58.49	
(7.5%) REL		1.00	
SAAB-340			
DRY ROT		44.16	138.58
(7.5%) REL		0.00	0.92
WET ROT			124.94
(7.5%) REL			1.00
EMB-120			
DRY ROT			123.38
(7.5%) REL			0.99
WET ROT			107.46
(7.5%) REL			1.00
FOKKER-100			
DRY ROT			100.23
(7.5%) REL			1.00
WET ROT			90.54
(7.5%) REL			1.00

ROT - Runway Occupancy Time in Secs
REL - Reliability
Average ROT = 102.94

Press any key to continue

Figure 6.14 Partial ROT / Reliability Table for Example 1.

TURNOFF LOCATIONS
AND THEIR
GEOMETRIES

AIRPORT CONDITIONS
Temperature (C) : 25.00
Elevation (m) : 0.0
Wind Speed (m/s) : 0.00
Weather (%) : Dry - 50 & Wet - 50

RUNWAY EXIT LOCATION DISPLAY

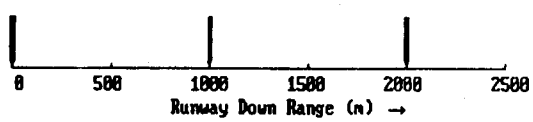

Runway Down Range (m) →

EXIT #	LOCATION	EXIT #	LOCATION
1	0.00	3	2000.00
2	1000.00		

Enter the Exit Number
to view the complete
Turnoff Geometry.
(Enter '0' to exit)
Example) 2
====>

Figure 6.15 Turnoff Locations and Their Geometries for Example 1.

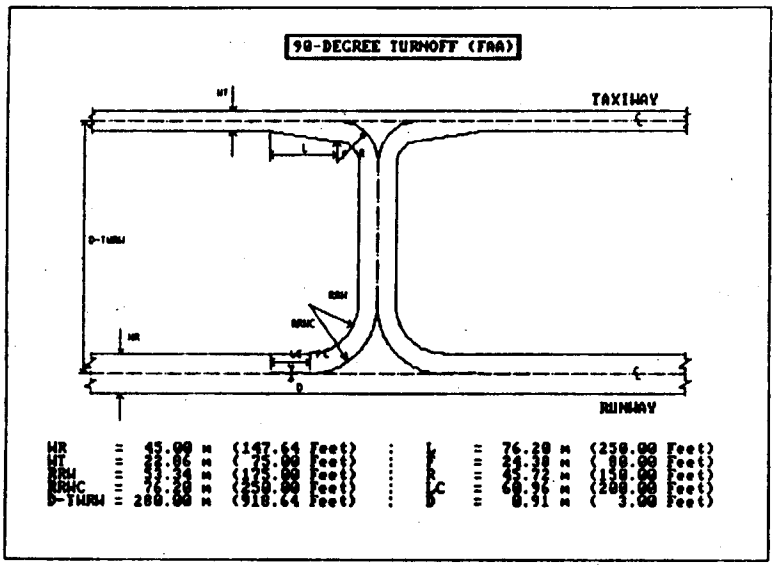

Figure 6.16 Existing 90-Degree Standard Turnoff Geometry for Example 1.

example and only those screens having significant changes from those of Example 1 will be treated in detail.

There are two ways to approach this revised problem. The first one is to use the existing data file from Example 1 and make the proper modifications through the complete input sequence. The second approach is to start a new problem with the same parameters as Example 1 and complete the pieces of information left out in the previous problem. Taking the second approach is simpler for the novice but the first one saves time.

The first significant change is made to the 'Analysis Type' menu (see Fig. 6.5) where now the second choice is selected, 'Improve an Existing Runway'. From this point on the same screens as those associated with Example 1 will be applicable. A reliability parameter needs to be specified in the third 'Input' screen to estimate the degree of exit reliability expected from the new turnoffs. For this example we use 90% as reliability parameter and we will specify the number of exits to be built at the end of the simulation stage. Another aspect that

we need to specify in this new scenario concerns the desired entry exit speeds for the new turnoffs. This is crucial as part of the input as REDIM will use the entry turnoff speeds selected in the 'Weather and Exit Speeds' menu to design geometrically the optimal turnoffs. For the improved runway the exit speeds and weather conditions are shown in Fig. 6.17. Note that it is possible to leave voids of speed data as far as these are not used in the program. For example, its is allowed to leave blanks for the speed values associated with TERP categories D and E as there are no aircraft belonging to these categories in this example.

After the pertinent changes have been made to the Input Module screens the user is expected to go back to the 'Main Menu' screen (pressing the 'Esc' key) and start the analytical procedures of REDIM. Selection of item 3 in Fig. 6.5 begins the dynamic simulation analysis. Just as for the previous example, there is some feedback information displayed on the screen in terms of partial ROT values for every candidate solution generated (see Fig. 6.18). The dynamic computations take on the average 9 seconds per aircraft-scenario combination. Currently, the model is restricted to 25 aircraft per run (i.e., 50 aircraft-scenario combinations) due to internal array size limitations. This, however, seems to be sufficient for most of the airport scenarios to be encountered and should not restrict the validity of the results. Once the dynamic simulation is done, the analyst enters the number of new turnoffs to be constructed and the optimization module routines are executed. Fig. 6.19 illustrates a partial view of the optimization results using 5 exits. That is, constructing two new high-speed turnoffs to complement the three existing ones.

The new average ROT value being 45.91 seconds represents a significant improvement over the previous example. The suggested new locations are 727 and 1495 meters from the active threshold. Fig. 6.19 also details the percentages of each aircraft-scenario combination exiting through each turnoff and their corresponding individual ROT times. It should be noticed that REDIM constraints adjacent turnoff locations within a prescribed distance D_{min} to abide current FAA standards. The current value for D_{min} is considered to be 213 meters (i.e., 700 ft.) but this can be modified by the user in the 'Airport Environmental Screen' (see Fig. 6.9). Running REDIM under the same runway environmental conditions but increasing the number of new turnoffs to three instead of two as before a 15% improvement is observed in the

```
INPUT

Input the value and Press enter ( ↵ ) key to store data.

Input the successful exit probability (%) : 90

The successful exit means that
the aircraft take the specified exit
at a lower speed than specified.
```

Figure 6.17 Definition of the Reliability Parameter for Example 2.

```
========>   Minimum ROT =   34.57111
            Location    =   1142.181
SAAB-340   wet  with specified exit spd =  25 m/s
========>   Minimum ROT =   37.72971
            Location    =   1253.188
EMB-120    dry  with specified exit spd =  25 m/s
========>   Minimum ROT =   36.70969
            Location    =   1279.125
EMB-120    wet  with specified exit spd =  25 m/s
========>   Minimum ROT =   40.11147
            Location    =   1406.762
FOKKER-100 dry  with specified exit spd =  30 m/s
========>   Minimum ROT =   35.14109
            Location    =   1359.422
FOKKER-100 wet  with specified exit spd =  30 m/s
========>   Minimum ROT =   38.43119
            Location    =   1495.364
BAe-146    dry  with specified exit spd =  30 m/s
========>   Minimum ROT =   31.86889
            Location    =   1123.91
BAe-146    wet  with specified exit spd =  30 m/s
========>   Minimum ROT =   34.40303
            Location    =   1221.074
Please input the number of new exits :
```

Figure 6.18 Partial Dynamic Simulation Results for Improved Single Runway.

average ROT time (from 45.91 to 38.57 seconds). Fig. 6.20 shows a partial ROT table for this new scenario. Note that the new turnoff location are: 727, 1279 and 1495 meters from the active threshold. As one might suspect an increase in the number of high-speed turnoffs yields better runway service times (i.e., lower values of WAROT) at the expense of capital cost. It can also be shown with several consecutive runs of the model that the gains in WAROT are small for a large number of exits ($n > 6$).

Figures 6.21-6.23 depict graphically the location and geometries generated by REDIM in the 5-turnoff runway scenario. Fig. 6.22 shows a characteristic compound plot of the five turnoff geometries, three already available (i.e., standard FAA 90-Deg. turnoffs) and two more projected. Fig. 6.23 represents the complete turnoff geometry of the fourth turnoff located 1495 m. from the runway threshold. In the 'Print the Report' Option the user receives a complete report on the optimization results as well as the input parameters selected for that particular run. The report is divided into two sections: I) input data analysis and II) analysis results. The former is in term subdivided into six categories corresponding to each one of the program input screens; 1) type of analysis, 2) aircraft mix, 3) airport operational data, 4) airport environmental data, 5) runway gradients, and 6) weather and speed characteristics. The analysis results section of the report contains three sub-sections; 1) average ROT, 2) exit locations, type and turnoff assignment table, and the actual centerline turnoff coordinates. Figs. 6.24-6.25 show partial listings of the report generated for Example 2 (5-turnoff case).

ROT / RELIABILITY TABLE
(This is for Improving an Existing Runway)

Exit # / Location (m) / Exit Type	1 0.0 90-Deg	2 726.9 New	3 1000.0 90-Deg	4 1495.4 New	5 2000.0 90-Deg
PA-38-112					
DRY ROT (5.0%)		35.02			
WET ROT (5.0%)		34.45			
PA-28-161					
DRY ROT (5.0%)		36.12			
WET ROT (5.0%)		35.73			
BE-58					
DRY ROT (5.0%)				71.42	
WET ROT (5.0%)				68.08	
BE-300					
DRY ROT (5.0%)				64.01	
WET ROT (5.0%)				60.86	

ROT - Runway Occupancy Time in Secs
Reliability in % = 90
Average ROT = 45.91

Figure 6.19 Partial ROT/Table Results for Improved Single Runway with 5 exits.

ROT / RELIABILITY TABLE
(This is for Improving an Existing Runway)

Exit # / Location (m) / Exit Type	1 0.0 90-Deg	2 726.9 New	3 1000.0 90-Deg	4 1279.1 New	5 1495.4 New	6 2000.0 90-Deg
CE-402C						
DRY ROT (7.5%)		24.98				
WET ROT (7.5%)		24.54				
SAAB-340						
DRY ROT (7.5%)				41.09		
WET ROT (7.5%)				39.04		
EMB-120						
DRY ROT (7.5%)				37.08		
WET ROT (7.5%)					47.04	
FOKKER-100						
DRY ROT (7.5%)					41.09	
WET ROT (7.5%)					39.04	

ROT - Runway Occupancy Time in Secs
Reliability in % = 90
Average ROT = 38.32

Figure 6.20 Partial ROT/Table Results for Improved Single Runway with 6 exits.

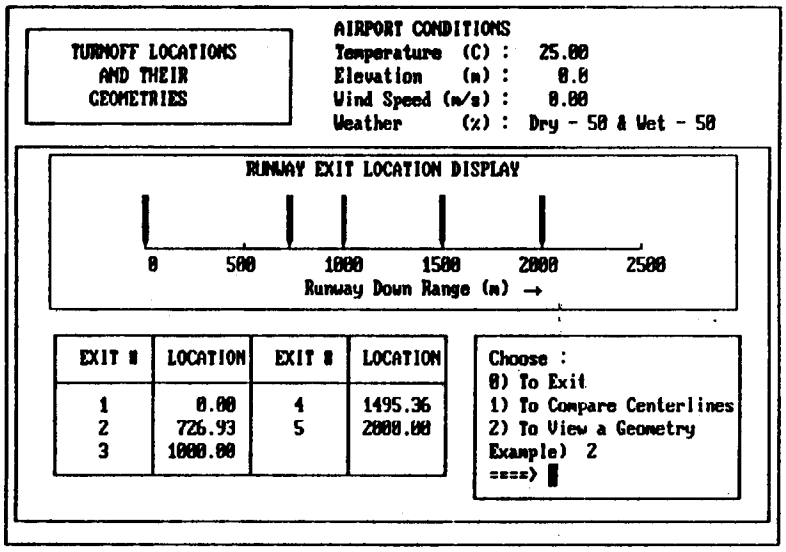

Figure 6.21 Runway Exit Locations for Example 2 with 5 Turnoffs.

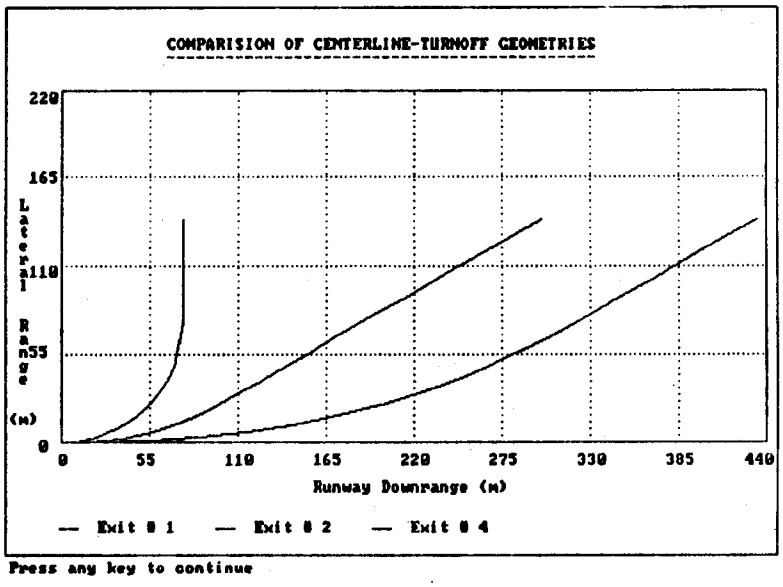

Figure 6.22 Centerline Geometry Comparison for Example 2 with 5 Turnoffs.

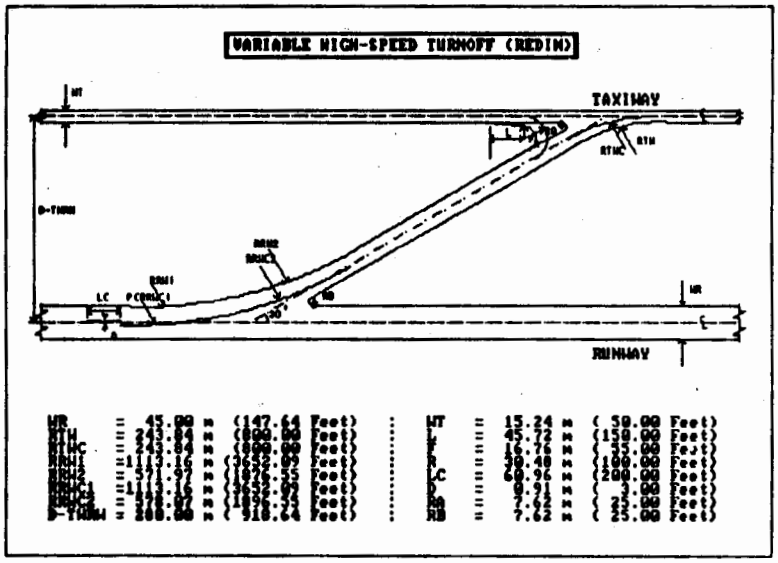

Figure 6.23 Complete Turnoff Geometry for Fourth Exit of Example 2 (5 Exits).

```
*****************************************************************************

RRRRRRRR   EEEEEEEE   DDDDDDD    IIIIIIIIII   MMM     MMM
RR    RR   EE         DD    DD       II      MMMM   MMMM
RRRRRRRR   EE         DD     DD      II      MM MM MM MM
RRRR       EEEEEEEE   DD     DD      II      MM  MMM  MM
RR RR      EE         DD     DD      II      MM   M   MM
RR  RR     EE         DD    DD       II      MM       MM
RR   RRR   EEEEEEEE   DDDDDDD    IIIIIIIIII   MM       MM

                RUNWAY  EXIT  DESIGN  INTERACTIVE  MODEL

*****************************************************************************

I. INPUT DATA SUMMARY

I-1. Analysis type and Existing Exits

  Analysis type = Improvement of an Existing Runway

  Exit #   Location (m)     Type
     1          0          90-deg
     2       1000          90-deg
     3       2000          90-deg
```

Figure 6.24 Input Data Summary Report for Example 2.

I-2. Aircraft Mix and Characteristics

acf name	%	WB (m)	WT (m)	LM (%)	MASS (kg)	LD (m)	CL MAX	WA (m^2)	WS (m)	NWT (m)
PA-38-112	10.0	1.5	3.0	77.4	757.0	486.0	1.575	11.6	10.4	2.1
PA-28-161	10.0	2.0	3.0	82.3	1109.0	416.0	1.694	15.8	10.7	2.4
BE-58	10.0	2.7	2.9	84.6	2500.0	751.5	1.486	18.5	11.5	2.9
BE-300	10.0	4.6	5.2	89.0	6363.0	857.2	2.076	28.2	16.6	5.3
CE-402C	10.0	3.2	5.5	88.1	3107.0	655.8	2.100	21.0	13.4	3.8
SAAB-340	10.0	7.1	6.7	90.9	12020.0	1140.4	2.578	41.8	21.4	7.7
EMB-120	10.0	7.0	6.6	90.5	11250.0	1269.5	2.272	39.4	19.8	7.6
FOKKER-100	15.0	14.0	5.0	89.5	39915.0	1360.0	2.533	93.5	28.1	16.8
BAe-146	15.0	11.2	4.7	92.3	36740.0	1130.0	3.385	77.3	26.3	12.6

WB = Wheelbase WT = Wheeltrack LM = Load on Main Gear
MASS = Landing Mass LD = Landing Run Distance CL MAX =
WA = Wing Area WS = Wing Span NWT = Dist. Nose Gear to Wingtip

I-3. Operational Data

1st free roll time	:	2.0 (sec)	std. dev.	0.5
2nd free roll time	:	1.0 (sec)	std. dev.	0.2
taxing speed	:	8.0 (m/s)	std. dev.	1.0
safety fac. for skid	:	50.0 (%)		

I-4. Environmental Data

wind speed	:	0.0 (m/s)	wind direction	:	0.0
airport elevation	:	0.0 (m)	temperature	:	25.0 (C-deg)
min. exit interval	:	213.0 (m)	runway orientation	:	0.0
runway width	:	45.0 (m)	distance to taxiway	:	280.0 (m)

I-5. Runway Gradients

runway length : 2000 (m)

gradients (%)

```
    -0.5   -0.5   -0.5   -0.5   -0.5   -0.5   -0.5   -0.5   -0.5   -0.5
   I------+------+------+------+------+------+------+------+------+------I
                                   1000                                2000
```

I-6. Weather and Exit Speeds

weather & exit speed (m/s)

	DRY	WET
Probability (%)	50.0	50.0
TERPS A	20.0	20.0
TERPS B	25.0	25.0
TERPS C	30.0	30.0
TERPS D	30.0	30.0
TERPS E	0.0	0.0

Figure 6.24 Input Data Summary Report for Example 2 (Continuation).

II. ANALYSIS RESULTS

II-1. Average ROT

average ROT = 45.91 (sec)

II-2. Exit Locations, Types, and Turn-off Assignment.

Exit #	1	2	3	4	5
Location (m)	0	727	1000	1495	2000
Type	90-d	new	90-d	new	90-d
PA-38-112					
dry		35.0			
wet		34.4			
PA-28-161					
dry		36.1			
wet		35.7			
BE-58					
dry				71.4	
wet				68.1	
BE-300					
dry				64.0	
wet				60.9	
CE-402C					
dry		25.0			
wet		24.5			
SAAB-340					
dry				55.5	
wet				52.3	
EMB-120					
dry				50.1	
wet				47.0	
FOKKER-100					
dry				41.1	
wet				39.0	
BAe-146					
dry				46.9	
wet				45.1	

Figure 6.25 Analysis Results Format for Example 2.

I-3. Turn-off Centerline Geometries.

Exit 1		Exit 2		Exit 3		Exit 4	
X	Y	X	Y	X	Y	X	Y
5.1	0.2	19.8	0.5	5.1	0.2	29.9	0.2
10.1	0.7	39.3	2.6	10.1	0.7	59.4	1.2
15.2	1.5	58.1	6.7	15.2	1.5	88.6	3.3
20.3	2.8	76.1	12.7	20.3	2.8	117.4	6.5
25.4	4.3	93.1	20.5	25.4	4.3	145.7	11.0
30.4	6.3	109.0	29.6	30.4	6.3	173.5	16.8
35.5	8.8	124.7	38.6	35.5	8.8	200.7	23.8
40.6	11.7	140.1	47.5	40.6	11.7	227.2	32.1
45.6	15.2	155.3	56.3	45.6	15.2	253.0	41.7
50.7	19.4	170.1	64.9	50.7	19.4	278.0	52.4
55.8	24.3	184.8	73.4	55.8	24.3	302.1	64.3
60.8	30.4	199.2	81.7	60.8	30.4	325.4	77.2
65.9	38.1	213.3	89.8	65.9	38.1	348.2	90.4
71.0	48.7	227.2	97.9	71.0	48.7	370.7	103.4
76.1	76.1	240.8	105.7	76.1	76.1	393.0	116.3
76.1	140.0	254.2	113.5	76.1	140.0	415.0	129.0
		267.3	121.0			434.2	140.1
		280.2	128.5				
		292.8	135.7				
		300.2	140.0				

Exit 5	
X	Y
5.1	0.2
10.1	0.7
15.2	1.5
20.3	2.8
25.4	4.3
30.4	6.3
35.5	8.8
40.6	11.7
45.6	15.2
50.7	19.4
55.8	24.3
60.8	30.4
65.9	38.1
71.0	48.7
76.1	76.1
76.1	140.0

Figure 6.25 Analysis Results Format for Example 2 (Continuation).

7.0 Conclusions

The end result of this model is to recommend a high-speed geometry that will minimize the runway occupancy time under realistic airport scenarios. As it was explained in Chapter 6 the model is able to predict turnoff locations and geometries that optimize the weighted average ROT parameter for a given set of airport conditions. The obvious question is how sensitive are the model results in terms of some of the input parameters such as aircraft mix, wind conditions, airfield parameters and so on. This question arises naturally since these variables are highly dynamic and fluctuate during the day and from season to season.

Looking at existing data on runway occupancy time [Koenig, 1978; Ruhl, 1989] it is believed that REDIM is behaving in a realistic fashion for a multitude of scenarios tested. Fig. 7.1 illustrates the results for San Francisco International Airport runway 27R where two independent sets of data were compared with the predictions made by REDIM for the same scenario. Fig. 7.2 depicts the results of REDIM and the observations reported by Koenig [Koenig, 1978]. In all cases the differences are below 5% from each other. A generalized trend on ROT times versus mix index for various numbers of exits is illustrated in Fig. 7.3. In this figure it is seen the sensitivity of the model to the number of exits. Without any doubt one of the most important parameters influencing ROT times.

7.1 Suggested High-speed Standard Geometry

The implementation of realistic high-speed turnoffs seems to be one the most debatable issues faced by airport engineers. On one hand it is well known that the location of the runway turnoffs affects significantly geometry of every turnoff; However, for a finite aircraft population a single turnoff location scheme is needed to minimize the desired average ROT performance index. The problem seems then to be that each planner should use variable geometry turnoffs for every scenario. This makes the number of geometry choices almost limitless for the

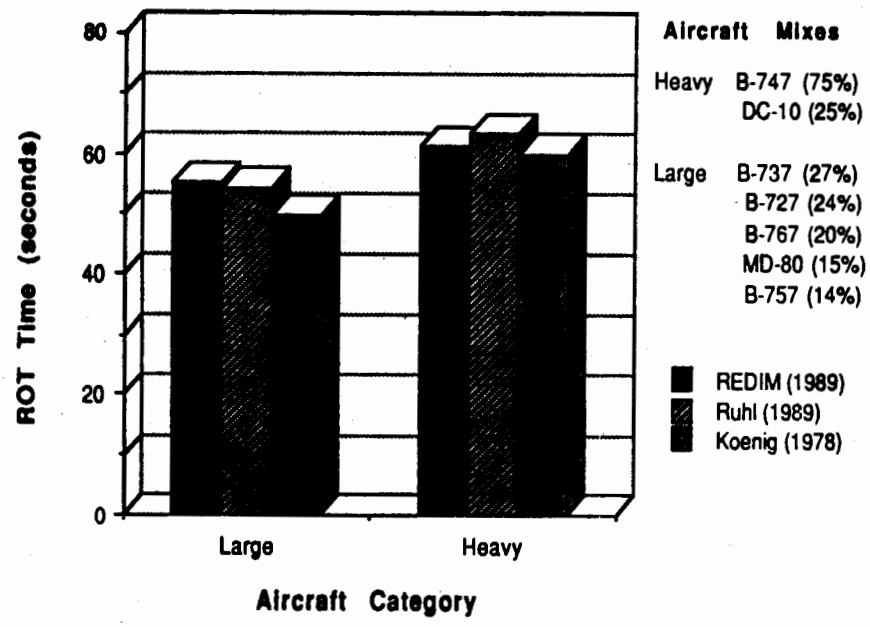

Figure 7.1 Comparison of REDIM Results at San Francisco Intl. Runway 28R.

hundredths of airport scenarios around the nation. This issue is not time consuming with the use of REDIM, but even a complex model like the one addressed in this report makes use of generalizations in order to reduce the magnitude of the problem within a confined set of choices.

In dealing with a new standard geometry our approach to the standardization problem is very similar to that confronted by the Horonjeff team three decades ago. If a standard is to be accepted by the aviation community it not only needs to be proven in simulators and in fields demonstrations, but also needs to address the needs of the builder in terms of a simple definition of the geometry. This is probably the most difficult task to address since a fully variable geometry is obtained as the result of the turning equations of motion of aircraft negotiating a high-speed turnoff. The specification of such a geometry (i.e., fully variable geometry) is difficult to justify in practice since every position coordinate in a two-dimensional plane needs to be known. From an operational point of view it is possible to approximate slow-varying turnoff geometries [i.e., spirals and clotoids] with large radius of curvature

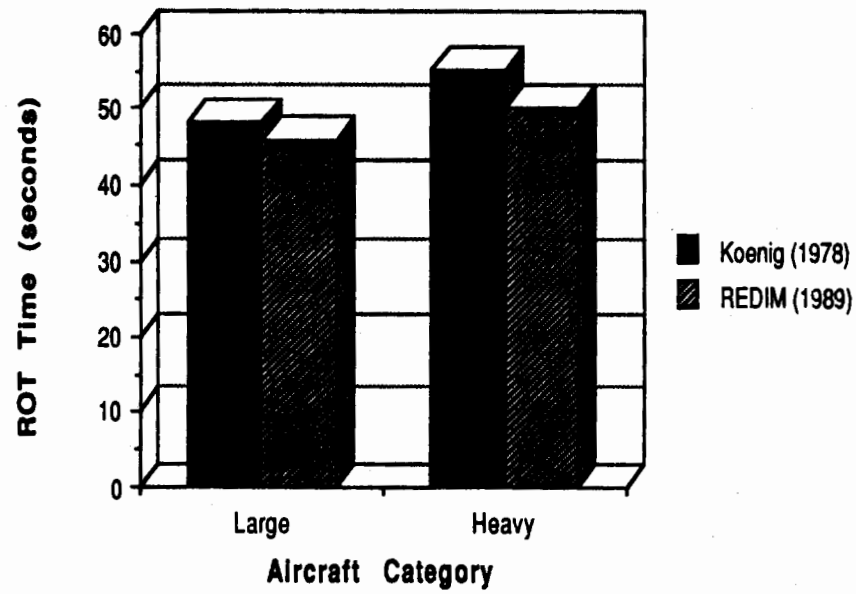

Figure 7.2 Comparison of REDIM Results at Denver Intl. Runway 26R.

entrance curve followed by a reduced radius of curvature circular segment. This approach was suggested by Robert Horonjeff in the late 50's (Horonjeff, et al, 1959) but interestingly enough his results have not been universally accepted by all the aviation authorities in terms of adopting a large entrance curve as geometric design standard. The current FAA practice uses a single radius of curvature to define the geometry of a high-speed turnoff (i.e., 1800 ft for 30-Deg. angled exits). In our findings with REDIM we have to acknowledge that Horonjeff's suggestions were justifiable and that possibly the simplest approach to define a new standard is to consider two circular arcs with a common tangency point as a viable solution to approximate a fully variable turnoff geometry (see Fig. 7.4). This approach is revisited in this section to show the selection process behind the variable geometry standard.

From Fig. 7.4 it is seen that two radii of curvature defined R_1, R_2, and a turnoff exit angle, ψ form the basis for the suggested approximation. The first radius of curvature approximates the jerk-limited curve corresponding to a specified entry speed (V_e) whereas the second one, R_2, models the aircraft "steady-state rotational" inertia characteristics as it negotiates the

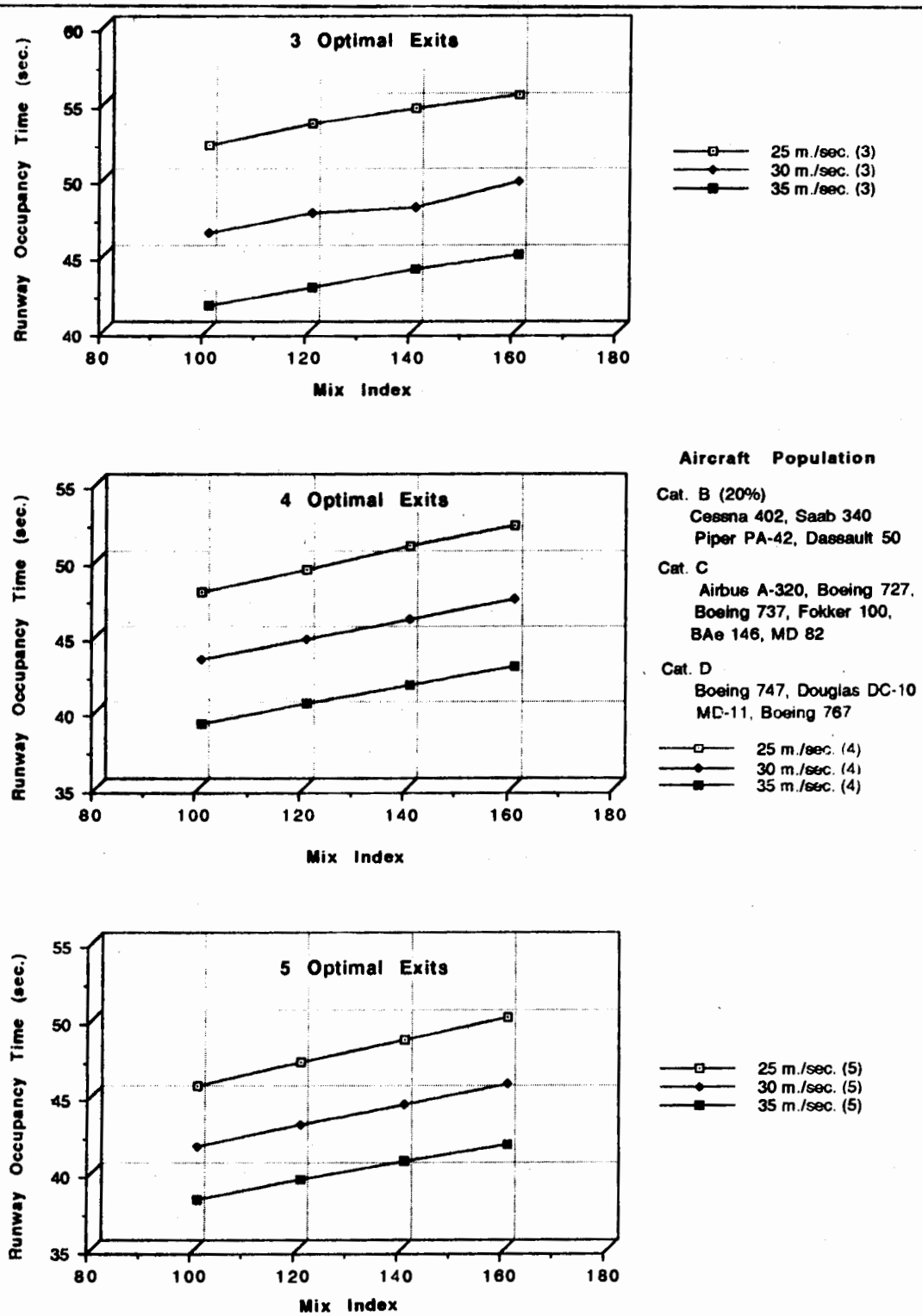

Figure 7.3 General ROT Trends for 3, 4 and 5 Optimal Locations.

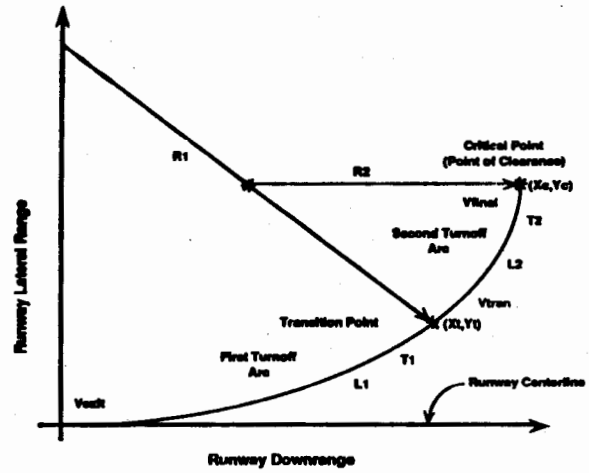

Nomenclature

(Xc,Yc)	Clearance Point Coordinates (meters)
(Xt,Yt)	Transition Point Coordinates (meters)
L1	First Arc Length (meters)
L2	Second Arc Length (meters)
T1	Second Turnoff Arc Travel Time (seconds
T2	First Turnoff Arc Travel Time (seconds)
Vexit	Aircraft Exit Speed at the Start of the Turn (m./sec.)
Vtran	Aircraft Speed at the Transition Point (m./sec.)
Vfinal	Aircraft Speed at the Clearance Point (m./sec.)
R1	First Turnoff Arc Radius (meters)
R2	Second Turnoff Arc Radius (meters)

Figure 7.4 Definition of the High-Speed Turnoff Geometry.

turnoff. Through many simulations using REDIM it became evident that extracting two specific values of R an excellent approximation to this fully variable turnoff geometry could be obtained. The values of R_1 and R_2 then were obtained as a function of turnoff time and aircraft category.

The rationale behind the time factor in this recommendation is to account for the aircraft inertia resistance motion which can be categorized as a "pseudo-first order model" (see Eqns. 3.18-19 for $\dot{R}$) where the radius of curvature changes slowly as a function of time. Looking at Fig. 7.5 it is observed that an equivalent "time constant" characterizing the aircraft rotational motion about the z axis as it negotiates a high-speed turnoff is proportional to the aircraft mass and moment of inertia about this axis among other factors. Knowing this fact a straight correlation between the values of R_2 and an extraction time were established. Table 7.1

summarizes the nominal extraction times used in REDIM to approximate the variable turnoff trajectory.

In REDIM nomenclature these times are labeled as easement curvature time, TR1, and steady-state curvature time, TR2. Note that for heavy transport-type aircraft (i.e., > 300,000 lbs) larger time lags to achieve a "steady-state" radius of curvature are a direct result of larger time constants in the model.

Fig. 7.4 also illustrates the two corresponding encompassing the approximate turnoff track. Arcs with lengths L_1 and L_2 are defined as follows,

$$L_1 = R_1 \ \theta_1 \qquad \{7.1\}$$

$$L_2 = R_2 \ \theta_2 \qquad \{7.2\}$$

where, L_1 and L_2 represent the turnoff characteristic lengths. R_1 and R_2 are the radii of curvature defining the turnoff, and θ_1 and θ_2 are the arcs defined by R_1 and R_2, respectively measured in radians. The turnoff arcs are characteristic for each aircraft since the transition and runway clearance point are aircraft speed and geometry dependent. It should be kept in mind that L_1 is a linear function of aircraft speed if the jerk-limited equation is used and if the values of a_n and J_n are substituted in Eqn. 7.3.

$$L_1 = \frac{a_n \ V_e}{J_n} = \frac{a_{max} \ V_e}{J_{max}} \qquad \{7.3\}$$

The analyst, however, does not need to be concerned in REDIM since the actual turnoff track values are presented in tabular form. The approximation is primarily used to depict the geometry on the computer screen.

Table 7.1 REDIM Model Extraction Times for Estimating R_1 and R_2.		
Category	R_1	R_2
A	1 sec.	4 sec.
B	1 sec.	5 sec.
C	1 sec.	6 sec.
D	1 sec.	6 sec.
E	1 sec.	6 sec.

7.2 Comparison of REDIM Geometries

The geometries generated by REDIM are dictated primarily by the jerk and normal acceleration in the first few seconds of the trajectory and by the aircraft rotational inertia limitations in the longer term (i.e., 3 or more seconds into the turn). In general, the geometries obtained in REDIM differ from the FAA standard acute angle exit geometry in terms of their initial and steady state radii of curvature. Fig. 7.6 depicts two exit geometries corresponding to and exit speed of 27 m.sec. (60 MPH). The top geometry corresponds to the standard acute angle exit and is shown for the sake of comparison. The bottom geometry was generated by REDIM for a Boeing 727-200 operating on a wet runway. Note that in both examples the final exit angle has been maintained at 30 degrees and as can be seen the REDIM geometry is characterized by two radii of curvature (R1=979.6 m. and R2=447.8 m.) resulting in a slightly larger arc length to reach the final exit angle. Also shown in Fig. 7.6 is a superposition of both geometries revealing in greater detail their differences. Notice that the width of the turnoff has also been maintained at 30.5 m. (i.e., 100 ft.) for the purpose of illustration. It is important to realize that currently REDIM evaluates the centerline of the aircraft trajectory and it designs the turnoff edges according to the aircraft design group classification. It seems advisable,

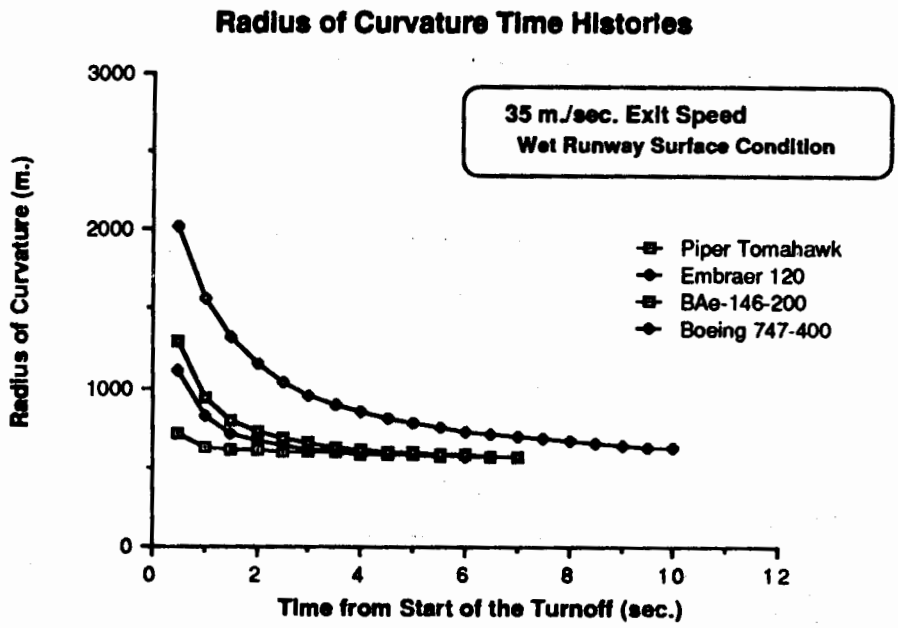

Figure 7.5 Time Variations of Radius of Curvature for Representative Aircraft.

however, to increase the existing turnoff widths in order to increase the pilot's confidence while negotiating a turn at high speed.

Fig. 7.7 illustrates similar results for a Boeing 747-200. In this particular case the differences are more notorious as the larger aircraft mass and inertia penalize its maneuverability on the ground. Again, the lateral distance and the turnoff width has been maintained according to existing FAA standards. Fig. 7.8 illustrates the geometry for the same Boeing 747-200 when the entry speed is 35 m./sec. (78 MPH). In this case the turnoff width has been increased to 45.8 mts. in order provide better situational awareness to the pilot. It is believed that increases in the width of all high speed exits will, in general, induce pilots to maintain faster exit speeds than those seen today at major airports. When one considers night and wet pavement conditions and factors a reasonable skidding friction parameter the resulting geometries require significant longitudinal and lateral distances to allow sizeable speed reductions on the turnoff. It has been estimated that 230 mts. (750 ft.) seems to be the minimum lateral distance

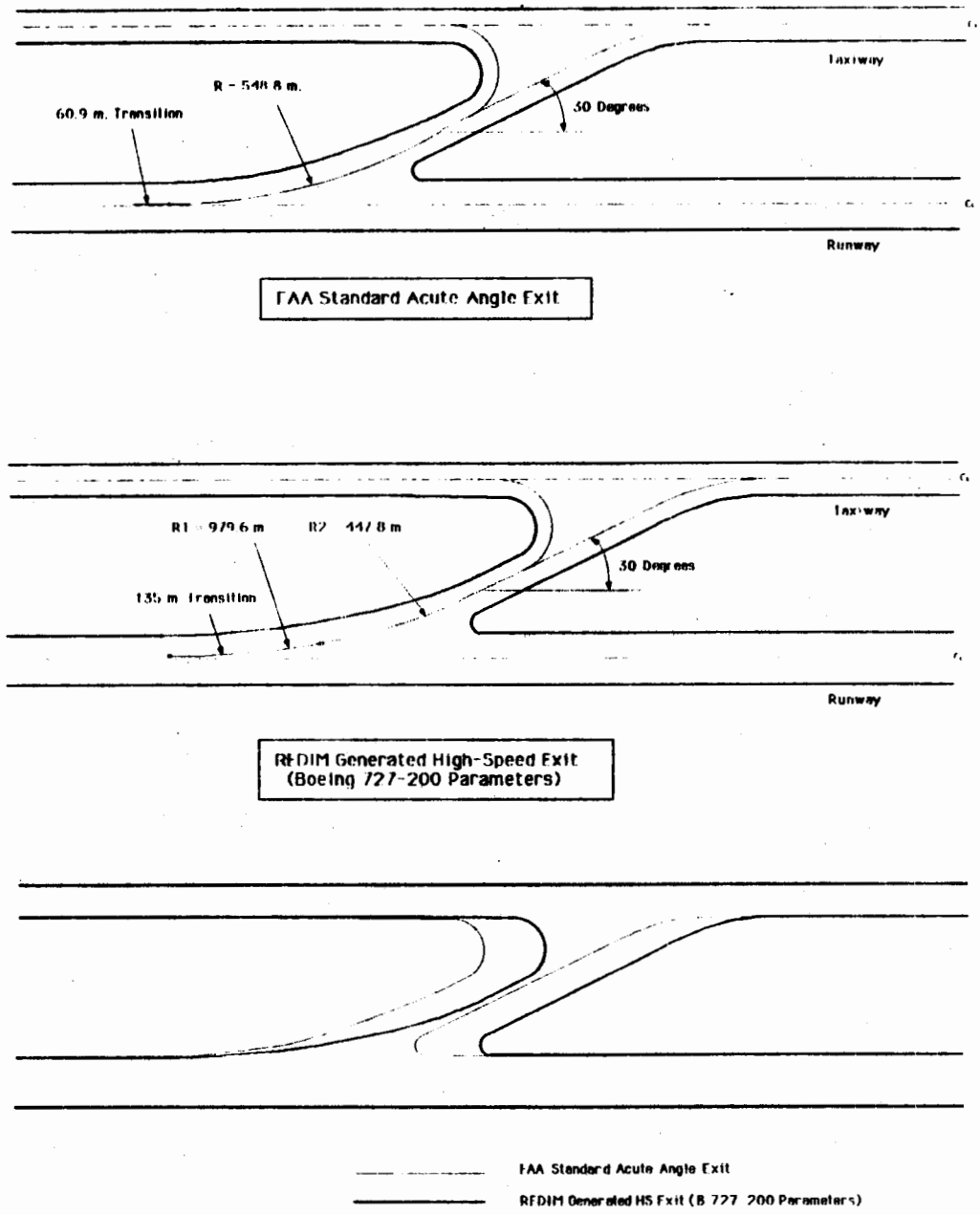

Figure 7.6 Medium Size Transport Turnoff Geometries Comparison (27 m./sec.)

allowing safe negotiation of a 35 m./sec. entry speed turn. This distance depends upon the terminal speed required at the taxiway junction point and will be the subject of further analysis in the Phase II of this research.

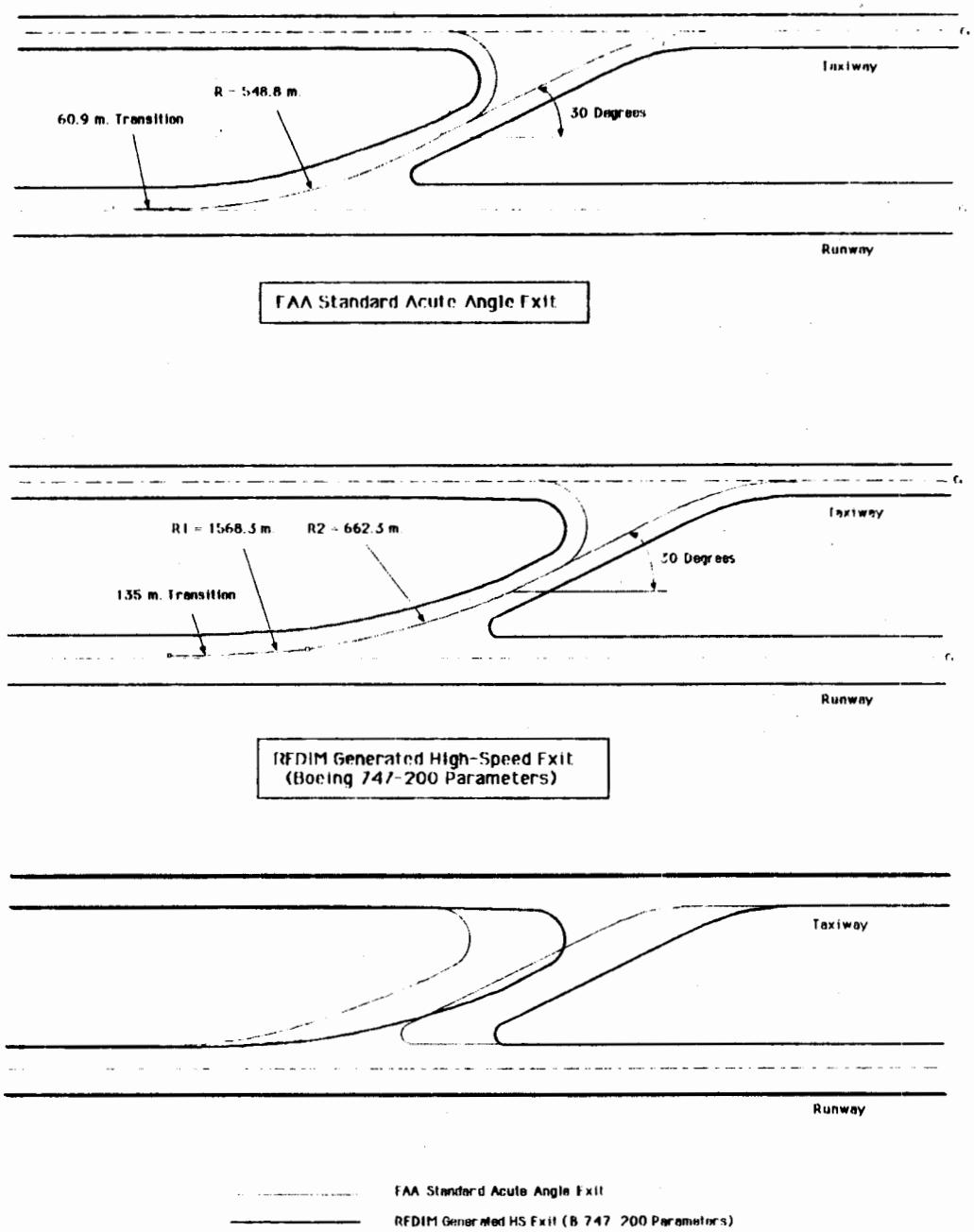

Figure 7.7 Heavy Transport Turnoff Geometries Comparison (27 m./sec.)

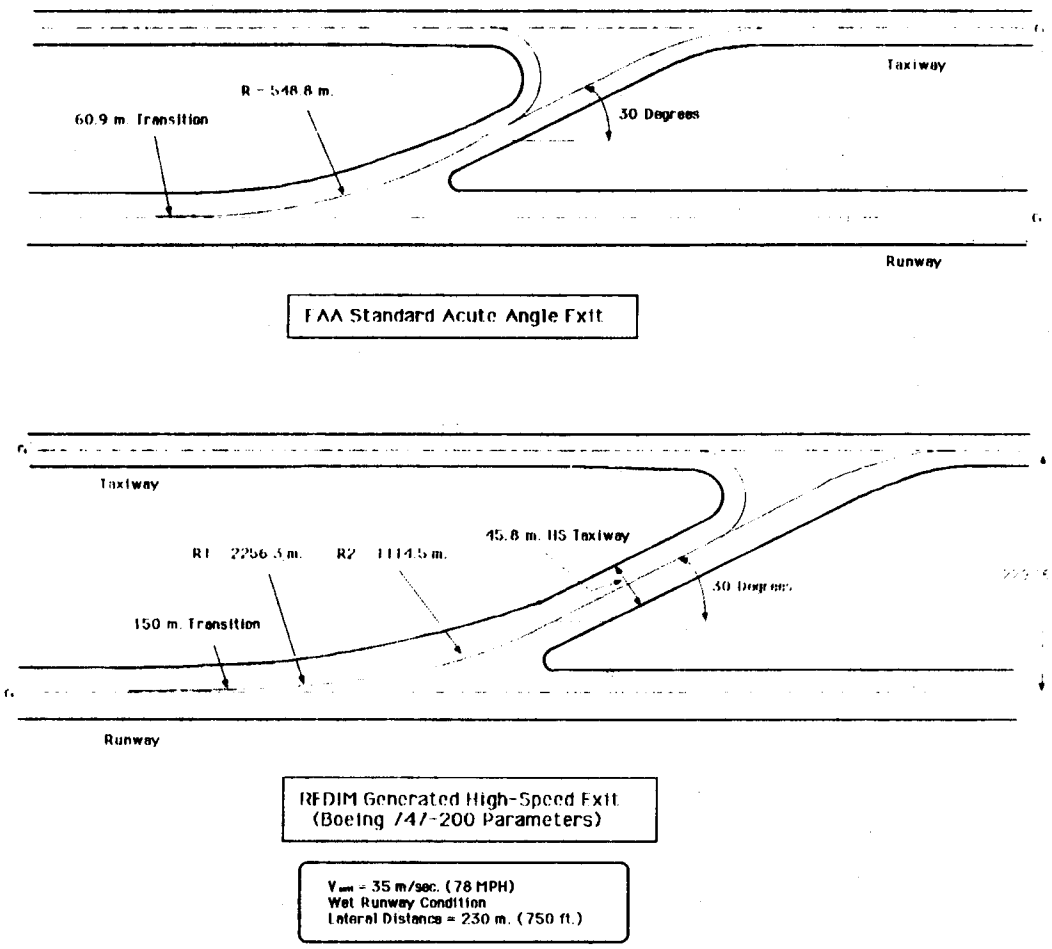

Figure 7.8 Heavy Transport Turnoff Geometries Comparison (35 m./sec.)

8.0 Model Recommendations

Although the REDIM model addresses a large variety of parameters affecting the aircraft landing dynamics and the airport environmental characteristics several features of the model need further investigation in order to calibrate and verify some of the assumptions made during the model development. Among these features are: 1) a postoptimization technique to account for time varying aircraft mixes and airport environmental parameters, 2) human behavioral factors such as the verification of the lateral acceleration and jerk perception thresholds used in the model and the incorporation of pilot behavioral factors influencing the selection of vehicle deceleration schedules for various runway lengths. 3) added flexibility in the turnoff angle parameters (i.e., turnoff angle and other lateral spacing restrictions), and We now try to address each one of these topics in more detail pointing out some of the obstacles and methods that could be used to implement these recommendations at a later research stage.

8.1 Postoptimization Algorithm

A post-optmization processor that could factor day-to-day aircraft traffic mix variability and environmental conditions could be a very practical addition to the existing model. The major constraint to this seems to be the computer storage limitations required to handle the larger size matrices generated by this new postoptimization process. Currently REDIM is limited to 50 aircraft/runway condition pairs in a single run to limit the numerical computations to a manageable level. If a global optimization scheme is be implemented under varying input parameters throughout the life cycle of the facility this would necessitate complete knowledge of the time variations of some parameters accounted for in REDIM throughout the period of interest (i.e., the airport design life-cycle). This of course could only be done for a few variables such as aircraft mix and airfield environmental conditions (i.e., airfield temperature, wind conditions, etc.) in order to maintain a reasonable matrix size to execute the problem

on a personal computer. Another valuable alternative in this regard could also be the addition of an iterative procedure that would search for a user defined ROT threshold value to be used as runway exit location/geometry design parameter. This procedure could be executed in several steps allowing at least two parameters to be varied independently to achieve the desired ROT value. Parameters of great influence in this regard are the number of exits and the exit speeds associated with each one of them. A typical searching algorithm to achieve a "goal" ROT value would cycle these two parameters sequentially until the desired ROT value is obtained.

8.2 Human Behavioral Factors

Another aspect deserving attention in this section is that dealing with some of the safety margins and assumptions made in the present modeling effort. In the overall conceptualization of REDIM safety margins were implemented in some of the dynamic module subroutines to account for the usual uncertainties associated with manual control tasks, such as the landing of an aircraft, the activation of braking devices, etc. However, the reduction of these uncertainties could significantly reduce the runway occupancy time (ROT) by reducing the margins of safety needed to cope with the original assumptions. This phenomena is similar to the anticipated reductions in the aircraft interarrival time (IAT) to the runway threshold through an improvement of the aircraft delivery accuracy (e.g., by reducing the final approach IAT separation buffers). The underlying assumptions made in this model have tried to establish a good balance between operational safety and the efficiency of the runway subsystem. This compromise was necessary because the model is expected to be applied in a variety of scenarios where the manual control uncertainties could be quite high. That is, the model could be either applied to small community airports where the proficiency and accuracy of the pilots might dictate slightly larger safety margins or to large transport-type airports where an increased number of automated landing rollout operations could take place in the future. It is expected that REDIM will be calibrated with the help of simulation and experimental results in order to gain more confidence in the output results of the model. This

calibration is, in fact, one of the most important steps to follow the development of REDIM. It is anticipated that the second phase of this research will devote time to validate the current model. It should be clearly understood by the analyst that scenario-specific factors such as obstructions, runway length, lighting conditions, etc. could affect the pilot's behavior to execute manual landings. For example, it is well known that the runway exit location and length have a large influence in ROT as pilots adjust their piloting behavior under scenario specific circumstances such as displaced thresholds and short runways. Therefore a series of empirical observations are recommended in the future in order to modify REDIM to account for some of these human operational factors.

8.3 *Turnoff Angle Parameters*

The turnoff angle plays a very important role in the estimation of the runway occupancy times (ROT's). Through simulations it can be shown that as much as 25% of the runway occupancy time is due to the turnoff for high speed exits. As such it is advisable to add more fexibility to the model by allowing the user to vary the turnoff angle. This new addition will be highly beneficial for analysis involving airport improvements where severe lateral separation restrictions pose a problem. In those cases the analyst could specify small turnoff angles to achieve a desired taxiway-turnoff intersection speed. In practice it has been shown (Fig 6.2) that turnoff exit angles lower that 18 degrees do not reduce the runway occupancy time as the aircraft travels for large periods of time on the turnoff. This in turn reduces the ROT times to a extend provided that the exit angle is not reduced below 20 degrees which seems to be a compromise bethween minimum ROT and the time to clear the runway. It is suggested that the final exit angle should be made variable in order to provide the user a mechanism to design fast turnoffs under drastic lateral restrictions (i.e., the presence of a parallel taxiway).

Bibliography

1. Anderson, J.E., *Transit Systems Theory*, Lexington Books, Lexington Massachusetts, 1979.

2. *Aviation Week and Space Technology* , McGraw-Hill Publishing Company, various issues 1986-1990.

3. Barrer, J.N. and Dielh, J.M., "Toward a Goal-Oriented Plan for Identifying Technology to Increase Airfield Capacity" , The MITRE Corporation, McLean, Virginia, 1988.

4. Branstetter, J.R., J. A. Houck, and A. D. Guenther, "Flight Simulation of a Wide-Body Transport Aircraft to Evaluate MLS-RNAV Procedures" , Journal of Aircraft, Volume 25, No. 6, June 1988.

5. *Business and Commercial Aviation,* McGraw-Hill Publishing Company, various issues 1989.

6. Carr, H., P. Reaveley, and L.B. Smith IV, "New Turnoffs for Optimal Runway Occupancy Times" , Airport Forum, No. 3, 1980, pp. 21-26.

7. Colligan, W. E., "A Systems Dynamics Model of the Terminal Operations of the National Airspace System Plan" , Project and Report, Systems Engineering, Virginia Tech University, 1988.

8. Daellenbach, H.G., "Dynamic Programming Model for Optimal Location of Runway Exits" , Transportation Research, Volume 8, Pergamon Press, 1974, pp. 225-232.

9. Denardo, E. V., *Dynamic Programming, Models and Applications* , Englewood Cliffs, New Jersey, 1982.

10. Desmond, J., "Improvements in Aircraft Safety and Operational Dependability from a Projected Flight Path Guidance Display" , AIAA Paper 861732, August 1986.

11. Elmaghraby, S. E., *Manuscript on Dynamic Programming* , Department of Operational Research, North Carolina State University, Used as Text of IEOR 6424 at Virginia Tech, 1989.

12. Federal Aviation Administration, *Airport Capacity Enhancement Plan* , DOT/FAA/CP 88-4, Washington, D.C., April 1988.

13. Federal Aviation Administration, *Air Traffic Activity and Delays Report for April 1988* , Air Traffic Operations Service, NAS Analysis Branch, May 1988.

14. Federal Aviation Administration, *Airoprt Design Standards : Transport Airport* , FAA/AC 150/5300-12, February 1983.

15. Federal Aviation Administration, *Airoprt Design Standards : Airports Served by Air Carriers, Taxiways* , FAA/AC 150/5335-1A, May 1970.

16. Gosling, G.D., A. Kanafani, and S. Hockaday, *Measures to Increase Airfield Capacity by Changing Aircraft Runway Occupancy Characteristics,* Research Report UCB-ITS-RR-81-7, Institute of Transportation Studies, University of California, Berkeley, 1981.

17. Green, W., Swanborough, G. and Mowinski, J., *Modern Commercial Aircraft* , Crescent Books, New York, 1987.

18. Hakimi, S. L., "Optimum Distribution of Switching Centers in a Communication Network and Some Graph Theoretic Problems," Operations Research, Vol. 13, 1965, pp. 462-475.

19. Harrin, E.N., *Low Tire Friction and Cornering Forces on a Wet Surface* , NACA TN 4406, September, 1958.

20. Harris, R.M., "Models for Runway Capacity Analysis" , MITRE Technical Report No. 4102, The MITRE Corporation, Washington Operations, December 1972.

21. Haury, R. L., "Fast Exit" , Civil Engineering of ASCE, October 1987, pp. 75-77.

22. Hillier, S.H. and G. J. Lieberman, *Introduction to Operations Research* , Holden-Day, Inc., Oakland, Califonia, 1986.

23. Hobeika, A.G., "Optimal Location of Runway Turnoffs in an Airport Environment" , Research Proposal submitted to NASA/Langley, June, 1988.

24. Horne, W.B., Smiley, R.F., and Stephenson, B.H., *Low-Speed Yawed Rolling and Some Other Elastic Characteristics of Two 56-in Diameter, 24 Ply-Rating Tires,* NACA TN 3235, August 1954.

25. Horonjeff, R., Finch, D.M., Belmont, D.M., and Ahlborn, G., *Exit Taxiway Location and Design* , Institute of Transportation and Traffic Engineering, University of California, Berkeley, August 1958.

26. Horonjeff, R., Grassi, R.C., Read, R.R., and Ahlborn, G., *A Mathematical Model for Locating Exit Taxiways* , Institute of Transportation and Traffic Engineering, University of California, Berkeley, December 1959.

27. Horonjeff, R., Read, R.R., and Ahlborn, G., *Exit Taxiway Locations* , Institute of Transportation and Traffic Engineering, University of California, Berkeley, September 1960.

28. Horonjeff, R. and McKelvey, F.X., *Planning and Design of Airports* , 3rd Edition, McGraw-Hill Book Company, New York, 1983.

29. Hosang, V.A., *Field Survey and Analysis of Aircraft Distribution on Airport Pavements* , Report DOT-FA71WAI-218, Washington, D.C., February, 1975.

30. Jane's all the World's Aircraft 1987-1988, Jane's Publishing Co. Ltd., England, 1988.

31. Joline, E.S., "Optimization of Runway Exit Configurations," Transportation Engineering Journal, American Society of Civil Engineers, Vol. 100, February 1974. pp. 85-102.

32. Koenig, S.E., "Analysis of Runway Occupancy Times at Major Airports" , MITRE Report MTR-7837, The MITRE Corporation, McLean, Virginia, 1978.

33. Lebron, J.E., *Estimates of Potential Increases in Airport Capacity Through ATC System Improvements in the Airport and Terminal Areas* , The MITRE Corporation, McLean, Virginia, FAA-DL5-87-1 (MTR-87W203), October 1987.

34. Los Angeles City Department of Airports, *Task Force Delay Study, Los Angeles International Airport Improvement Program* , Los Angeles Task Force Study Group.

35. Miller and Thomas, "Takeoff and Landing Problems - Design for Runway Conditions" , Journal of Aeronautical Society, Vol. 67, No. 633, September 1963, pp. 571-576.

36. Nicolai, L.M, *Fundamentals of Aircraft Design*, METS, Inc., San Jose, California, 1975.

37. Roskam, I. and E. Lan, *Airplane Aerodynamics and Performance* , Roskam Aviation and Engineering Corporation, Ottawa, Kansas, 1981.

38. Roskam, J., *Airplane Design: Part I* , Roskam Aviation and Engineering Corporation, Ottawa, Kansas, 1985.

39. Rossow, V.J, and Tinlin, B.E., " Research on Aircraft/Vortex-Wake Interactions to Determine Acceptable Level of Wake Intensity ", Journal of Aircraft, Volume 25, No. 6, June 1988.

40. Ruhl, T.A., "Empirical Analysis of Runway Occupancy with Applications to Exit Taxiway Location and Automated Exit Guidance," Transportation Research Board Meeting, January 7-11, Washington, 1990.

41. Schoen, M.L. et al, "Probabilistic Computer Model of Optimal Runway Turnoffs" , NASA Contractor Report 172549, April 1985.

42. Simpson, R.W., Odoni, A.R. and Salas-Roche, F., "Potential Impacts of Advanced Technologies on the ATC Capacity of High-Density Terminal Areas" , NASA Contractor Report 4024, October 1986.

43. Swedish, W.J., "Evaluation of the Potential for Reduced Longitudinal Spacing on Final Approach," MITRE Report MTR-79-000280, August, 1979.

44. Smith, J.M., *Mathematical Modeling and Digital Simulation for Engineers and Scientists* , John Wiley and Sons Inc., New York, 1987.

45. Tansel. B. C., R. L. Francis, and T. J. Lowe, "Location on Networks : A survey, Part I, The p-centered and p-median Problems," Management Science, Vol. 29, No. 4, April 1983, pp. 482-497.

46. Tosic', V., D. Teodorovic', and O. Babic', "Optimum Runway Exit Location," Transportation Planning and Technology, Vol 10, 1985, pp. 135-145.

47. Torenbeek, E., *Synyhesis of Subsonic Airplane Design*, Van Niemoff, Netherlands, 1981.

48. Transportation Research Board, National Research Council, *Future Development of the U. S. Airport Network*, TRB, NRC, Washington, D. C., 1988.

49. United States Department of Transportation, Transportation Systems Center, *Symposium on Aviation System Concepts for the 21st Century* , September 28 and 29, 1988.

50. Walpole. R.E, and Myers, R.H., *Statistics for Engineers and Scientists*, 2nd Edition, McMillan Company, New York, 1978.

51. Williams, J., *Aircraft Performance Prediction Methods and Optimization*, AGARD Lecture Series No. 56, NATO, 1972.

52. Witteveen, N. D., *Modified Rapid Runway Exit Taxiways To Reduce Runway Occupancy Time*, Presented at 21st International Air Transport Association Conference on System Demand and System Capacity, Montreal, Canada, September 1987.

53. Wong, J. Y., *Theory of Ground Vehicles*, John Wiley and Sons, New York, 1958.

54. Yager, T.J., and White, E.J., *Recent Progress Towards Predicting Aircraft Ground Handling Performace*, NASA Technical Memorandum 81952, Hampton, VA, 1981.

Appendix A. Glossary of Aircraft Characteristics

	A	B	C	D	E	F	G	H	I	J
1	CODE NAME	NAME	MAX. ANGLE	WINGSPAN	WHEELBASE	% LOAD	LAND.MASS	WING AREA	YAW INERTIA	CL MAXIMUM
2			(DEGREES)	(METERS)	(METERS)	(PERCENT)	(KILOGRAMS)	(SQ METERS)	(KG -SQ M)	(DIM)
3										
4	COMMERCIAL AIRCRAFT									
5										
6	A-300-600	AIRBUS A300	35.00	44.80	18.60	92.50	140,000	260.00	1.5348E+07	3.0009
7	A-310-300	AIRBUS A310	36.00	43.90	15.21	91.60	123,000	219.00	1.2282E+07	3.1912
8	A-320-200	AIRBUS A320	38.00	33.91	12.63	90.50	64,500	122.10	4.0426E+06	2.9941
9	FOKKER-100	FOKKER 100	32.00	28.08	14.00	89.50	39,915	93.50	1.7695E+06	2.5326
10	BAe 146-200	BAe 146	30.00	26.34	11.20	92.30	38,740	77.30	1.5342E+06	3.2889
11	B-727-200	BOEING 727	38.00	36.75	16.75	92.50	72,200	157.30	4.9088E+06	2.5585
12	B-737-300	BOEING 737	36.00	28.88	12.35	93.50	51,710	105.40	2.7632E+06	2.8425
13	B-737-400	BOEING 737	36.00	28.88	12.50	92.50	54,885	105.40	3.0617E+06	2.5527
14	B-747-200B	BOEING 747	43.00	59.64	25.60	94.80	285,765	511.00	5.2423E+07	2.7359
15	B-747-400	BOEING 747	44.00	63.30	25.60	94.00	285,765	511.00	5.2423E+07	2.7359
16	B-757-200	BOEING 757	35.00	38.05	18.29	93.50	89,810	185.25	7.1474E+06	2.8366
17	B-767-300	BOEING 767	37.50	47.57	19.69	92.20	129,273	283.3	1.3380E+07	2.4480
18	MD-83	MCDONDOUG.	36.00	32.87	22.07	90.30	63,276	118.00	3.9114E+06	2.9319
19	MD-87	MCDON DOUG.	39.00	32.87	19.18	91.20	58,067	118.00	3.3737E+06	2.9018
20	DC-10-30	DOUGLAS ACF	42.00	50.40	22.05	94.00	182,798	367.70	2.4293E+07	2.6595
21	MD-11	MCDONDOUG	49.00	53.00	28.27	93.60	195,044	338.90	2.7162E+07	2.8279
22										
23	CODE NAME	NAME	MAX. ANGLE	WINGSPAN	WHEELBASE	% LOAD	LAND.MASS	WING AREA	YAW INERTIA	CL MAXIMUM
24			(DEGREES)	(METERS)	(METERS)	(PERCENT)	(KILOGRAMS)	(SQ METERS)	(KG -SQ M)	(DIM)
25										
26	SINGLE ENGINE	PISTON AIRCRAFT								
27										
28	PA-38-112	PIPER TOMAHAWK	40.00	10.36	1.45	77.45	757	11.59	1.9203E+03	1.5748
29	PA-28-161	PIPER WARRIOR II	39.00	10.67	2.03	82.18	1,109	15.79	3.7055E+03	1.6935
30	PA-28-236	PIPER DAKOTA II	40.00	10.92	1.98	81.73	1,363	15.90	5.2849E+03	1.6477
31	PA-32-301	PIPER SARATOGA	38.00	11.02	2.36	85.92	1,636	16.63	7.2365E+03	1.5472
32	PA-46-310P	PIPER MALIBU	45.00	13.66	2.44	83.31	1,777	18.28	8.3029E+03	1.9504
33	BE-F33A	BEECH DONANZA	41.00	10.21	2.13	81.51	1,545	16.81	6.5575E+03	2.1300
34	CE-172	CESSNA SKYHAWK	43.00	10.92	1.70	77.93	1,090	15.90	3.5969E+03	2.0407
35	CE-208	CESSNA STATIONAIR	39.00	10.92	2.11	81.20	1,723	16.17	7.9116E+03	3.1719
36	CE-182	CESSNA SKYLINE	42.00	10.92	1.69	76.85	1,338	16.16	5.1191E+03	2.4647
37	CE-210P	CESSNA CENTURION	40.00	11.20	1.83	77.60	1,772	16.50	8.3029E+03	1.9925
38										
39										
40	CODE NAME	NAME	MAX. ANGLE	WINGSPAN	WHEELBASE	% LOAD	LAND.MASS	WING AREA	YAW INERTIA	CL MAXIMUM
41			(DEGREES)	(METERS)	(METERS)	(PERCENT)	(KILOGRAMS)	(SQ METERS)	(KG -SQ M)	(DIM)
42										
43										
44	MULTIENGINE AIRCRAFT (INCLUDING TURBOPROPS)									
45										
46	BE-58	BEECH BARON 58	39.00	11.53	2.72	84.73	2,500	18.52	1.5016E+04	1.4859
47	BE-300	BEECH KING AIR	32.00	16.61	4.56	89.13	6,363	28.16	7.4990E+04	2.0760
48	CE-402C	BUSINESSLINER	42.00	13.45	3.18	88.12	3,107	20.98	2.1831E+04	1.4304
49	CE-421	GOLDEN EAGLE	40.00	12.53	3.20	87.19	3,266	19.97	2.3789E+04	1.4310
50	BE-2000	BEECH STARSHIP	90.00	16.46	6.86	92.27	6,363	26.13	7.4990E+04	2.3520
51	CE-F406	CESS. CARAVAN II	40.00	15.04	3.81	85.37	4,250	23.50	3.7434E+04	1.6213
52	PA-34-220T	PIPER SENECA III	46.00	11.85	2.13	82.13	2,160	19.36	1.1675E+04	1.5439
53	PA-42-1000	PIPER CHEYENNE	32.00	14.53	3.23	87.22	5,477	27.25	5.7930E+04	1.7171
54	P180	PIAGGIO AVANTI	40.00	13.84	5.80	91.41	4,777	20.82	4.5779E+04	1.7075
55										
56	TURBOJET AND TURBOFAN BUSINESS AIRCRAFT									
57										
58		NAME	MAX. ANGLE	WINGSPAN	WHEELBASE	% LOAD	LAND.MASS	WING AREA	YAW INERTIA	CL MAXIMUM
59			(DEGREES)	(METERS)	(METERS)	(PERCENT)	(KILOGRAMS)	(SQ METERS)	(KG -SQ M)	(DIM)
60										
61	CE-550	CESSNA CITATION II	41.00	15.90	5.55	92.61	5,773	30.00	6.3424E+04	1.7680
62	CE-650	CESS. CITATION III	40.00	16.31	6.50	92.95	9,090	26.37	1.3857E+05	2.9561
63	LEARJET 31	LEARJET 31	36.00	13.34	6.15	93.42	6,940	24.57	8.7076E+04	2.4130
64	LEARJET 55C	LEARJET 55	31.00	13.34	7.01	93.27	8,165	24.57	1.1519E+05	2.1736
65	G1159C	GRUMMAN IV	41.00	23.72	11.62	93.70	26,535	89.29	8.7620E+05	1.5472
66	BAe 125-800	BAe 125	43.00	15.66	6.41	93.10	10,590	34.75	1.8024E+05	2.1704
67	IA-1124A	WESTWIND II	42.00	13.65	7.79	94.77	8,636	28.55	1.2687E+05	2.1403
68	BE-400	BEECHJET	40.00	13.25	5.86	92.68	6,454	22.42	7.6846E+04	2.3380
69	IA-1125	ASTRA	42.00	16.05	7.34	94.38	9,409	29.43	1.4705E+05	2.5508
70	DA-100	FALCON 100	42.00	13.08	5.30	92.77	8,020	24.13	1.1170E+05	3.0140
71	DA-200	FALCON 200	41.00	16.30	5.74	90.94	13,090	41.03	2.5960E+05	2.7255
72	DA-50	FALCON 50	47.00	18.86	7.24	92.19	17,857	46.84	4.4309E+05	3.5907
73	CL-601-3A	CHALLENGER	38.00	19.61	7.99	92.86	16,363	42.00	3.8121E+05	2.1780
74										
75	TURBOPROP COMMUTER AIRCRAFT									
76										
77		NAME	MAX. ANGLE	WINGSPAN	WHEELBASE	% LOAD	LAND.MASS	WING AREA	YAW INERTIA	CL MAXIMUM
78			(DEGREES)	(METERS)	(METERS)	(PERCENT)	(KILOGRAMS)	(SQ METERS)	(KG -SQ M)	(DIM)
79										
80	SAAB-340	SAAB 340	38.00	21.44	7.14	90.88	12,020	41.80	2.2416E+05	2.5779
81	BAe 31	JETSTREAM	36.00	15.85	4.60	87.18	6,600	25.20	7.9863E+04	2.1346
82	EMB-120	BRASILIA	38.00	19.78	6.97	90.77	11,250	39.43	2.0001E+05	2.2722
83	DHC-6-300	TWIN OTTER	38.00	19.81	4.53	87.16	5,579	39.02	5.9799E+04	2.5620
84	DHC-7-100	DASH-7	37.00	28.35	8.38	90.89	19,050	79.90	4.9527E+05	2.9330
85	DHC-8-100	DASH-8	38.00	25.91	9.60	91.63	15,375	54.35	3.4245E+05	3.2894
86	BEECH 1900	BEECH 1900	30.00	16.61	7.25	93.72	7,302	28.15	9.5042E+04	2.0658
87	SA-227-AT/41	FAIR MERLIN IVC	35.00	16.60	5.38	88.74	6,590	28.73	7.9655E+04	1.8267
88	EMB-110-P1	BANDEIRANTE	30.00	15.33	5.10	90.70	5,712	29.10	6.2275E+04	2.4852
89	CASA 212-300	AVIOCAR	38.00	19.00	5.55	88.07	7,465	40.00	9.8724E+04	1.8490
90	CASA 235-100	CASA-235	37.00	25.81	6.92	89.70	14,229	73.00	2.9970E+05	1.9817
91	ATR-72	AEROS/AERITALIA	32.00	27.05	10.70	93.26	21,385	61.00	6.0434E+05	2.6089
92	ATR-42-300	AEROS/AERITALIA	35.00	24.57	8.78	92.71	15,500	54.50	3.4726E+05	3.2170
93	FOKKER 50	FOKKER 50	43.00	29.00	9.70	92.13	18,890	70.00	4.8813E+05	2.5417
94	BAe ATP	BAe ATP	42.00	30.63	9.70	92.62	21,773	77.00	6.2334E+05	2.2519
95	DO-228-201	DORNIER 228	35.00	16.97	6.29	91.05	6,213	31.84	7.1973E+04	2.6203
96	SHORTS 330	SHORTS 330 REG	42.00	22.76	6.15	87.93	10,251	42.10	1.7043E+05	2.7543

	K	L	M	N	O	P	Q	R	S	T
1	CODE NAME	FAR 25	BRAKING DISTANCE	V. STALL	V. TOUCHDOWN	AIR DIST.	DECELERATION	FREE ROLL	FREE ROLL DIST.	N. FLARE
2		LANDING (M.)	(METERS)	(M/SEC.)	(M/SEC.)	(METERS)	(M/SEC-SEC)	TIME (SEC.)	(METERS)	(G'S)
3										
4	COMMERCIAL AIRCRAFT									
5										
6	A-300-600	1555.00	999.61	53.61	61.65	370.44	1.90	3.00	184.95	1.15
7	A-310-300	1480.00	933.88	53.09	61.06	368.95	2.00	3.00	183.17	1.15
8	A-320-200	1540.00	987.88	53.09	61.06	368.95	1.89	3.00	183.17	1.15
9	FOKKER-100	1360.00	815.02	51.96	59.75	365.72	2.19	3.00	179.26	1.15
10	BAe 146-200	1130.00	612.89	47.42	54.54	353.50	2.43	3.00	163.61	1.15
11	B-727-200	1560.00	1004.61	53.61	61.65	370.44	1.89	3.00	184.95	1.15
12	B-737-300	1393.00	844.14	52.58	60.46	367.47	2.17	3.00	181.39	1.15
13	B-737-400	1497.00	941.61	53.61	61.65	370.44	2.02	3.00	184.95	1.15
14	B-747-200B	2112.00	1536.70	56.70	65.21	379.68	1.38	3.00	195.62	1.15
15	B-747-400	2134.00	1558.70	56.70	65.21	379.68	1.36	3.00	195.62	1.15
16	B-757-200	1460.00	912.78	52.32	60.17	366.74	1.98	3.00	180.50	1.15
17	B-767-300	1650.00	1088.03	54.64	62.84	373.46	1.81	3.00	188.51	1.15
18	MD-83	1585.00	1026.33	54.12	62.24	371.94	1.89	3.00	186.73	1.15
19	MD-87	1430.00	884.38	52.06	59.87	366.01	2.03	3.00	179.61	1.15
20	DC-10-30	1630.00	1067.54	54.72	62.92	373.69	1.85	3.00	188.77	1.15
21	MD-11	2130.00	1552.14	57.09	65.66	380.89	1.39	3.00	196.97	1.15
22										
23	CODE NAME	FAR 25	BRAKING DISTANCE	V. STALL	V. TOUCHDOWN	AIR DIST.	DECELERATION	FREE ROLL	FREE ROLL DIST	N. FLARE
24		LANDING (M.)	(METERS)	(M/SEC.)	(M/SEC.)	(METERS)	(M/SEC-SEC)	TIME (SEC.)	(METERS)	(G'S)
25										
26	SINGLE ENGINE PISTON AIRCRAFT									
27										
28	PA-38-112	485.96	215.00	25.77	29.64	211.68	2.04	2.00	59.28	1.3
29	PA-28-161	418.00	181.00	25.77	29.64	211.68	2.43	2.00	59.28	1.3
30	PA-28-236	526.00	252.00	28.87	33.20	213.97	2.19	2.00	66.39	1.3
31	PA-32-301	491.00	223.00	30.93	35.57	215.64	2.84	2.00	71.13	1.3
32	PA-46-310P	463.00	275.00	29.90	34.38	214.79	2.15	2.00	68.76	1.3
33	BE-F33A	404.00	259.00	26.29	30.23	212.04	1.79	2.00	60.46	1.3
34	CE-172	408.00	180.00	23.20	26.68	209.97	1.98	2.00	53.35	1.3
35	CE-208	457.00	233.00	23.20	26.68	209.97	1.53	2.00	53.35	1.3
36	CE-182	402.00	180.00	23.20	26.68	209.97	1.98	2.00	53.35	1.3
37	CE-210P	505.00	233.00	29.38	33.79	214.38	2.45	2.00	67.58	1.3
38										
39										
40	CODE NAME	FAR 25	BRAKING DISTANCE	V. STALL	V. TOUCHDOWN	AIR DIST.	DECELERATION	FREE ROLL	FREE ROLL DIST.	N. FLARE
41		LANDING (M.)	(METERS)	(M/SEC.)	(M/SEC.)	(METERS)	(M/SEC-SEC)	TIME (SEC.)	(METERS)	(G'S)
42										
43										
44	MULTIENGINE AIRCRAFT (INCLUDING TURBOPROPS)									
45										
46	BE-58	751.47	439.00	38.14	43.87	310.47	2.19	2.00	87.73	1.25
47	BE-300	857.18	540.00	41.75	48.02	315.16	2.13	2.00	96.03	1.25
48	CE-402C	655.77	340.00	40.72	46.83	313.77	3.23	2.00	93.66	1.25
49	CE-421	693.57	375.00	42.78	49.20	316.57	3.23	2.00	98.40	1.25
50	BE-2000	922.77	607.00	40.72	46.83	313.77	1.81	2.00	93.66	1.25
51	CE-406	667.86	350.00	42.27	48.61	315.86	3.38	2.00	97.22	1.25
52	PA-34-220T	527.63	220.00	34.02	39.12	305.63	3.48	2.00	78.25	1.25
53	PA-42-1000	851.30	532.00	43.30	49.79	317.30	2.33	2.00	99.59	1.25
54	P180	743.81	420.00	46.39	53.35	321.81	3.39	2.00	106.70	1.25
55										
56	TURBOJET AND TURBOFAN BUSINESS AIRCRAFT									
57										
58		FAR 25	BRAKING DISTANCE	V. STALL	V. TOUCHDOWN	AIR DIST.	DECELERATION	FREE ROLL	FREE ROLL DIST.	N. FLARE
59		LANDING (M.)	(METERS)	(M/SEC.)	(M/SEC.)	(METERS)	(M/SEC-SEC)	TIME (SEC.)	(METERS)	(G'S)
60										
61	CE-550	798.10	320.00	41.75	48.02	334.06	3.60	3.00	144.05	1.15
62	CE-650	842.53	356.00	43.22	49.70	337.43	3.47	3.00	149.10	1.15
63	LEARJET 31	883.00	396.00	43.30	49.79	337.62	3.13	3.00	149.38	1.15
64	LEARJET 55C	941.90	418.00	49.48	56.91	353.18	3.87	3.00	170.72	1.15
65	G1159C	1026.54	465.00	55.46	63.78	370.19	4.37	3.00	191.35	1.15
66	BAe 125-800	867.37	356.00	47.42	54.54	347.76	4.18	3.00	163.61	1.15
67	IA-1124A	860.30	348.00	47.58	54.71	348.16	4.30	3.00	164.14	1.15
68	BE-400	863.46	370.00	44.41	51.07	340.26	3.52	3.00	153.20	1.15
69	IA-1125	819.79	324.00	44.80	51.52	341.22	4.10	3.00	154.57	1.15
70	QA-100	804.67	325.00	42.03	48.33	334.68	3.59	3.00	144.99	1.15
71	DA-200	872.00	385.00	43.30	49.79	337.62	3.22	3.00	149.38	1.15
72	DA-50	885.17	410.00	41.24	47.42	332.90	2.74	3.00	142.27	1.15
73	CL-601-3A	1016.13	467.00	53.53	61.55	364.46	4.06	3.00	184.66	1.15
74										
75	TURBOPROP COMMUTER AIRCRAFT									
76										
77		FAR 25/23	BRAKING DISTANCE	V. STALL	V. TOUCHDOWN	AIR DIST.	DECELERATION	FREE ROLL	FREE ROLL DIST.	N. FLARE
78		LANDING (M.)	(METERS)	(M/SEC.)	(M/SEC.)	(METERS)	(M/SEC-SEC)	TIME (SEC.)	(METERS)	(G'S)
79										
80	SAAB-340	1140.45	708.00	42.27	48.61	335.23	1.67	2.00	97.22	1.15
81	BAe 31	1098.03	656.00	44.33	50.98	340.07	1.98	2.00	101.96	1.15
82	EMB-120	1269.46	825.00	44.85	51.57	341.32	1.61	2.00	103.14	1.15
83	DHC-6-300	635.80	256.00	29.90	34.38	311.03	2.31	2.00	68.76	1.15
84	DHC-7-100	823.09	418.00	36.08	41.49	322.10	2.06	2.00	82.99	1.15
85	DHC-8-100	943.50	534.00	37.11	42.68	324.14	1.71	2.00	85.36	1.15
86	BEECH 1900	910.46	466.00	44.85	51.57	341.32	2.85	2.00	103.14	1.15
87	SA-227-AT/41	894.46	450.00	44.85	51.57	341.32	2.96	2.00	103.14	1.15
88	EMB-110-P1	1252.90	850.00	35.57	40.90	321.09	0.98	2.00	81.80	1.15
89	CASA 212-300	768.10	345.00	40.21	46.24	330.62	3.10	2.00	92.47	1.15
90	CASA 235-100	795.80	375.00	39.69	45.64	329.51	2.78	2.00	91.29	1.15
91	ATR-72	1047.84	596.00	46.39	53.35	345.14	2.39	2.00	106.70	1.15
92	ATR-42-300	979.73	568.00	37.63	43.27	325.19	1.65	2.00	86.55	1.15
93	FOKKER 50	1025.74	598.00	41.24	47.42	332.90	1.88	2.00	94.85	1.15
94	BAe ATP	1092.46	648.00	44.85	51.57	341.32	2.05	2.00	103.14	1.15
95	DO-228-201	752.57	354.00	34.84	39.72	319.14	2.23	2.00	79.43	1.15
96	SHORTS 330	1032.73	621.00	37.63	43.27	325.19	1.51	2.00	86.55	1.15

	U	V	W	X	Y	Z	AA	AB	AC	AD
1	STD. Vapp	CODE NAME	VERT. DIST. TO CG	TOTAL LENGTH	ASPECT RATIO	WHEELTRACK	WHEEL ANGLE	PROJ. DISTANCE	TURNING ANGLE	DIST. CG-MG
2	(m/sec.)		(METERS)	(METERS)	(DIMENSIONLESS)	(METERS)	(DEGREES)	(METERS)	(DEGREES)	(METERS)
3										
4		COMMERCIAL AIRCRAFT								
5										
6	3.86	A-300-600		54.08	7.72	9.60	14.47	9.30	0.00	
7	3.82	A-310-300		46.60	8.80	9.60	17.51	9.15	0.00	
8	3.82	A-320-200			9.39	7.59	16.72	7.27	0.00	
9	3.74	FOKKER-100			8.43	5.04	10.20	4.96	0.00	
10	3.41	BAe 146-200	3.05	28.60	8.98	4.72	11.90	4.62	52.86	
11	3.86	B-727-200			8.59	6.38	10.75	6.25	0.00	
12	3.76	B-737-300			7.91	5.23	11.95	5.12	0.00	
13	3.86	B-737-400			7.91	5.23	11.81	5.12	0.00	
14	4.08	B-747-200B			6.96	11.00	12.12	10.75	0.00	
15	4.08	B-747-400			7.84	11.00	12.12	10.75	0.00	
16	3.76	B-757-200			7.82	7.32	11.31	7.18	0.00	
17	3.93	B-767-300			7.99	9.30	13.29	9.05	0.00	
18	3.89	MD-83			9.16	5.08	6.56	5.05	0.00	
19	3.75	MD-87			9.16	5.08	7.54	5.04	0.00	
20	3.94	DC-10-30			6.91	10.67	13.60	10.37	0.00	
21	4.11	MD-11			8.29	10.67	10.69	10.48		
22										
23	STD. Vapp	CODE NAME	VERT. DIST. TO CG	TOTAL LENGTH	ASPECT RATIO	WHEELTRACK	WHEEL ANGLE	PROJ. DISTANCE	TURNING ANGLE	DIST. CG-MG
24	(m/sec.)		(METERS)	(METERS)	(DIMENSIONLESS)	(METERS)	(DEGREES)	(METERS)	(DEGREES)	(METERS)
25										
26		SINGLE ENGINE PISTON AIRCRAFT								
27										
28	1.85	PA-38-112	1.22	7.04	9.26	3.05	46.44	2.10	49.26	0.33
29	1.85	PA-28-161	1.35	7.25	7.21	3.05	36.91	2.44	47.91	0.36
30	2.08	PA-28-236	1.35	7.54	7.50	3.05	37.60	2.42	48.17	0.36
31	2.23	PA-32-301	1.24	8.45	7.30	3.39	35.68	2.75	42.01	0.33
32	2.15	PA-46-310P	1.52	8.66	11.46	3.75	37.54	2.97	45.63	0.41
33	1.89	BE-F33A	1.47	8.13	6.20	2.92	34.43	2.41	50.67	0.39
34	1.67	CE-172	1.40	8.20	7.50	2.53	36.65	2.03	54.06	0.38
35	1.67	CE-208	1.48	9.80	7.37	3.09	36.21	2.49	49.89	0.40
36	1.67	CE-182	1.46	8.66	7.38	2.74	39.03	2.13	53.91	0.39
37	2.11	CE-210P	1.53	8.59	7.60	2.64	35.80	2.14	55.01	0.41
38										
39										
40	STD. Vapp	CODE NAME	VERT. DIST. TO CG	TOTAL LENGTH	ASPECT RATIO	WHEELTRACK	WHEEL ANGLE	PROJ. DISTANCE	TURNING ANGLE	DIST. CG-MG
41	(m/sec.)		(METERS)	(METERS)	(DIMENSIONLESS)	(METERS)	(DEGREES)	(METERS)	(DEGREES)	(METERS)
42										
43										
44		MULTIENGINE AIRCRAFT (INCLUDING TURBOPROPS)								
45										
46	2.74	BE-58	1.55	9.12	7.18	2.92	28.22	2.57	50.30	0.42
47	3.00	BE-300	1.85	13.34	9.80	5.23	29.83	4.54	39.19	0.50
48	2.93	CE-402C	1.41	11.09	8.62	5.48	40.75	4.15	34.18	0.38
49	3.08	CE-421	1.53	11.09	7.86	5.30	39.63	4.08	36.85	0.41
50	2.93	BE-2000	1.98	14.05	10.37	5.13	20.50	4.81	39.49	0.53
51	3.04	CE-F406	2.08	11.89	9.63	4.28	23.32	3.73	48.10	0.56
52	2.45	PA-34-220T	1.42	8.72	7.25	3.38	39.43	2.65	47.00	0.38
53	3.12	PA-42-1000	1.54	13.23	7.75	5.72	41.52	4.28	35.72	0.41
54	3.34	P180	1.86	14.68	9.70	2.85	13.80	2.77	53.35	0.50
55										
56		TURBOJET AND TURBOFAN BUSINESS AIRCRAFT								
57										
58	STD. Vapp		VERT. DIST. TO CG	TOTAL LENGTH	ASPECT RATIO	WHEELTRACK	WHEEL ANGLE	PROJ. DISTANCE	TURNING ANGLE	DIST. CG-MG
59	(m/sec.)		(METERS)	(METERS)	(DIMENSIONLESS)	(METERS)	(DEGREES)	(METERS)	(DEGREES)	(METERS)
60										
61	3.00	CE-550	1.53	14.39	8.43	5.36	25.77	4.83	32.37	0.41
62	3.11	CE-650	1.71	16.90	10.09	2.84	12.32	2.77	50.94	0.45
63	3.12	LEARJET 31	1.51	14.83	7.24	2.51	11.53	2.46	50.84	0.40
64	3.56	LEARJET 55C	1.76	16.79	7.24	2.51	10.15	2.47	54.93	0.47
65	3.99	G1159C	2.73	26.70	6.30	4.17	10.17	4.10	53.06	0.73
66	3.41	BAe 125-800	1.65	15.60	7.06	2.79	12.28	2.73	50.43	0.44
67	3.42	IA-1124A	1.52	14.75	6.53	3.35	12.13	3.28	42.86	0.41
68	3.19	BE-400	1.60	14.75	7.83	2.84	13.62	2.76	49.22	0.43
69	3.22	IA-1125	1.54	16.08	8.75	2.77	10.68	2.72	48.53	0.41
70	3.02	DA-100	1.43	13.86	7.09	2.86	15.10	2.76	46.00	0.38
71	3.12	DA-200	1.94	17.15	6.48	3.69	17.82	3.51	47.84	0.52
72	2.97	DA-50	2.11	18.50	7.59	3.98	15.37	3.84	47.71	0.57
73	3.85	CL-601-3A	2.13	20.85	9.16	3.18	11.25	3.12	53.79	0.57
74										
75		TURBOPROP COMMUTER AIRCRAFT								
76										
77	STD. Vapp		VERT. DIST. TO CG	TOTAL LENGTH	ASPECT RATIO	WHEELTRACK	WHEEL ANGLE	PROJ. DISTANCE	TURNING ANGLE	DIST. CG-MG
78	(m/sec.)		(METERS)	(METERS)	(DIMENSIONLESS)	(METERS)	(DEGREES)	(METERS)	(DEGREES)	(METERS)
79										
80	3.04	SAAB-340	2.43	19.72	11.00	6.71	25.17	6.07	38.67	0.65
81	3.19	BAe 31	2.20	14.37	9.97	5.94	32.85	4.99	41.40	0.59
82	3.23	EMB-120	2.40	20.00	9.92	6.58	25.27	5.95	38.89	0.64
83	2.15	DHC-6-300	2.17	15.77	10.06	3.71	22.27	3.43	51.65	0.58
84	2.60	DHC-7-100	2.85	24.54	10.06	7.16	23.13	6.58	40.88	0.76
85	2.67	DHC-8-100	3.00	22.54	12.35	7.87	22.29	7.28	39.48	0.80
86	3.23	BEECH 1900	1.70	17.63	9.80	5.23	19.83	4.92	34.64	0.46
87	3.23	SA-227-AT/41	2.26	18.09	9.59	4.57	23.01	4.21	47.05	0.61
88	2.56	EMB-110-P1	1.77	15.10	8.08	4.94	25.84	4.45	38.52	0.47
89	2.89	CASA 212-300	2.47	16.15	9.03	3.10	15.60	2.99	58.85	0.66
90	2.86	CASA 235-100	2.66	21.38	9.13	3.90	15.74	3.75	54.79	0.71
91	3.34	ATR-72	2.69	27.17	12.00	4.10	10.84	4.03	53.18	0.72
92	2.71	ATR-42-300	2.39	22.77	11.08	4.10	13.14	3.99	50.12	0.64
93	2.97	FOKKER 50	2.85	25.48	12.01	7.20	20.36	6.75	40.17	0.76
94	3.23	BAe ATP	2.67	26.00	12.18	8.46	23.56	7.75	34.55	0.72
95	2.48	DO-228-201	2.10	18.56	9.04	3.30	14.70	3.19	52.76	0.56
96	2.71	SHORTS 330	2.77	17.39	12.30	4.24	19.02	4.01	54.11	0.74

Appendix B. Optimality Through a Discrete Search

Suppose there exist feasible ranges r (r = 1 to R) for each aircraft-surface condition combination, where ROT's within each range are increasing from left to right. Assuming that N exits are to be located on the runway at any points such that there is at least one exit for each feasible range, and that the exits are separated by at least a distance of D_{min}, the optimal exit locations, which minimize the weighted sum of ROT, can be found from a finite collection of points. Let L_r and R_r be the left hand and the right hand interval end points for the range r, respectively. L_r and R_r are actually distances measured from the start of the active runway threshold. Define a set of **breakpoints** as points on the runway which are of the type $L_r + q\ D_{min}$ for $q \geq 0$ and integer valued, for r = 1 to R. Then the optimal locations are found from the set of breakpoints by the following theorem.

THEOREM 1 Assume that N is large enough so that the above problem has a feasible solution. Then at optimality, each location will coincide with some breakpoint.

PROOF We will prove this by induction on the exit index. Consider the leftmost exit location. This exit must coincide with L_r for some $r \in \{1, \ldots R\}$ because if not, by sliding its location leftwards until it coincides with such a location, we will maintain feasibility (since all aircraft which could take this exit can continue to do so), and the objective value will strictly improve. Inductively, suppose that the result is true for the location of exit 1,

. . . , t, and consider exit t + 1, where t $\{1, \ldots, N\text{-}1\}$. If exit t + 1 coincides with some L_r for $R \in \{1, \ldots, R\}$, then the result is true. If exit t + 1 is at a distance D_{min} from exit t to its left, then by the induction hypothesis, and the construction of breakpoints, the result is again true. If neither of these cases holds, then we can slide the location of exit t + 1 leftwards until one of these conditions holds, thereby maintaining feasibility and improving the objective value. Hence, the result must be true for the location of exit t + 1, and this completes the proof.

COROLLARY 1 For any pair of exits t and t+1 separated by a distance greater than D_{min}, the location of exit t+1 must lie in $\{ L_1, ..., L_R \}$

PROOF Evident from the proof of Theorem 1.

COROLLARY 2 Given that the ROT's are nondecreasing, rather than strictly increasing within each feasible range, there exists an optimal solution in which the exit locations coincide with the defined breakpoints.

PROOF Evident from the proof of Theorem 1.

COROLLARY 3 (Improvement problem) Given existing exit locations at points $D_1, ..., D_e$, define additional breakpoints as the points $D_i + q\ D_{min}$ for $q \geq 1$ and integer, for $i = 1, \ldots, e$. Furthermore, delete from the set of breakpoints thus defined, those which lie at a distance less than D_{min} from an existing exit location (on either side of it). Then again, any optimal solution will have the new exit locations coinciding with these defined breakpoints.

PROOF Can be constructed similar to that of Theorem 1.

REMARK By Corollary 1, for N and D_{min} small enough, optimal locations of exits will coincide with the points L_r, $r = 1, \ldots, R$. For larger values of these parameters, the other breakpoints will begin to play a role. This is of consequence since the points L_r represent the critical locations given by the simulations of aircraft landing movement. Also, given our emphasis, Corollary 3 is of most importance.

Appendix C. Approximation of Turnoff Times

The estimation of the turnoff time plays a very important role in the mathematical optimization module of REDIM as the dynamic programming technique used tries to minimize a time related performance index. It was said in Chapter 4 of this report that in order to save valuable computational time it was necessary to approximate the time spent by aircraft in the turnoff maneuver under two scenario conditions (dry and wet). Furthermore, every secondary candidate solution (i.e., those generated from the actual aircraft landing simulations to comply with Bellman's principle of optimality as explained in Appendix B) has an associated turnoff time (TOT) for every aircraft and scenario condition and thus the estimation of these times would consume large amounts of time if performed through the complete simulation scheme used to estimate primary candidates and described in Section 3.3 of this report.

Since the geometry for every primary candidate is completely known from the simulation results it is possible to extract two representative values of the radius of curvature, R1 and R2, to approximate the turnoff geometry until the aircraft has cleared the runway as depicted in Fig. C.1. It should be emphasized that although this is an approximation the results are usually accurate if R1 and R2 are selected appropriately. In the late fifties Horonjeff [Horonjeff, 1959] used this scheme to approximate high-speed turnoff tracks with satisfactory results.

Through hundredths of simulations of the REDIM model its was observed that the values of R1 and R2 could be extracted from the turnoff simulation as a function of time and aircraft category. This segmentation per category was somewhat expected from equations 3.13-3.18 in Section 3.4 if one realizes that the aircraft turning capability is related to the inertia, centripetal and scrubbing forces resisting the aircraft turning motion. Results depicting the time rate of change variations of the radius of curvature for representative aircraft using REDIM are shown in Fig. C.2. It was then decided through examination of all the data to estimate R1 as the instantaneous radius of the curvature occuring one second after the turning maneuver started whereas R2 was varied selectively between four and six seconds depending upon the aircraft category. The four-second R2 is used with category A aircraft which display

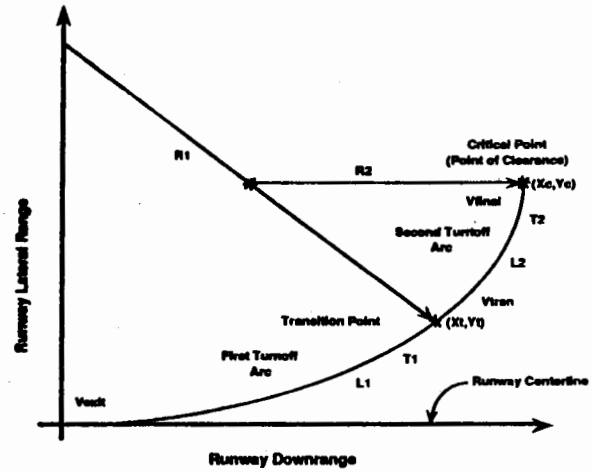

Nomenclature

(Xc,Yc)	Clearance Point Coordinates (meters)
(Xt,Yt)	Transition Point Coordinates (meters)
L1	First Arc Length (meters)
L2	Second Arc Length (meters)
T1	Second Turnoff Arc Travel Time (seconds
T2	First Turnoff Arc Travel Time (seconds)
Vexit	Aircraft Exit Speed at the Start of the Turn (m./sec.)
Vtran	Aircraft Speed at the Transition Point (m./sec.)
Vfinal	Aircraft Speed at the Clearance Point (m./sec.)
R1	First Turnoff Arc Radius (meters)
R2	Second Turnoff Arc Radius (meters)

Figure C.1 Turnoff Time Approximation Nomenclature.

very fast behavior in the turnoff dynamics whereas the six-second R2 is used to predict heavy transport aircraft turnoff dynamics having larger time lags to achieve a "steady-state" radius of curvature. In REDIM nomenclature these times are labeled as easement curvature time, TR1, and steady-state curvature time, TR2.

Once the exact turnoff path is known the next step is to estimate the time required to clear the runway. This is done under the assumption that a turning aircraft decelerates due to rolling friction alone. Actual aircraft speed measurements performed by by Horonjeff [Horonjeff et al, 1959, 1960] and Hosang [Hosang, 1978] in high-speed taxiways show nearly constant deceleration rates similar to those associated with a moderate value of rolling friction alone. This can be attributed to the small aircraft castor angles present while negotiating a high-speed turnoff. A conservative value of F_{roll} of .03 has been used throughout the program to model the rolling friction deceleration rates experienced by every aircraft.

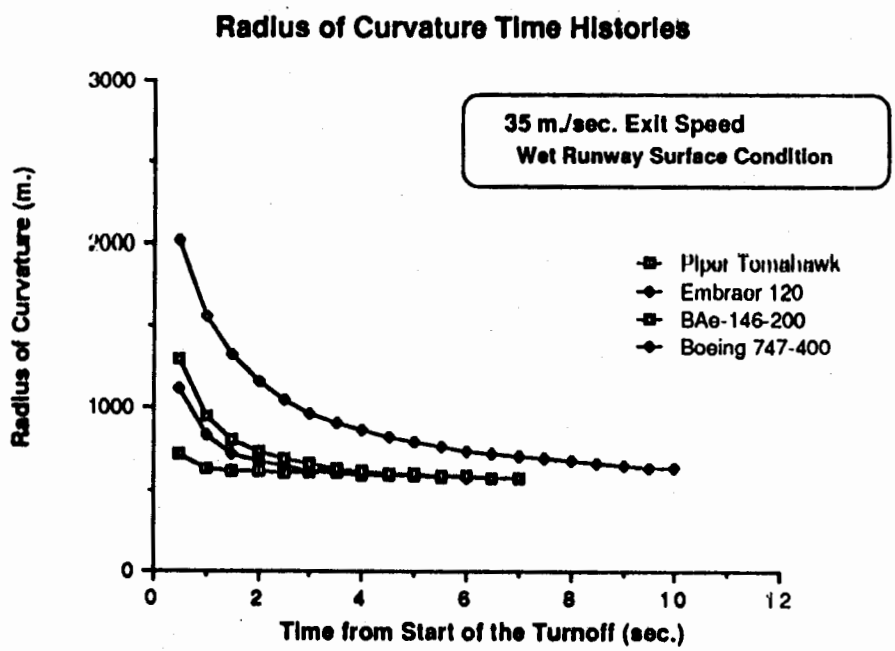

Figure C.2 Time Variations of Radius of Curvature for Representative Aircraft.

Fig. C.1 illustrates how the turnoff time is estimated using two simple radii of curvatire to approximate the actual turnoff track. Two turnoff arcs with lengths L_1 and L_2 are defined as follows,

$$L_1 = R_1 \ \theta_1 \qquad \{C.1\}$$

$$L_2 = R_2 \ \theta_2 \qquad \{C.2\}$$

where, L_1 and L_2 represent the turnoff characteristic lengths. R_1 and R_2 are the radii of curvature defining the turnoff, and θ_1 and θ_2 are the arcs defined by R_1 and R_2, respectively measured in radians. The turnoff arcs are characteristic for each aircraft since the transition and runway clearance point are aircraft speed and geometry dependent. A further simplification regarding the easement length, L_1 can be introduced using results derived from highway geometric design principles where the length of a spiral transition curve L_1 is made

a function of exit speed. Horonjeff later on showed that a short transition spiral could well be approximated with a large radius of curvature segment and this approximation is easily implemented in the model [Horonjeff, 1959].

$$L_1 = 2.914 + 3.1701\ V_{exit} \qquad for\ 8\ m/sec. \leq V_{exit} \leq 45\ m/sec. \qquad \{C.3\}$$

The aircraft speed at the transition point between the two radii of curvature is obtained from Eqn. C.4 whereas the speed at the runway clearance point is shown in Eqn. C.5.

$$V_{tran} = \{V_{exit}^2 - 2\ f_{roll}\ L_1\}^{.5} \qquad \{C.4\}$$

$$V_{final} = \{V_{tran}^2 - 2\ f_{roll}\ L_2\}^{.5} \qquad \{C.5\}$$

where, V_{exit} is the desired aircraft exit speed (m./sec.), V_{tran} is the transition speed (m./sec.), V_{final} is the final speed at the runway clearance point, (X_c, Y_c), g is the gravity constant (m./sec.-sec.) and f_{roll} is the rolling friction coefficient (dimensionless). The travel time across each of the turnoff segments is estimated as shown in Eqns. C.6 and C.7.

$$T_1 = \frac{V_{exit} + V_{tran}}{2} \qquad \{C.6\}$$

$$T_2 = \frac{V_{tran} + V_{final}}{2} \qquad \{C.7\}$$

where, T_1 and T_2 are the travel times from the start of the turnoff to the transition point (X_t, Y_t) and from transition point to runway clearing point (X_c, Y_c), respectively. The total turnoff time is the summation of these two previous contributions.

$$T_{tot} = T_1 + T_2 \qquad \{C.8\}$$

where, T_{tot} is the turnoff time until clearing the runway. This procedure to estimate the turnoff time is implemented for the secondary candidates whose locations are $q\ (D_{min})$ meters away from primary candidate solutions (for $q = 1, 2, ..., N$) as explained in Chapter 4 of this report. It should be noticed that the secondary candidate solutions obtained for small aircraft far downrange from an active threshold will usually be unfeasible for large aircraft since these

will not be able to negotiate the turnoff with the desired margin of safety. This process reduces even more the candidate set to be used in the optimization module.